Model Development Report: Putah Creek Watershed

SUBMITTED TO:
State Water Resources Control Board
1001 I Street, 14th Floor
Sacramento, CA 95814

PREPARED BY:

Paradigm Environmental
9320 Chesapeake Drive, Suite 100
San Diego, CA 92123

MARCH 18, 2026

THIS PAGE INTENTIONALLY LEFT BLANK

Contents

Figures

Tables

1 INTRODUCTION

This report provides a detailed discussion of the development and configuration of a hydrology model which was developed for the Putah Creek watershed to support decision making by the California State Water Resources Control Board (Water Board) regarding water supply, demand, and use. In April 2021, Governor Gavin Newsom issued a state of emergency proclamation for specific watersheds across California in response to exceptionally dry conditions throughout the state. The April 2021 proclamation, as well as subsequent proclamations, directed the Board to address these emergency conditions to ensure adequate, minimal water supplies for critical purposes. To support Water Board actions to address emergency conditions, hydrologic modeling and analysis tools are being developed to contribute to a comprehensive decision support system that assesses water supply and demand, and the flow needs for watersheds throughout California.

This model development report builds on the Putah Creek watershed modeling work plan (SWRCB 2024), which has additional information on the model background and over-arching model approach; the Loading Simulation Program in C++ (LSPC) was used to simulate hydrology within the watershed. The model provides an evaluation platform for (1) simulating existing instream flows that integrate current water management activities and consumptive uses, (2) evaluating the range of impacts of alternative management scenarios. Key components necessary to the development of this model are detailed in this report. Model development refers to basic building blocks for defining the surface water model domain. It includes catchment delineation, reach segments (cross-sections, hydraulic characteristics, and routing network), and Hydrologic Response Units (HRUs). Model development also includes creating and assigning representative climate forcing inputs.

- Section 2.1 describes the Catchment Delineation. Catchments are the highest resolution spatial boundaries in the model. Delineated catchments were compiled from best-available topographic layers and refined as needed to align outlets with monitoring gauges.
- Section 2.2 describes the Hydraulic Network. Hydraulic routing features include reaches, lakes/reservoirs, and other network routing elements that convey flow and pollutants from one catchment to another.
- Section 3 describes the Hydrologic Response Units. HRUs are the smallest spatial unit within the model, representing unique combinations of spatial data layers including land use/land cover, hydrologic soil group, and slope.
- Section 4 describes the climate forcing inputs (i.e., precipitation and potential evapotranspiration) that drive the model's rainfall-runoff response.
- Section 5 describes the representation of surface water withdrawals and irrigation in the model.
- Section 6 details the representation of Lake Berryessa within the model.
- Sections 7 presents an evaluation of the observed water balances in the watershed.
- Sections 8 and 9 detail the model calibration and validation procedures and results.

2 CATCHMENT NETWORK

2.1 Catchment Delineation

The United States Geological Survey (USGS) delineates watersheds nationwide based on surface hydrological features and organizes the drainage units into a nested hierarchy using hydrologic unit codes (HUC). These HUCs have a varying number of digits to denote scale ranging from 2-digit HUCs (largest) at the regional scale to 12-digit HUCs (smallest) at the subwatershed scale. The Putah Creek watershed is defined as a HUC-8 watershed comprised of 20 HUC-12 subwatersheds.

For units smaller than HUC-12 subwatersheds, the National Hydrography Dataset Plus v2 (NHDPlus) has further discretized the watershed into catchments ranging in size between 0.0003 square miles to over 7 square miles. Where necessary, catchments were either merged to eliminate braiding in the stream network or sub-delineated using the hydrologically conditioned 30-meter resolution digital elevation model (DEM), flow direction, and flow accumulation rasters available with the NHDPlus dataset to better represent points of interest. Catchments were merged in 19 cases; sub-delineation was necessary in 6 cases where a catchment had disconnected reach segments with points of diversion. Table 2-1 presents summary statistics of NHDPlus catchment sizes by HUC-12 subwatershed. Figure 2-1 is a map of HUC-12 subwatersheds and NHDPlus catchments within the Putah Creek HUC-8 watershed.

Table 2-1. Summary of final NHDPlus catchments within the Putah Creek watershed HUC-12 subwatersheds

HUC-12	HUC-12 Name	Catchment Count	Catchment Minimum (acres)	Catchment Average (acres)	Catchment Maximum (acres)	Catchment Total (acres)
180201620101	Upper Eticuera Creek	20	58.5	826.7	2,131.9	16,534.4
180201620102	Lower Eticuera Creek	39	11.8	724.6	2,671.0	28,260.8
180201620201	Upper Pope Creek	17	89.2	819.3	1,822.5	13,928.2
180201620202	Maxwell Creek	43	3.1	521.6	1,781.2	22,427.6
180201620203	Lower Pope Creek	41	9.8	504.7	2,452.4	20,694.0
180201620301	Saint Helena Creek	23	3.3	593.0	1,617.5	13,639.9
180201620302	Dry Creek – Putah Creek	29	23.6	705.1	3,141.8	20,448.1
180201620303	Big Canyon Creek	26	20.2	801.2	2,721.5	20,831.6
180201620304	Soda Creek	29	0.2	715.8	1,971.8	20,758.6
180201620305	Bucksnort Creek	25	12.5	673.4	2,961.0	16,835.1
180201620306	Hunting Creek	38	5.3	631.3	2,075.2	23,989.8
180201620307	Crazy Creek	30	24.2	843.9	2,438.1	25,317.8
180201620308	Butts Creek	71	4.7	499.3	1,950.6	35,452.9
180201620401	Capell Creek	52	3.6	539.7	1,750.0	28,066.0
180201620402	Jackson Creek	39	50.5	873.6	1,984.0	34,070.1
180201620403	Wragg Canyon	32	6.2	677.6	2,539.3	21,684.5
180201620501	Pleasants Creek	16	2.9	662.3	2,189.1	10,596.8
180201620502	Dry Creek	21	11.8	669.1	2,815.9	14,050.9
180201620503	McCune Creek	58	1.3	331.4	1,947.8	19,223.2
180201620504	South Fork Putah Creek	20	14.0	579.0	4559.2	11,580.4
Total		**669**	**--**	**--**	**--**	**418,390.6**

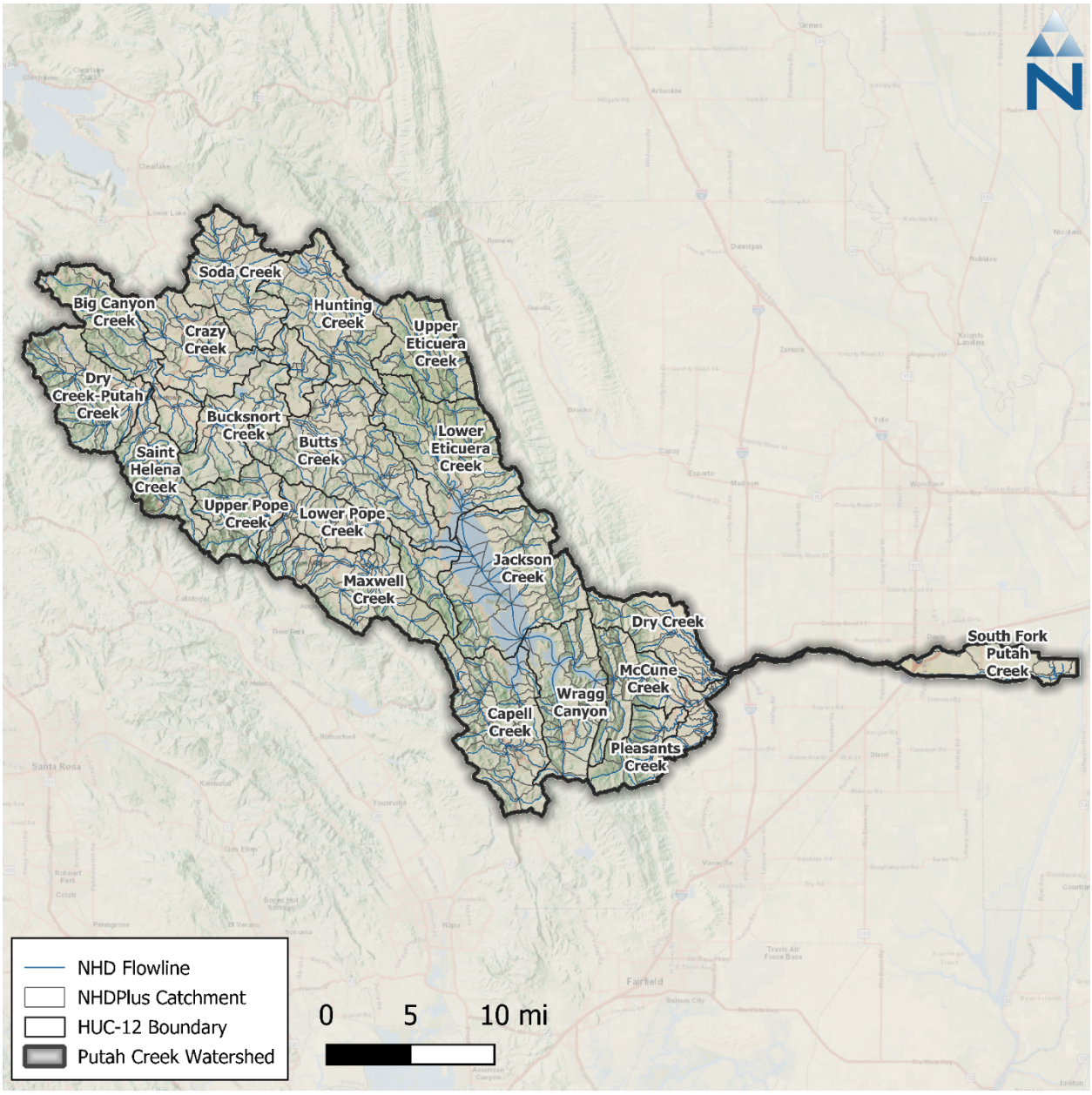

Figure 2-1. Final NHDPlus catchment segmentation and flowlines for the Putah Creek watershed.

2.2 Routing and Connectivity

Once catchments have been delineated, the connectivity of flow within and between each catchment needs to be specified so that water can be routed from upstream to downstream areas. Within the Putah Creek watershed model, surface flow is conveyed through a reach network with no more than one representative reach segment for each catchment. Within a catchment, water from all other upstream physical conveyance is routed directly to the top of and through the representative stream segment.

The reach network for the Putah Creek watershed is based on the NHD flowlines available with the NHDPlus dataset. These flowlines were edited as described in Section 2.1 to eliminate braiding and are shown in Figure 2-1. Within the NHDPlus schema, catchments can be related to flowlines

through the catchment *FEATUREID* and flowline *COMID*. The flowline *COMID* was joined to the PlusFlowlineVAA (value-added attributes) table available with the NHDPlus dataset to determine flow routing.

2.3 Stream Characteristics

The discharge for each stream segment is calculated in LSPC using Manning's equation, presented below as Equation 1:

$$Q = VA = (\frac{1.49}{n})AR^{\frac{2}{3}}\sqrt{S} \qquad \text{Equation 1}$$

where (A) is the cross-sectional area in square feet, (R) is the hydraulic radius in feet, (V) is the velocity in feet per second, (S) is the longitudinal slope, and (n) is the channel roughness coefficient.

Length and slope are derived from the PlusFlowlineVAA table, which includes precalculated reach characteristics based on local conditions. For reaches that were merged, split, or edited, the slope was recalculated as the length-weighted average slope (derived from the DEM described in Section 3.4) based on the new reach length. The default cross-section representation in LSPC is a symmetrical trapezoidal channel defined using the terms shown in Figure 2-2. Stream segments are represented in the model as having the same cross-section for the entire reach length. Numerous studies have developed empirical relationships between stream channel geometry and upstream contributing area (Bent & Waite, 2013; McCandless, 2003a, 2003b; McCandless & Everett, 2002); these were used to derive channel geometry for each stream segment in LSPC. An initial estimate of n = 0.04 representing natural streams with vegetation was used for all reach segments and may be updated as needed during model calibration (Arcement & Schneider, 1989).

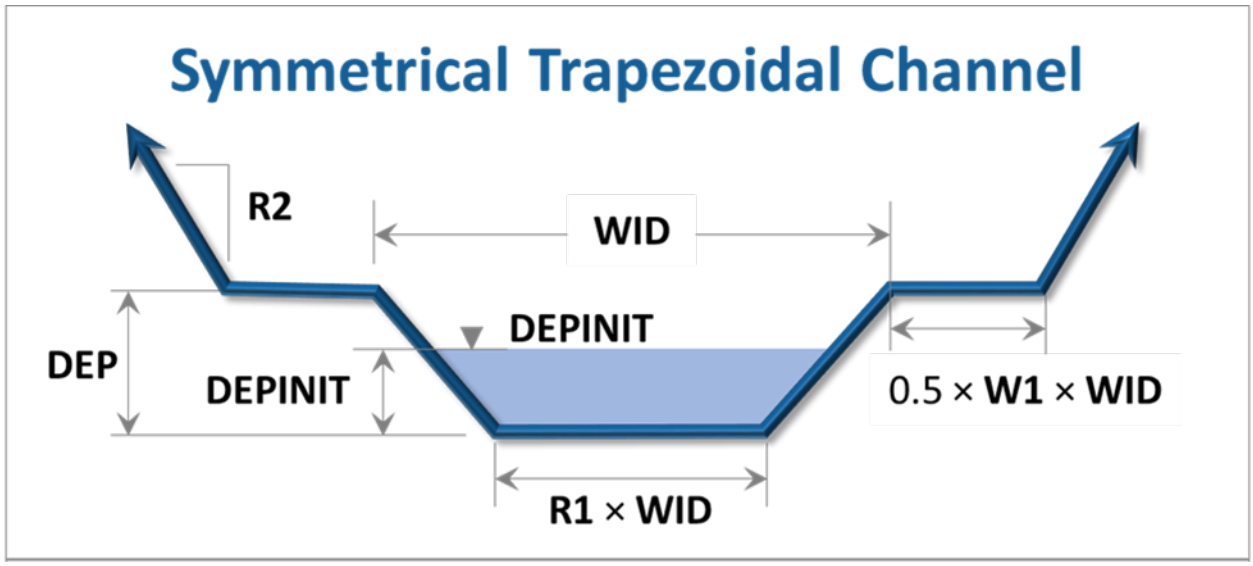

WID	Estimated Bankfull-Width	**R1**	Ratio of channel bottom width to **WID**
DEP	Estimated Bankfull-Depth	**R2**	Side slope for floodplain
DEPINIT	Initial water depth	**W1**	Floodplain width parameter

Figure 2-2. Example cross-section representation in LSPC.

3 HYDROLOGIC RESPONSE UNITS

Within LSPC, land is categorized into HRUs, which are the core hydrologic modeling land units in the watershed model. Each HRU represents areas of similar physical characteristics attributable to certain processes. The HRU development process uses data types that are typically closely associated with hydrology (and water quality, when applicable) in the watershed. For the Putah Creek watershed, this includes data such as land cover, cropland, soil type, and slope. The HRUs are developed by overlaying these datasets in raster format and identifying the unique combinations over the catchments. Ultimately, some consolidation of HRUs was implemented to balance the model computational efficiency and optimal spatial resolution, resulting in a set of meaningful HRUs for model configuration. Percent tree canopy was also summarized as a secondary attribute by HRU and used to estimate initial values for the interception storage and lower-zone evapotranspiration rate for model configuration.

Table 3-1 lists the spatial data used in the HRU analysis along with the corresponding data sources. The following subsections summarize the data that were used to develop each of these spatial layers and the processes for consolidating them as HRUs.

Table 3-1. Summary of input datasets detailing data source and type

GIS Layer	Data Source	Site	Description	Date Downloaded
Digital Elevation Model	USGS 3D Elevation Program (3DEP)	Science Base	2024 – 27.49m resolution grid	August 1, 2024
Land Cover	MRLC (NLCD)	MRLC	2021 – 30m resolution grid	June 30, 2023
Cropland	USDA (CDL)	USDA	2022 -– 30m resolution grid	January 2, 2023
Percent Imperviousness	MRLC (NLCD)	MRLC	2021 – 30m resolution grid	June 30, 2023
Percent Tree Canopy	MRLC	MRLC	2021 – 30m resolution grid	October 5, 2023
Soil Survey Geographic Database (SSURGO)	USDA (NRCS)	USDA	2022 – polygon layer	October 5, 2023
U.S. General Soil Map (STATSGO2)	USDA (NRCS)	USDA	2016 – polygon layer	December 29, 2022

3.1 Land Cover

The land cover data were obtained from the 2021 National Land Cover Database (NLCD) maintained by the Multi-Resolution Land Consortium (MRLC), a joint effort between multiple federal agencies. The primary objective of the MRLC NLCD is to provide a current data product in the public domain with a consistent characterization of land cover across the United States. The 2021 NLCD provides a 16-class scheme at a 30-meter grid resolution.

Table 3-2 summarizes the NLCD 2021 land cover distribution for the Putah Creek watershed; Figure 3-1 shows the land cover for the Putah Creek watershed. Grassland is the dominant land cover classification covering approximately 55% of the watershed area. When combined, evergreen forest, the undeveloped categories of deciduous forest, mixed forest, shrub/scrub, and grassland/herbaceous account for close to 88% of the total watershed area. Developed land cover makes up less than 3.2% of the total watershed area and is classified mostly as "Developed, Open

Space," which suggests that much of the developed area is dispersed. Approximately 3.7% of the total watershed area is categorized as cultivated cropland. For HRU development, similar NLCD classes (e.g., forest) were grouped.

Table 3-2. Distribution of 2021 NLCD land cover classes within the Putah Creek watershed

NLCD Class	Description	Model Group[1]	Area (acres)	Area (%)
22	Developed, Low Intensity	Developed_Low_Intensity	2,868.4	0.7%
23	Developed, Medium Intensity	Developed_Medium_Intensity	1,188.3	0.3%
24	Developed, High Intensity	Developed_High_Intensity	233.1	0.1%
21	Developed, Open Space	Developed_Open_Space	8,727.4	2.1%
31	Barren Land (Rock/Sand/Clay)	Barren	230.0	0.1%
41	Deciduous Forest	Forest	1,156.4	0.3%
42	Evergreen Forest	Forest	17,104.8	4.1%
43	Mixed Forest	Forest	10,756.3	2.6%
52	Shrub/Scrub	Scrub	110,369.7	26.4%
71	Grassland/Herbaceous	Grassland	228,679.3	54.7%
81	Pasture/Hay	Pasture	418.5	0.1%
82	Cultivated Crops	Agriculture	15,474.8	3.7%
90	Woody Wetlands	Forest	880.2	0.2%
95	Emergent Herbaceous Wetlands	Grassland	2,175.7	0.5%
11	Open Water	Water	18,086.6	4.3%
		Total	**418,349.5**	**100.0%**

1. Developed land cover will be refined and redistributed into effective Developed_Impervious and Developed_Pervious areas as described in Section 3.6. All other model groups are mapped for consolidation as shown.

Color Gradient: Lowest | Low | Med | High | Highest

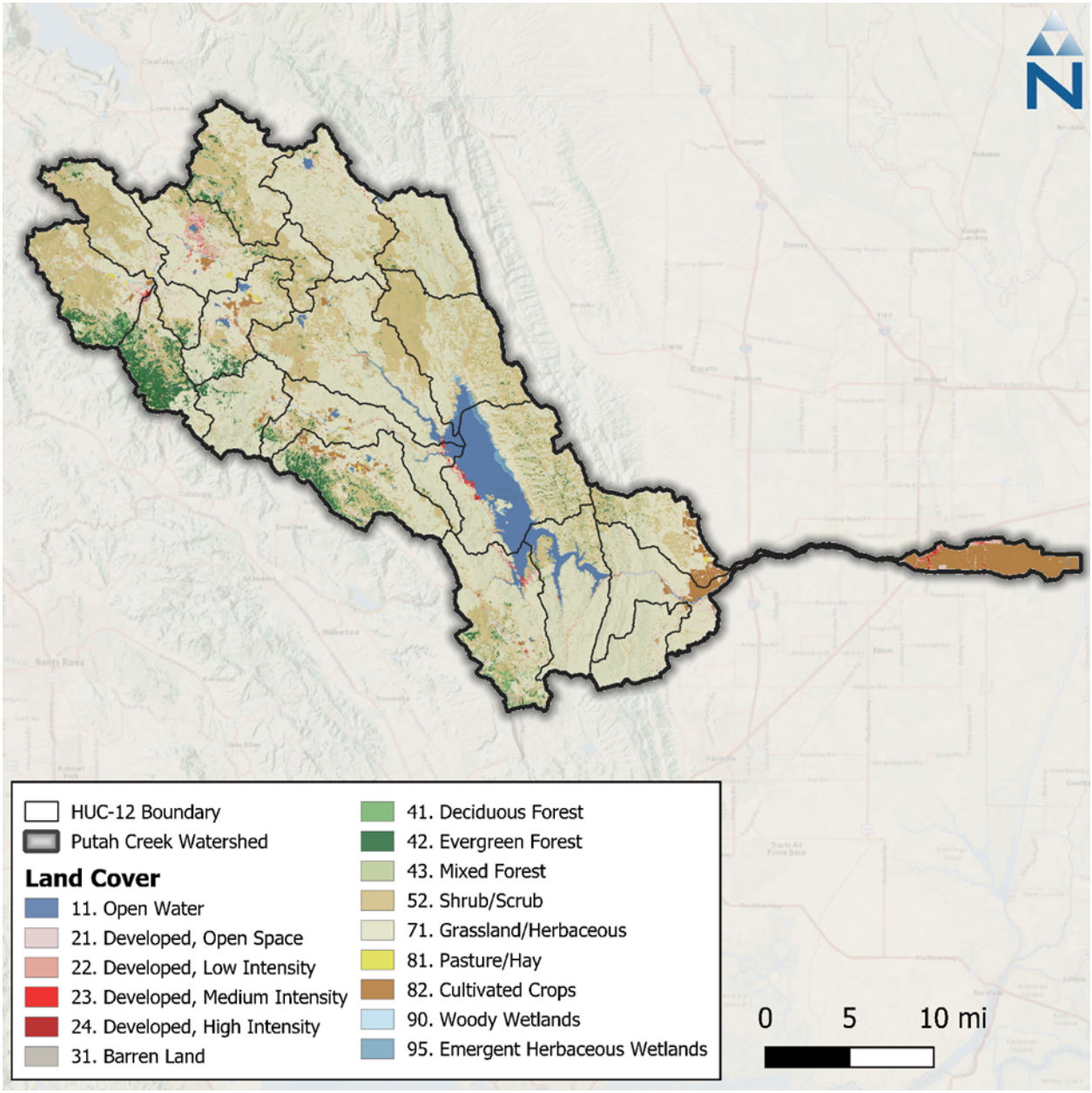

Figure 3-1. NLCD 2021 land cover within the Putah Creek watershed.

3.2 Agriculture and Crops

Land cover data for the Putah Creek watershed (see Section 3.1) were analyzed to identify predominant cropland vegetation classes. This analysis revealed that only 0.1% of the watershed area was classified as Pasture/Hay (class 81), 26% was classified as Shrub/Scrub (class 52), and 55% was classified as Grassland/Herbaceous (class 71); of these areas, a portion may include areas of cultivated crops that were not automatically recognized through processing of the remote sensing data or include cultivated crops on a rotating schedule. To reflect these situations, supplemental information published by the United States Department of Agriculture (USDA) was used.

The USDA Cropland Data Layer (CDL) is an annually updated raster dataset that geo-references crop-specific land use (USDA 2024). The dataset comes as a 30-meter resolution raster with a linked

lookup table of 85 standard crop types that can be used to classify agricultural land. Figure 3 2 shows the spatial distribution of these classes through the study area, and Table 3 3 summarizes their areal coverage. The CDL Land use layer was intersected with the NLCD Land Cover layer, and CDL Agriculture and Pasture land use classifications overwrote the original NLCD classifications. The combined Land Use/Land Cover (LULC) increased "Cropland" to nearly 20,000 acres (4.7%), which was classified as "Agriculture" in the final HRU layer—"Pasture" area was also updated to match CDL land use. The LULC intersection redistributes HRU area between originally classified Grassland, Pasture, and Agriculture categories from NLCD.

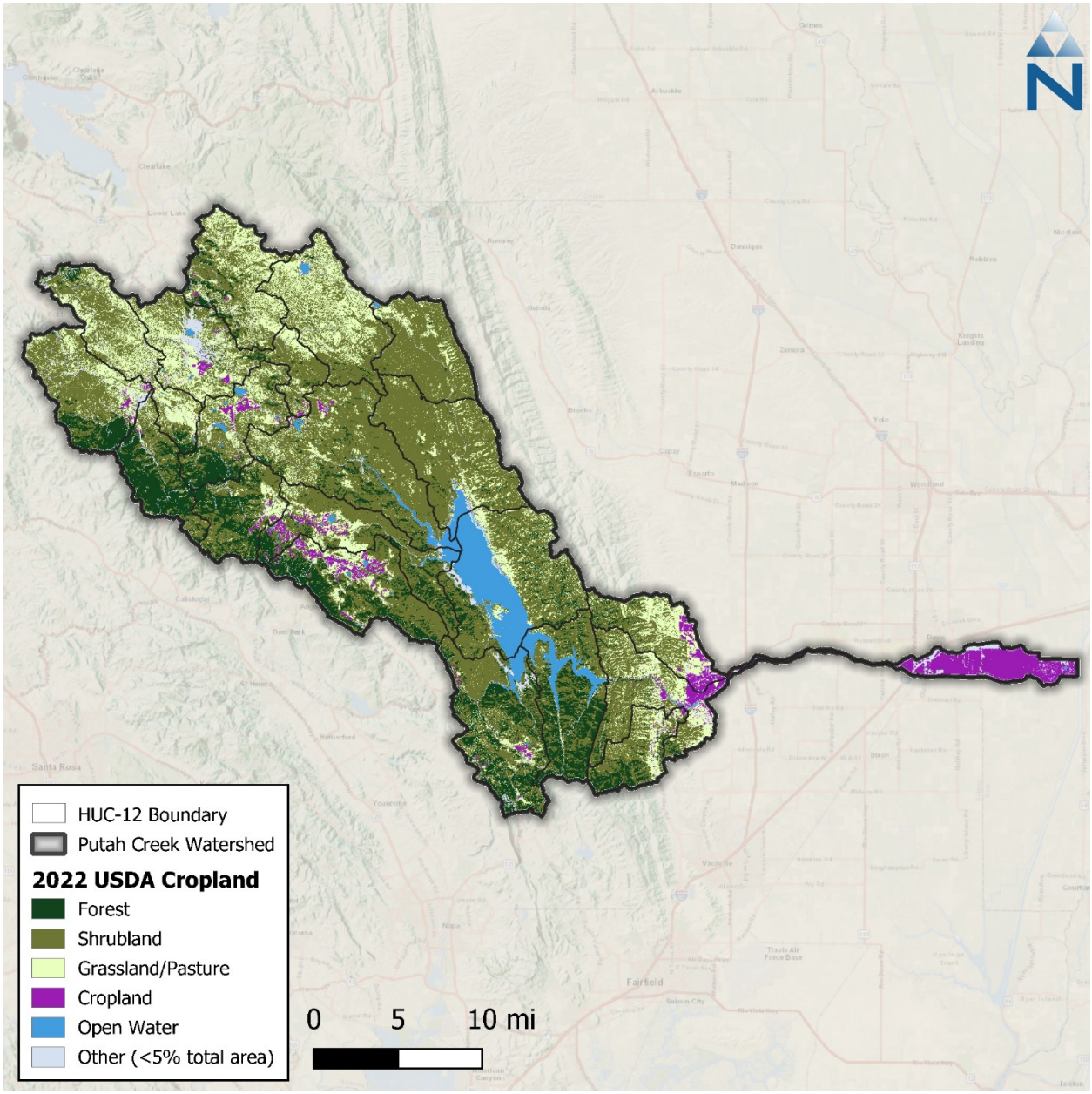

Figure 3-2. USDA 2022 Cropland Data within the Putah Creek watershed.

Table 3-3 USDA 2022 Cropland Data summary within the Putah Creek watershed

Crop Type	Area (acres)	Area (%)
Forest	62,412.6	15.0%
Shrubland	219,723.7	53.0%
Grassland/Pasture	83,714.2	20.0%
Cropland	18,764.5	4.0%
Open Water	18,768.0	4.0%
Other (<5% Total Area by Category)	14,966.4	4.0%
Total	**418,349.5**	**100.0%**

Color Gradient: Lowest | Low | Medium | High | Highest

3.3 Soils

Soil data for the Putah Creek watershed were obtained from the Soil Survey Geographic Database (SSURGO) published by the Natural Resource Conservation Service (NRCS). Four primary hydrologic soil groups (HSG) are used to characterize soil runoff potential. Group A generally has the lowest runoff potential, whereas Group D has the highest runoff potential. The SSURGO soils database is composed of a GIS polygon layer of map units and a linked tabular database with multiple layers of soil properties.

Table 3-4 and Figure 3-3 present summaries of the SSURGO hydrologic soil groups for the Putah Creek watershed. The dominant soil group in the watershed is Group D (54.7%), contains Clay Loam, Silty Clay Loam, and Sandy Clay. Group C (35.9%) is the next most common soil group in the watershed, containing sandy clay loam that typically has low infiltration rates. Group A makes up less than 2% of the watershed. Less than 1% of the watershed has mixed soils. For modeling purposes, mixed soils will be grouped with the nearest primary group as follows: A/D → B, B/D → C, and C/D → D. About 8.4% of the watershed HSG area is classified as unknown in the SSURGO database and reside primarily in the north and within Lake Berryessa. For these areas, the corresponding HSG from the STATSGO dataset was used to supplement the data gaps; this reduced the unknown soil areas to about 4% (predominately with Lake Berryessa). Since most of the soil in the watershed is Group D, the remaining unknown soil areas are also considered to be Group D in this analysis.

Table 3-4. NRCS Hydrologic soil groups in the Putah Creek watershed

Soil Group	Model Group	Area (acres)	Area (%)
A	A	6,666.9	1.6%
B	B	16,020.8	3.8%
C	C	150,235.8	35.9%
C/D	D	167.0	0.0%
D	D	228,925.4	54.7%
Unclassified	D	16,333.5	3.9%
	Total	**418,349.5**	**100.0%**

Color Gradient: Lowest | Low | Medium | High | Highest

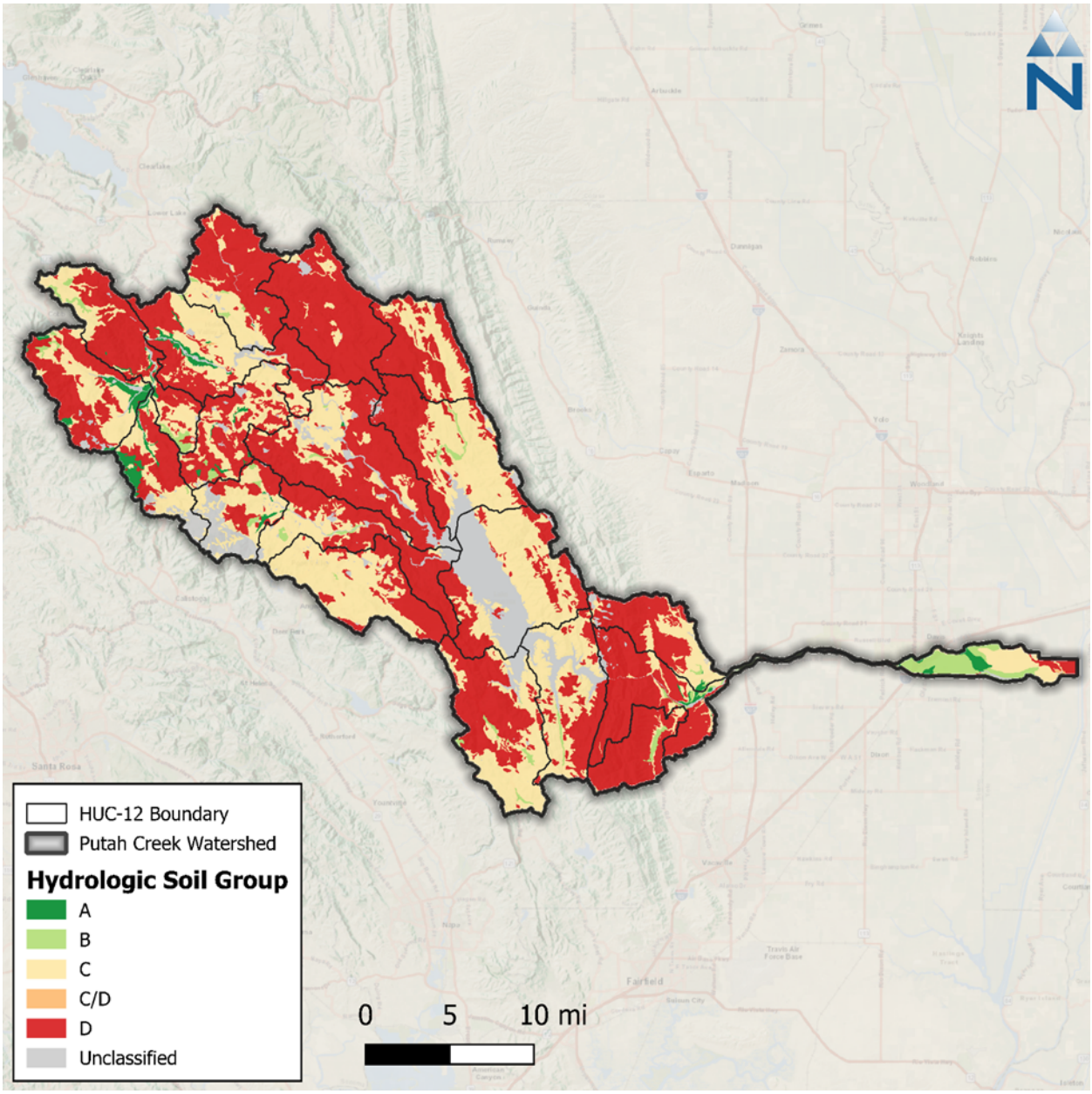

Figure 3-3. SSURGO hydrologic soil groups within the Putah Creek watershed.

3.4 Elevation and Slope

The United States Geological Survey (USGS) 3D Elevation Program (3DEP) publishes DEMs expressing landscape elevation through a raster grid data product with a 1 arc-second (approximately 30-meter) horizontal resolution. The 1 arc-second data covering the Putah Creek watershed had a resolution of 27.49-meters and thus was resampled to 30-meters for consistency with the rest of the datasets for the HRU analysis. The Putah Creek watershed ranges in elevation from approximately 1.7 meters along the southeastern extension of the watershed to over 1,400 meters in the northwestern portion of the watershed.

The 30-meter DEM was used to generate a slope (percent rise) raster for the watershed. Figure 3-4 illustrates the cumulative distribution function (CDF) of the slope raster values across the model

domain as a percentage of the total watershed land area (i.e., excluding major water bodies). The CDF was used to identify appropriate bins for HRU slope categories during the HRU definition process. Slopes were categorized as low (< 5%), medium (5 to 15%), and high (>15%) according to their distribution and overlap with the land cover layer. Table 3-5 and Figure 3-5 present the distribution of slope categories within the watershed.

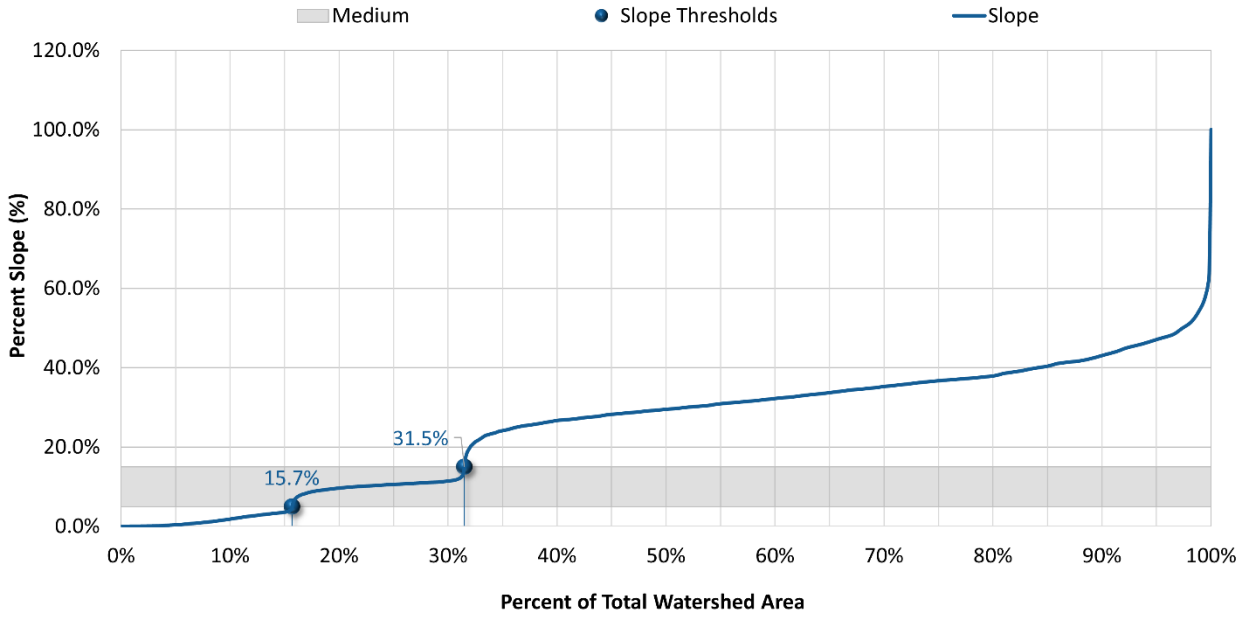

Figure 3-4. Cumulative distribution of slope categories within the Putah Creek watershed.

Table 3-5. Distribution of slope categories within the Putah Creek watershed

Slope (%)	Slope Category	HRU Group	Area (acres)	Area (%)
0-5	Low	Low	65,565.3	15.7%
5-15	Medium	Med	66,128.6	15.8%
>15	High	High	286,655.6	68.5%
		Total	**418,349.5**	**100.0%**

Color Gradient: Lowest | Low | Medium | High | Highest

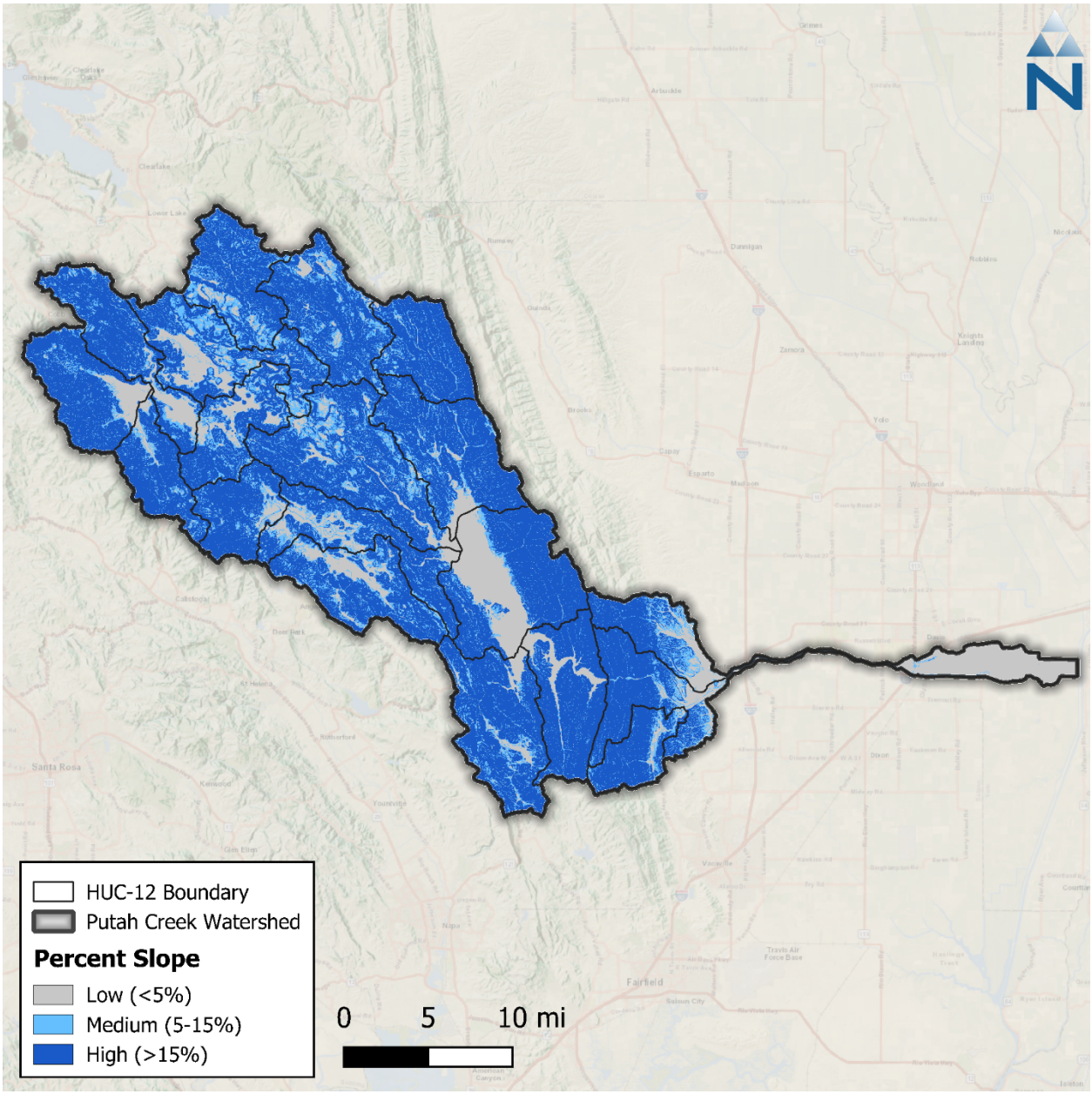

Figure 3-5. Percent Slope derived from the DEM within the Putah Creek watershed.

3.4.1 Length and Slope of Overland Flow

Overland flow lengths on high slopes are generally shorter and more direct and have faster travel times on high slopes, but generally longer and less direct with slower travel times on lower slopes. It was found during previous modeling efforts that using an empirical relationship shown in Figure 3-6, derived by inversely scaling length of overland flow (LSUR) with slope of overland flow (SLSUR), improved model prediction of peak flow timing. Figure 3-7 is the resulting cumulative distribution of LSUR and SLSUR in the Putah Creek watershed. Longer flow lengths on shallow sloped areas increase the opportunity for attenuation, surface storage, and infiltration. On the other hand, shorter flow lengths on steeper slopes retain the flashiness where applicable. Similar modeling efforts have historically used discrete/fixed values and ranges for SLSUR and LSUR to better manage the degrees of freedom among model variables. However, because SLSUR can be measured

by HRU from remotely-sensed data, applying a relationship to also estimate LSUR as a function of SLSUR preserves some natural variability throughout the watershed that (1) can provide some improvement relative to initial hydrology prediction using constant values and (2) helps to reduce the chance of adjusting other parameters during calibration that are better explained by the influence of LSUR and SLSUR.

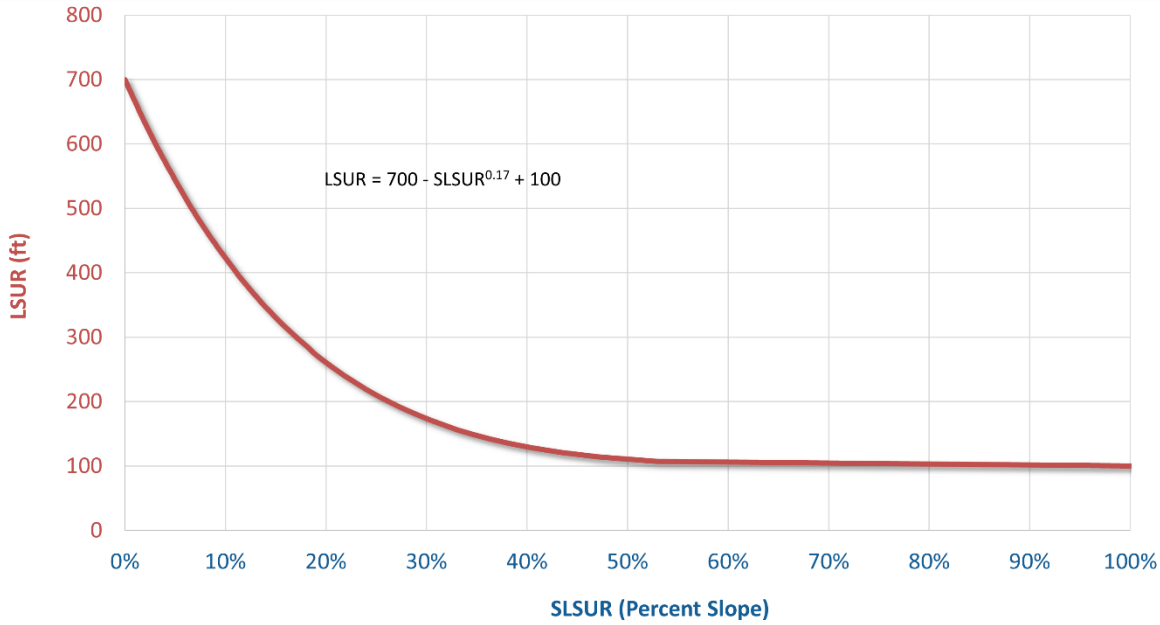

Figure 3-6. Empirical relationship of LSUR vs. SLSUR.

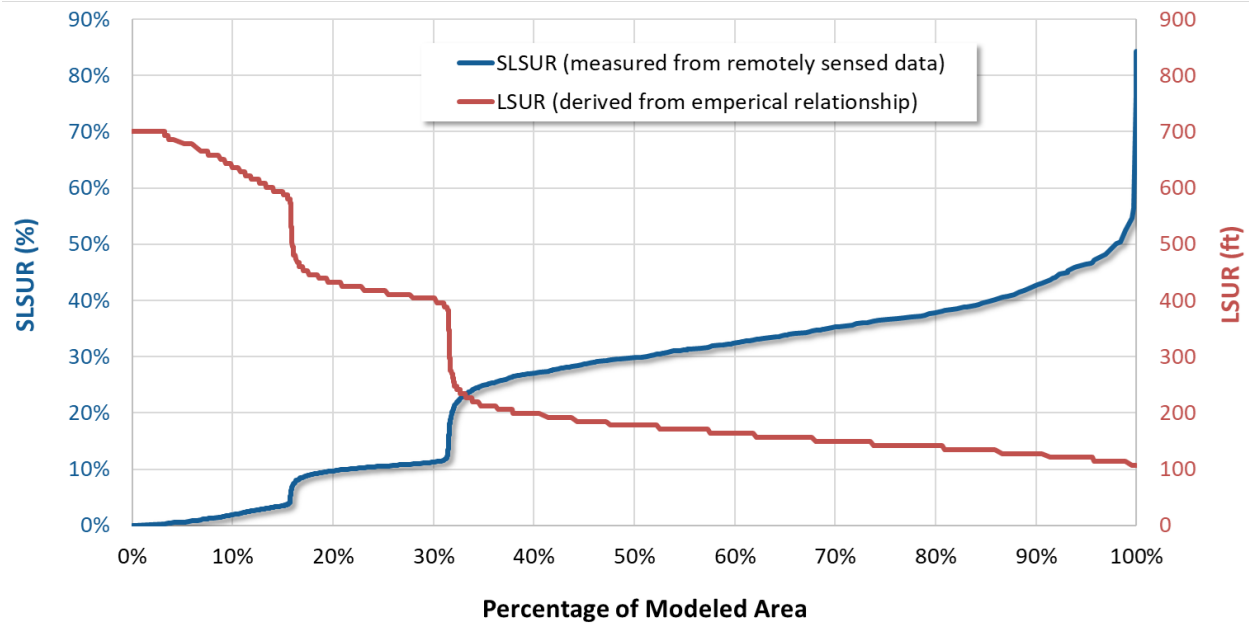

Figure 3-7. Cumulative distribution of LSUR and SLSUR in the Putah Creek watershed derived from the generalized empirical relationship.

3.5 Secondary Attributes

Secondary attributes can be included in the HRU development process to provide additional information not directly mapped in the HRU categories. Secondary attributes used for the Putah Creek watershed include impervious and tree canopy cover percentages. The impervious cover percentage is used for the translation of mapped impervious cover to effective impervious cover, while percent canopy estimates can inform certain hydrologic parameters but will not be represented in the HRUs as a category.

3.5.1 Impervious Cover

MRLC publishes a developed impervious cover dataset as a companion to the NLCD land cover. This dataset is also provided as a raster with a 30-meter grid resolution. Impervious cover is expressed in each raster pixel as a percentage of the total area ranging from 0 to 100 percent. Figure 3-8 shows the NLCD impervious 2021 cover dataset for the Putah Creek watershed. Because this dataset provides impervious cover estimates for areas classified as developed, non-zero values closely align with developed areas (NLCD classification codes 21 through 24). The percentage impervious cover was used in HRU development to further group developed land cover classes into pervious or impervious and to distinguish between mapped impervious area (MIA) and effective impervious area (EIA), as discussed in Section 3.6.1.

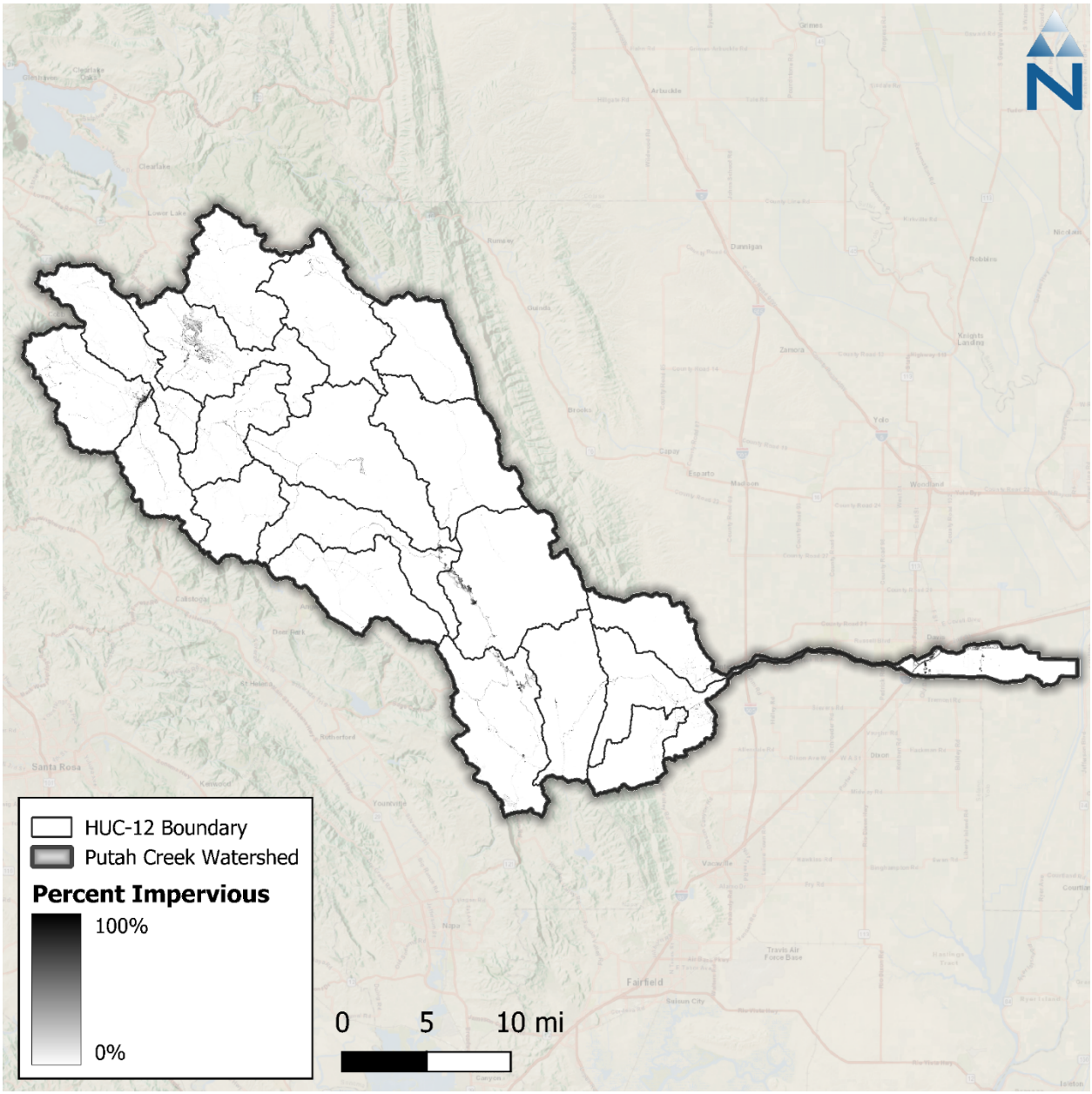

Figure 3-8. NLCD 2021 percent impervious cover in the Putah Creek watershed.

3.5.2 Tree Canopy

MRLC publishes a tree canopy dataset as a companion to the NLCD land cover dataset that estimates the percentage of tree canopy cover spatially. The United States Forest Service (USFS) developed the underlying data model, which is available through its partnership with the MRLC. This dataset is also provided as a raster with a 30-meter grid resolution. Similar to the impervious cover dataset, each raster grid cell expresses the percentage of grid cell area covered by tree canopy with values ranging from 0 to 100 percent. The Putah Creek watershed has the highest canopy coverage (up to 89%) along the western edge of the watershed (Figure 3-9). Tree canopy cover data was used to estimate model parameters such as interception storage and lower-zone evapotranspiration rates.

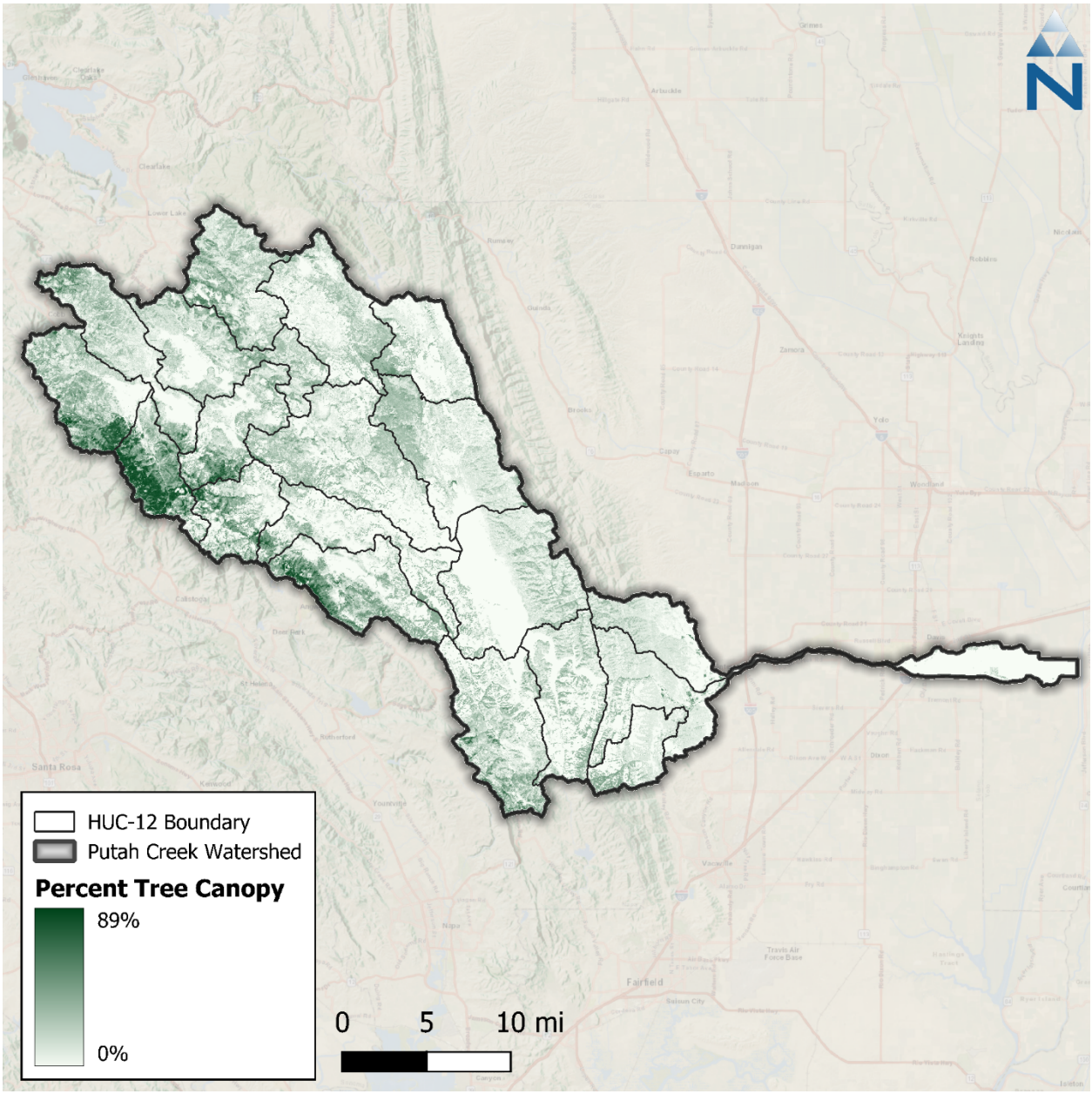

Figure 3-9. NLCD 2021 percent tree canopy cover in the Putah Creek Watershed.

3.6 HRU Consolidation

The five spatial datasets described above (land cover, cropland, impervious cover, soils, and slope) were spatially overlayed in GIS to derive a composite raster where each grid cell shows the combination of the values from the overlayed datasets. A zonal statistics operation was then performed in GIS to generate a summary table identifying unique grid cell values (i.e. HRUs) from the composite raster and corresponding areas across catchments. The combination of these datasets resulted in 132 potential HRUs. To balance model computational efficiency, the impervious HRUs were consolidated for soil and slope combinations to reduce the overall number of unique HRUs. This step was necessary to develop a model with a reasonable run time while maintaining the optimal model resolution to characterize hydrologic conditions adequately. The HRU refinement process involves analyzing the percentage of the model area attributed to each unique HRU

combination as shown in Table 3-6. The spatial distribution of mapped HRUs across the watershed is shown in Figure 3-10. Additionally, the impervious percentage is used to adjust and group developed land cover classes (Section 3.6.1) and agricultural areas located in catchments with irrigation points of diversion were assigned as Irrigation HRUs (Section 5.1). The final 98 modeled HRU categories are described in Section 3.6.2.

Table 3-6. Percent land cover distribution by mapped HRU category for the Putah Creek watershed

LULC	Total Area (%)	Soil Group (% LULC Area)				Slope (% LULC Area)		
		A	B	C	D	0-5	5-15	>15
Developed_Low_Intensity	0.7%	9.7%	12.4%	41.5%	36.4%	32.3%	30.4%	37.3%
Developed_Medium_Intensity	0.3%	12.7%	19.6%	39.3%	28.3%	50.7%	29.5%	19.8%
Developed_High_Intensity	0.1%	13.1%	30.4%	28.8%	27.7%	65.3%	27.0%	7.7%
Developed_Open_Space	2.1%	5.7%	9.4%	54.6%	30.3%	28.9%	29.4%	41.7%
Barren	0.0%	4.8%	44.1%	17.0%	34.0%	60.5%	22.8%	16.8%
Forest	6.9%	5.7%	4.3%	59.0%	31.0%	2.9%	12.1%	85.0%
Scrub	22.9%	0.4%	2.3%	42.5%	54.8%	4.7%	19.1%	76.1%
Grassland	38.1%	0.4%	1.7%	29.1%	68.8%	4.7%	12.4%	82.8%
Pasture	20.0%	1.9%	2.4%	34.3%	61.4%	18.0%	21.0%	61.0%
Agriculture	4.7%	7.5%	28.2%	48.6%	15.7%	82.5%	12.8%	4.6%
Water	4.3%	0.1%	4.6%	7.3%	88.0%	95.9%	3.0%	1.1%
Total	**100.0%**	**1.6%**	**3.8%**	**35.9%**	**58.7%**	**15.7%**	**15.8%**	**68.5%**

Color gradients indicate more Watershed Area and an increasing percentage of Soil and Slope, respectively.

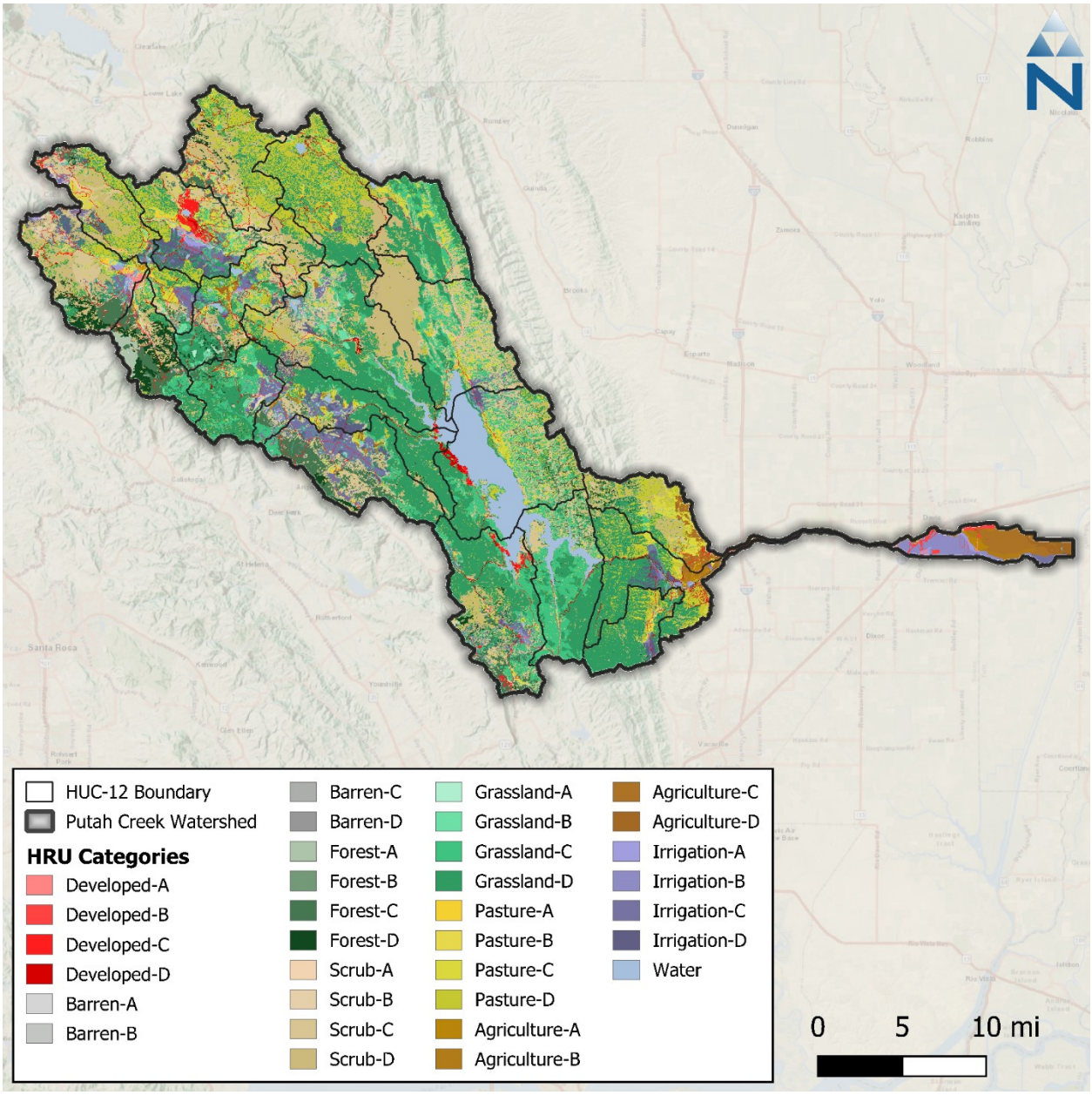

Figure 3-10. Mapped HRU categories within the Putah Creek watershed. Note that slope categories are grouped for visual clarity.

3.6.1 Directly Connected Impervious Area

The HRU approach not only highlights the predominant composition of an area within the catchment but also provides additional texture and physical basis for parameterizing and representing natural processes. Within a given modeled catchment, HRU segments are modeled as being parallel to one another. Each HRU segment flows directly to the routing stream segment without any interaction with neighboring HRU segments. However, in the physical environment, the lines between impervious and pervious land are not as clearly distinguished—impervious land may flow downhill over pervious land on route to a storm drain or watercourse.

For modeling purposes, Effective Impervious Area (EIA) represents the portion of the total, or Mapped Impervious Area (MIA), that routes directly to the stream segments. It is derived as a

function of the percent Directly Connected Impervious Area (DCIA), with other adjustments as needed to account for other structural and non-structural management practices in the flow network. Figure 3-11 illustrates the transitional sequence from MIA to DCIA. Impervious areas that are not connected to the drainage network can flow onto pervious surfaces, infiltrate, and become part of the pervious subsurface and overland flow. Because segments are modeled as being parallel to one another in LSPC, this process can be approximated using a conversion of a portion of impervious land to pervious land. On the open landscape, runoff from disconnected impervious surfaces can overwhelm the infiltration capacity of adjacent pervious surfaces during large rainfall/runoff events creating sheet flow over the landscape—therefore, the MIA→EIA translation is not actually a direct linear conversion. Finding the right balance between MIA and EIA can be an important part of the hydrology calibration effort.

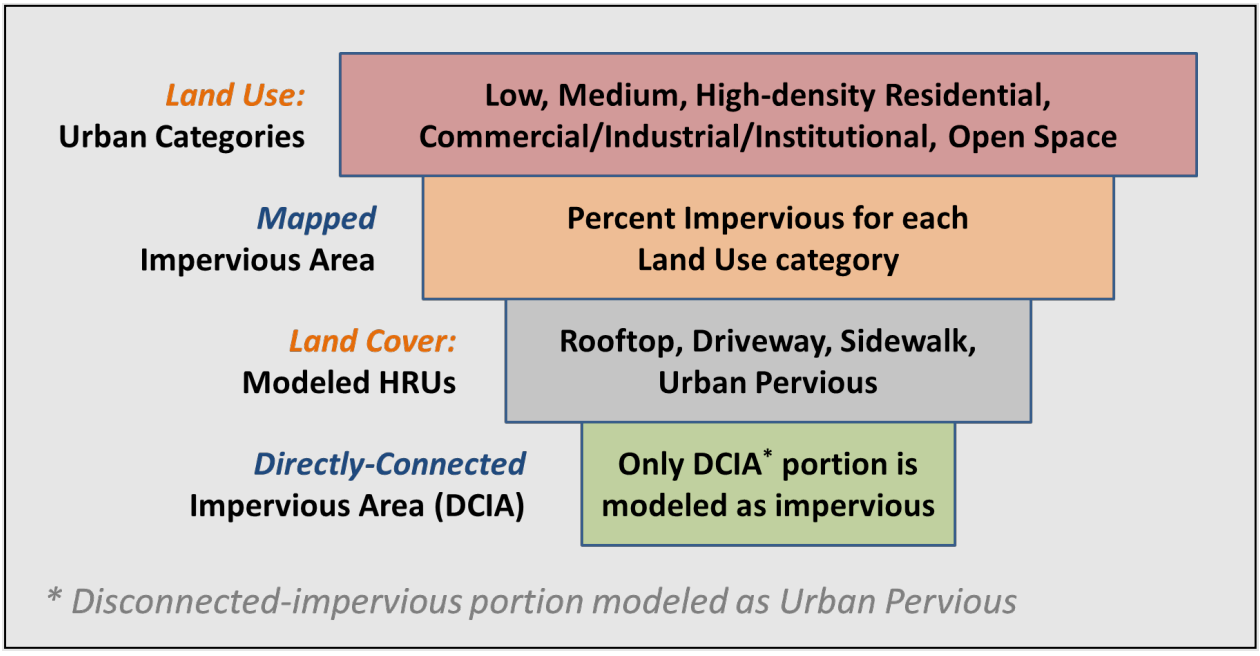

Figure 3-11. Generalized translation sequence from MIA to DCIA.

Empirical relationships like the Sutherland Equations (Sutherland, 2000) presented in Figure 3-12 show a strong correlation between the *density* of developed areas and DCIA. The curve for high-density developed land trends closer to the line of equal value than the curve for less developed areas. Similarly, as the density of the mapped impervious area approaches 100%, the translation to DCIA also approaches 100%. An initial estimate of EIA is equal to MIA × DCIA. This empirical approximation can be further refined during model calibration to account for other flow disconnections resulting from structural or non-structural Best Management Practices (BMPs) or other inline hydraulic routing features.

For the Putah Creek watershed, each developed land cover category was assigned a DCIA curve as shown in Table 3-7. The MIA, which is the impervious portion of each grid, was converted to EIA areas using these equations. Sutherland (2000) notes that areas with less than 1% MIA effectively behave like 100% pervious areas; therefore, EIA adjustments were only applicable to "Developed" areas. Table 3-8 is a summary of resampled MIA and calculated EIA by the land cover groups.

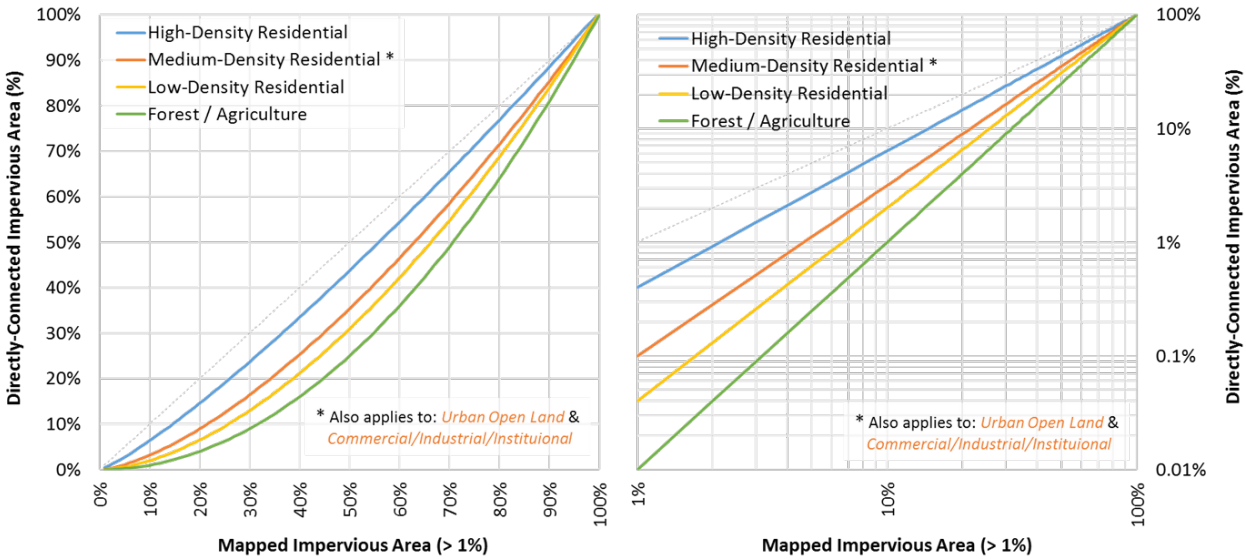

Figure 3-12. Mapped and directly connected impervious area relationships (Sutherland, 2000).

Table 3-7. Assignment of DCIA curves by land cover category

Land Cover	MIA	EIA	EIA:MIA	Equation
High Density Developed	87.5%	85.6%	98.0%	$DCIA=0.4(MIA)^{1.2}$
Medium Density Developed	61.6%	48.4%	79.0%	$DCIA=0.1(MIA)^{1.5}$
Low Density Developed	31.6%	14.3%	45.0%	$DCIA=0.04(MIA)^{1.7}$
Open Space	5.7%	0.4%	7.0%	$DCIA=0.01(MIA)^{2.0}$
Undeveloped*	0.0%	0.0%	0.0%	DCIA=0

* Assume no DCIA (100% disconnection, EIA = 0)

Color Gradient: Lowest | Low | Medium | High | Highest

Table 3-8. Distribution of impervious area by grouped NLCD/CDL land cover class

Model Group	Area Distribution (ac)		Impervious (acre)		Impervious (%)	
	Total	%	MIA	EIA	MIA	EIA
Developed_Low_Intensity	2,864.7	0.7%	905.9	408.4	31.6%	14.3%
Developed_Medium_Intensity	1,188.3	0.3%	732.4	575.4	61.6%	48.4%
Developed_High_Intensity	233.1	0.1%	203.8	199.4	87.4%	85.5%
Developed_Open_Space	8,641.6	2.1%	492.0	33.6	5.7%	0.4%
Barren	165.9	0.0%	0.0	0.0	0.0%	0.0%
Forest	28,798.0	6.9%	0.0	0.0	0.0%	0.0%
Scrub	95,864.2	22.9%	1.0	0.0	0.0%	0.0%
Grassland	159,355.9	38.1%	1.8	0.0	0.0%	0.0%
Pasture	83,730.9	20.0%	0.1	0.0	0.0%	0.0%
Agriculture	19,533.5	4.7%	4.0	0.0	0.0%	0.0%
Water	17,973.4	4.3%	0.0	0.0	0.0%	0.0%
Total	**418,349.5**	**100.0%**	**2,341.0**	**1,216.8**	--	--

Color gradients indicate model groups with more Watershed Area and Imperviousness, respectively.

3.6.2 Modeled HRU Categories

The combinations of LULC, HSG, and slope represent the physical characteristics that influence hydrology. After accounting for DCIA, the four developed land cover classes were rolled up as either a single "Developed Impervious" category or "Developed Pervious" stratified by HSG and slope. Agriculture HRUs (i.e., 4 HSGs × 3 slopes = 12 combinations) were further divided into irrigated and non-irrigated counterparts for a total of 24 HRUs. Altogether, a total of 98 HRU categories comprised the basic building blocks used in LSPC to represent hydrologic responses in the watershed. The "Agriculture" and "Pasture" HRU areas within catchments where streamflow was withdrawn for irrigation were re-assigned to their "Irrigation" HRU counterparts. Irrigation was simulated for those HRUs as described in Section 5.1. The final HRU distribution in the watershed is shown in Table 3-9.

Table 3-9. Modeled HRU distribution within the Putah Creek watershed

HRU ID	Land Use - Land Cover	HSG	Slope	Area (acres)	Area (%)
1000	Developed_Impervious	All	All	1,216.9	0.3%
2110	Developed_Pervious	A	Low	668.8	0.2%
2120	Developed_Pervious	A	Med	94.0	0.0%
2130	Developed_Pervious	A	High	48.0	0.0%
2210	Developed_Pervious	B	Low	821.8	0.2%
2220	Developed_Pervious	B	Med	230.0	0.1%
2230	Developed_Pervious	B	High	183.3	0.0%
2310	Developed_Pervious	C	Low	1,609.4	0.4%
2320	Developed_Pervious	C	Med	2,002.0	0.5%
2330	Developed_Pervious	C	High	2,371.8	0.6%
2410	Developed_Pervious	D	Low	501.5	0.1%
2420	Developed_Pervious	D	Med	1,145.7	0.3%

Table 3-9. Modeled HRU distribution within the Putah Creek watershed (continued)

HRU ID	Land Use - Land Cover	HSG	Slope	Area (acres)	Area (%)
2430	Developed_Pervious	D	High	2,034.5	0.5%
3110	Barren	A	Low	4.7	0.0%
3120	Barren	A	Med	3.3	0.0%
3130	Barren	A	High	0.0	0.0%
3210	Barren	B	Low	56.7	0.0%
3220	Barren	B	Med	16.2	0.0%
3230	Barren	B	High	0.2	0.0%
3310	Barren	C	Low	14.2	0.0%
3320	Barren	C	Med	8.2	0.0%
3330	Barren	C	High	5.8	0.0%
3410	Barren	D	Low	24.7	0.0%
3420	Barren	D	Med	10.0	0.0%
3430	Barren	D	High	21.8	0.0%
4110	Forest	A	Low	40.7	0.0%
4120	Forest	A	Med	64.5	0.0%
4130	Forest	A	High	1,529.4	0.4%
4210	Forest	B	Low	198.4	0.1%
4220	Forest	B	Med	222.8	0.1%
4230	Forest	B	High	804.4	0.2%
4310	Forest	C	Low	455.5	0.1%
4320	Forest	C	Med	2,431.9	0.6%
4330	Forest	C	High	14,111.6	3.4%
4410	Forest	D	Low	151.9	0.0%
4420	Forest	D	Med	751.9	0.2%
4430	Forest	D	High	8,035.1	1.9%
5110	Scrub	A	Low	113.4	0.0%
5120	Scrub	A	Med	91.0	0.0%
5130	Scrub	A	High	147.5	0.0%
5210	Scrub	B	Low	405.7	0.1%
5220	Scrub	B	Med	517.1	0.1%
5230	Scrub	B	High	1,295.7	0.3%
5310	Scrub	C	Low	2,207.9	0.5%
5320	Scrub	C	Med	8,675.4	2.1%
5330	Scrub	C	High	29,896.9	7.2%
5410	Scrub	D	Low	1,801.2	0.4%
5420	Scrub	D	Med	9,073.2	2.2%
5430	Scrub	D	High	41,639.5	10.0%
6110	Grassland	A	Low	415.9	0.1%
6120	Grassland	A	Med	112.1	0.0%

Table 3-9. Modeled HRU distribution within the Putah Creek watershed (continued)

HRU ID	Land Use - Land Cover	HSG	Slope	Area (acres)	Area (%)
6130	Grassland	A	High	137.7	0.0%
6210	Grassland	B	Low	758.1	0.2%
6220	Grassland	B	Med	595.8	0.1%
6230	Grassland	B	High	1335.5	0.3%
6310	Grassland	C	Low	2705.4	0.7%
6320	Grassland	C	Med	6020.2	1.4%
6330	Grassland	C	High	37710.7	9.0%
6410	Grassland	D	Low	3657.5	0.9%
6420	Grassland	D	Med	13067.9	3.1%
6430	Grassland	D	High	92839.3	22.2%
7110	Pasture	A	Low	746.8	0.2%
7120	Pasture	A	Med	74.3	0.0%
7130	Pasture	A	High	75.0	0.0%
7210	Pasture	B	Low	729.7	0.2%
7220	Pasture	B	Med	267.1	0.1%
7230	Pasture	B	High	294.7	0.1%
7310	Pasture	C	Low	4271.3	1.0%
7320	Pasture	C	Med	5011.9	1.2%
7330	Pasture	C	High	10273.5	2.5%
7410	Pasture	D	Low	2940.5	0.7%
7420	Pasture	D	Med	7899.0	1.9%
7430	Pasture	D	High	31983.6	7.7%
8110	Agriculture	A	Low	886.0	0.2%
8120	Agriculture	A	Med	37.6	0.0%
8130	Agriculture	A	High	0.9	0.0%
8210	Agriculture	B	Low	1580.8	0.4%
8220	Agriculture	B	Med	179.5	0.0%
8230	Agriculture	B	High	15.6	0.0%
8310	Agriculture	C	Low	5029.9	1.2%
8320	Agriculture	C	Med	591.6	0.1%
8330	Agriculture	C	High	180.4	0.0%
8410	Agriculture	D	Low	1654.8	0.4%
8420	Agriculture	D	Med	311.1	0.1%
8430	Agriculture	D	High	234.0	0.1%
9000	Water	All	All	17973.4	4.3%
10110	Irrigation	A	Low	1053.5	0.3%
10120	Irrigation	A	Med	59.6	0.0%
10130	Irrigation	A	High	107.6	0.0%
10210	Irrigation	B	Low	3639.0	0.9%

Table 3-9. Modeled HRU distribution within the Putah Creek watershed (continued)

HRU ID	Land Use - Land Cover	HSG	Slope	Area (acres)	Area (%)
10220	Irrigation	B	Med	598.7	0.1%
10230	Irrigation	B	High	217.5	0.1%
10310	Irrigation	C	Low	6286.2	1.5%
10320	Irrigation	C	Med	2956.3	0.7%
10330	Irrigation	C	High	3624.8	0.9%
10410	Irrigation	D	Low	2381.2	0.6%
10420	Irrigation	D	Med	2078.7	0.5%
10430	Irrigation	D	High	4992.1	1.2%
			Total	**418,349.5**	**100.0%**

Color Gradient: Lowest | Low | Med | High | Highest

4 CLIMATE FORCING INPUTS

The Putah Creek watershed LSPC model uses hourly climate data forcing inputs to drive the hydrology module. In general, hydrologic models are highly dependent on the quantity and quality of meteorological input data (Quirmbach & Schultz, 2002). Conventionally, meteorological boundary conditions for stormwater modeling rely on ground-based stations across an area; however, challenges arise when trying to associate point-sampled weather station data over complex and/or large terrain (Henn et al., 2018). Model representation of precipitation in regions with low station density is susceptible to distortion when using linearized downscaling methods (e.g., Thiessen polygons).

The approach described here supplements spatial and temporal gaps in observed meteorological data with gridded meteorological products from the Parameter-elevation Regressions on Independent Slopes Model (PRISM) and North American Land Data Assimilation System-2 (NLDAS). NLDAS and PRISM are Land Surface Model (LSM) datasets with 1/8th degree and 4-km spatial resolution, respectively, which are ideal for supplementing spatial gaps in the observed station network as well as patching missing or erroneous temporal gaps in the observed time series data. The use of a hybrid approach that blends ground-based stations with remotely sensed precipitation products, i.e., increasing the rainfall gauge density over the watershed, has been shown to improve the representation of rainfall and increase forecast accuracy more than using ground-based stations alone (Kim et al., 2018; Looper & Vieux, 2012; Xia, Mitchell, Ek, Cosgrove, et al., 2012; Xia, Mitchell, Ek, Sheffield, et al., 2012). This approach has been applied for large watershed-scale modeling applications in Los Angeles County (LACFCD, 2020).

Potential evapotranspiration (PEVT) is another critical forcing input for hydrology simulation. Section 4.2 describes how PEVT was derived for this modeling effort.

4.1 Precipitation

Figure 4-1 presents a summary of the hybrid approach to blend observed precipitation with gridded meteorological products. Observed data and gridded products were first processed in parallel (1) to identify the highest quality gauge data and (2) to merge gridded products to produce continuous hourly time series. Next, gridded products were used to fill spatial and temporal gaps in the observed precipitation coverage. The final coverage shown in Figure 4-2 comprises the highest quality observed time series, supplemented by gridded products only where spatial and temporal gaps occurred in the observed coverage. The parallel processing of observed and gridded precipitation is presented in Section 4.1.1. Section 4.1.2 describes how those outputs were synthesized into the model's final set of precipitation time series.

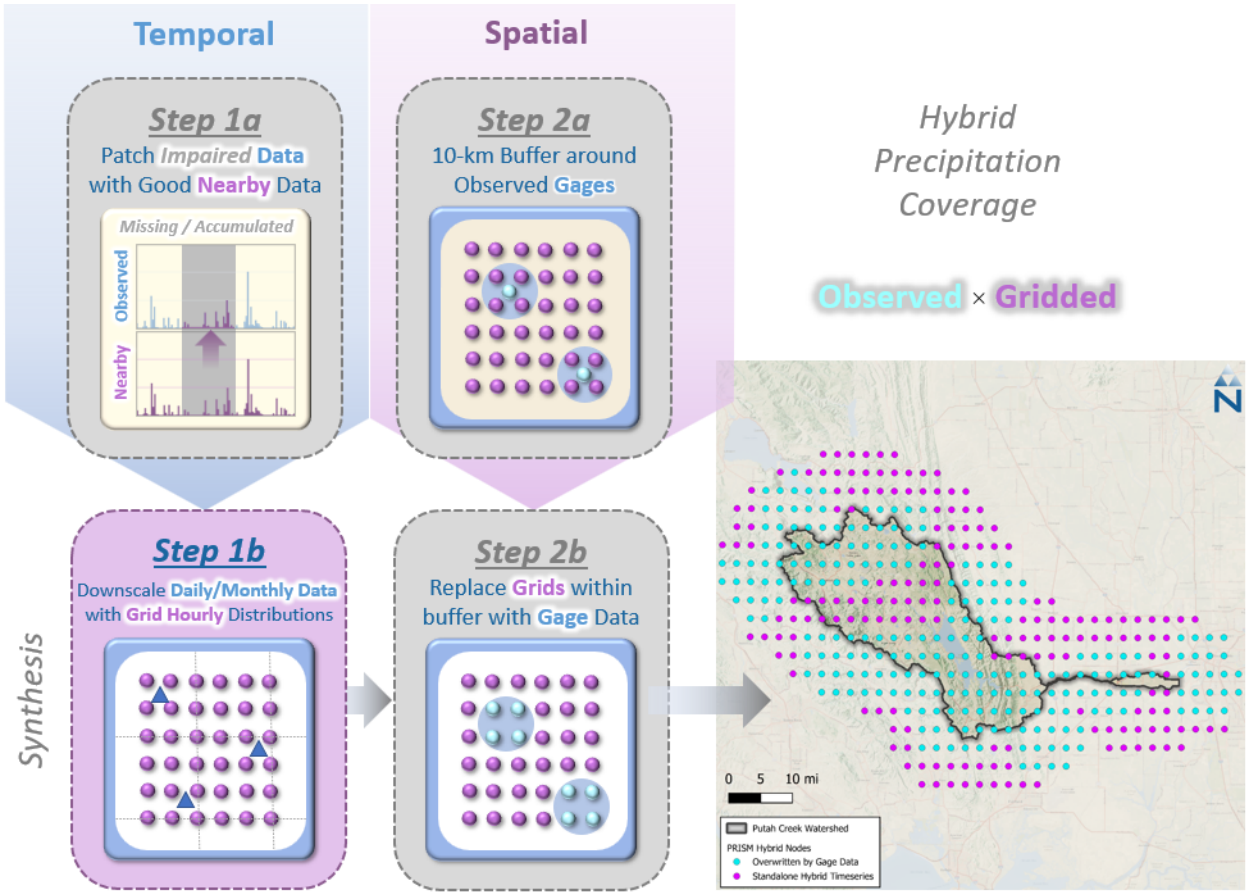

Figure 4-1. Hybrid approach to blend observed precipitation with gridded meteorological products.

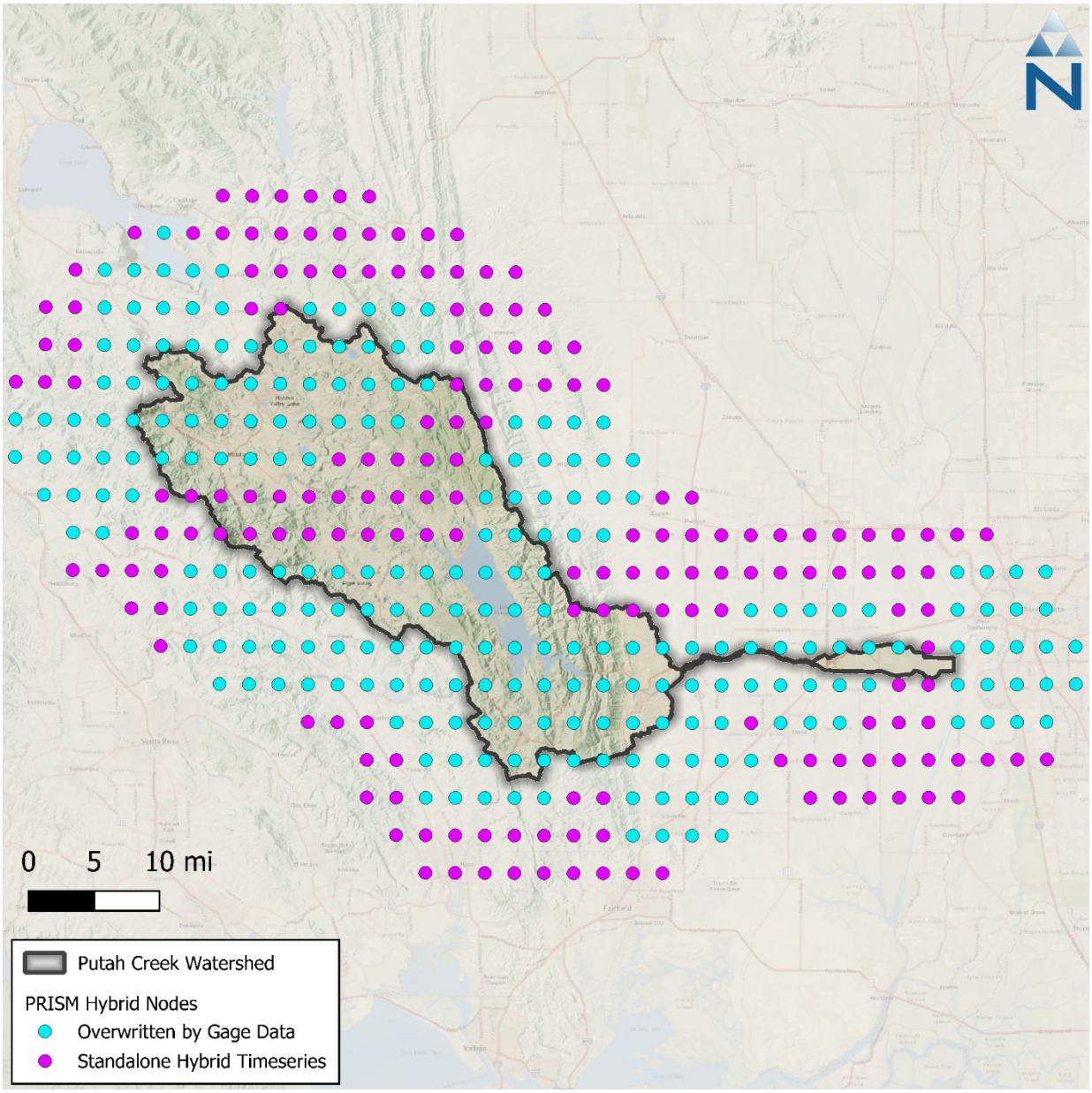

Figure 4-2. Spatial coverage of PRISM nodes by hybrid data source.

4.1.1 Parallel Processing of Observed Data and Gridded Products

Observations from 14 precipitation gauges, summarized in Table 4-1, were processed for use in the hybrid precipitation time series. These stations report daily precipitation totals, which were disaggregated to hourly based on the distribution of the nearest NLDAS grid cell, while maintaining observed daily totals. Eight of the gauges are from the Global Historical Climatology Network Daily (GHCND) database which is operated by the National Ocean and Atmospheric Association (NOAA). Six additional stations from the California Data Exchange Center (CDEC) and the Remote Automated Weather Stations (RAWS) were also used. The relationship between water year total precipitation and elevation for these stations is shown in Figure 4-3. The Putah Creek work plan had additional precipitation gauges listed, however those stations were dropped from further use as duplicates or were outside of the 10-km buffer used to create hybrid time series.

Table 4-1. Precipitation stations used to develop hybrid precipitation time series

Agency	Station ID[1]	Name	Start Date	End Date	Lat.	Long.	Elevation (meters)	Data Coverage (%)[2]
NOAA	GHCND:USW00023232	SACRAMENTO AIRPORT ASOS, CA US	11/10/1941	1/10/2025	38.51	-121.50	5.9	96%
	GHCND:USC00040212	ANGWIN PACIFIC UNION COLLEGE, CA US	12/31/1939	Present	38.57	-122.44	522.7	92%
	GHCND:USC00042294	DAVIS 2 WSW EXPERIMENTAL FARM, CA US	12/31/1892	Present	38.53	-121.78	18.3	92%
	GHCND:USC00044673	LAKE BERRYESSA, CA US	5/31/2005	7/31/2008	38.58	-122.25	138.7	100%
	GHCND:USC00044712	LAKE SOLANO, CA US	7/31/1975	Present	38.50	-122.00	57	99%
	GHCND:USC00045360	MARKLEY COVE, CA US	2/28/1970	Present	38.49	-122.12	146.3	99%
	GHCND:US1CALK0018	HIDDEN VALLEY LAKE 2.7 W, CA US	3/17/2021	Present	38.81	-122.57	355.7	99%
	GHCND:US1CANP0003	CALISTOGA .4 SSE, CA US	2/11/2009	Present	38.58	-122.58	106.1	94%
CDEC	ATL	ATLAS PEAK	1/1/1987	Present	38.49	-122.25	506.0	--
	WSP	WHISPERING PINES	1/1/1987	Present	38.81	-122.71	823.0	--
RAWS	ATLC1	ATLAS PEAK	1/20/2011	Present	38.47	-122.27	589.5	--
	BRO	BROOKS CALIFORNIA, CA US	5/2/1990	Present	38.74	-122.14	354	--
	KNO	KNOXVILLE CREEK CALIFORNIA, CA US	5/23/1985	Present	38.86	-122.42	670.6	--
	KON	KONOCTI CALIFORNIA, CA US	3/20/1995	Present	38.91	-122.70	659.3	--

1. Stations presented have at least 90% reported data coverage.
2. NOAA data coverage as reported; CDEC and RAWS estimated based on data flagging and count of time steps.

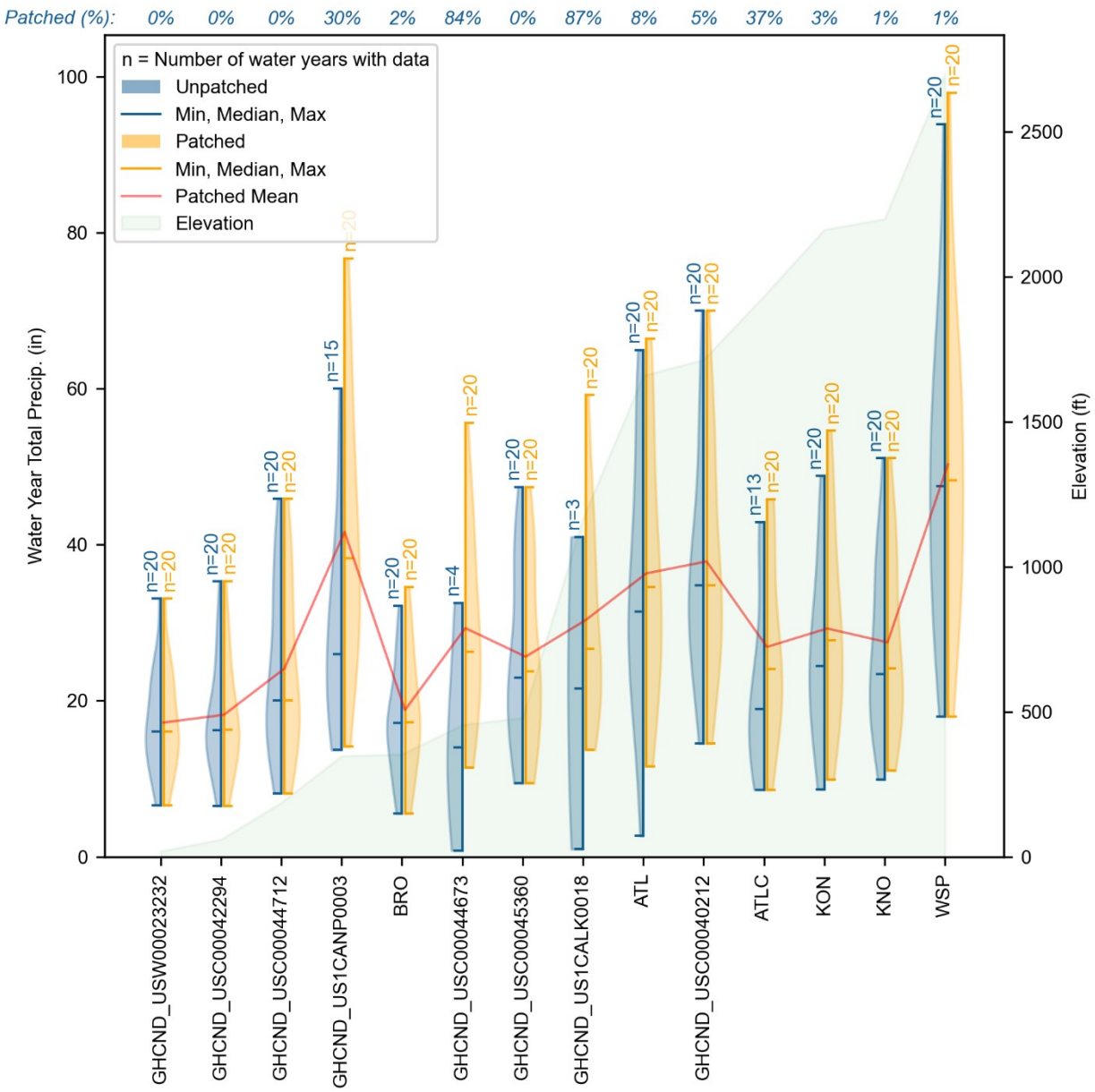

Figure 4-3. Water year precipitation totals and elevation of selected precipitation stations for 2004 - 2023.

The gridded meteorological products were processed in parallel with the observed data and used to patch spatial and temporal gaps in the observed data record, as shown in Figure 4-3. PRISM monthly precipitation time series data are available at a 4-km spatial resolution across the conterminous United States (Daly et al., 1994, 1997; Gibson et al., 2002). PRISM combines point data and spatial datasets (primarily DEMs) via statistical methods to generate estimates of annual, monthly, and event-based precipitation in a gridded format from as early as 1961 (Daly et al., 2000). PRISM has undergone several iterations of refinement, extensive peer review, and performance validation through case study applications.

NLDAS is a quality-controlled meteorological dataset designed specifically to support continuous simulation modeling activities (Cosgrove et al., 2003; Mitchell et al., 2004). NLDAS provides hourly predictions of meteorological data at a 1/8th degree spatial resolution for North America

(approximately 13.8-kilometer intervals), with retrospective simulations beginning in January 1979. For this model, hourly NLDAS precipitation distributions were mapped to the nearest PRISM grid cell and used to disaggregate the monthly PRISM totals to hourly—the resulting set of gridded precipitation time series reflects monthly PRISM totals that have hourly distributions from the nearest NLDAS grid. Using monthly PRISM totals with hourly NLDAS, as opposed to daily PRISM totals, eliminates the need to estimate distributions for occasional but rare instances where an hourly distribution does not coincide with a daily total.

4.1.2 Synthesis of Observed Data and Gridded Products

Where available, observed precipitation data were preferentially selected over gridded data where data quantity and quality were adequate. Impaired intervals are gaps in the observed record flagged as missing, deleted, or accumulated rainfall. Gridded time series are used to patch impaired intervals as follows. First, a 10-km buffer was created around each of the observed gauges that were prescreened for quality. Next, the 10-km gauge buffer was intersected with the PRISM grid layer. The time series at any grid falling within the buffer is ultimately overridden by the associated observed gauge time series, except for impaired intervals, where the gridded data are retained to patch those temporal impairments. Consequently, most of the observed data at a PRISM grid location will be identical to a neighboring grid within a 10-km buffer of the gauge but will have slightly different PRISM time series for impaired intervals.

After the creation of the hybrid precipitation time series, each catchment is assigned a time series based on the Thiessen polygon its centroid falls within. Figure 4-4 illustrates the final assignment of gauge-based or LSM-based hybrid time series by catchment. Figure 4-5 shows the distribution of monthly total precipitation across all hybrid time series within the watershed and Figure 4-6 illustrates the spatial distribution of annual average precipitation from the hybrid time series by catchment.

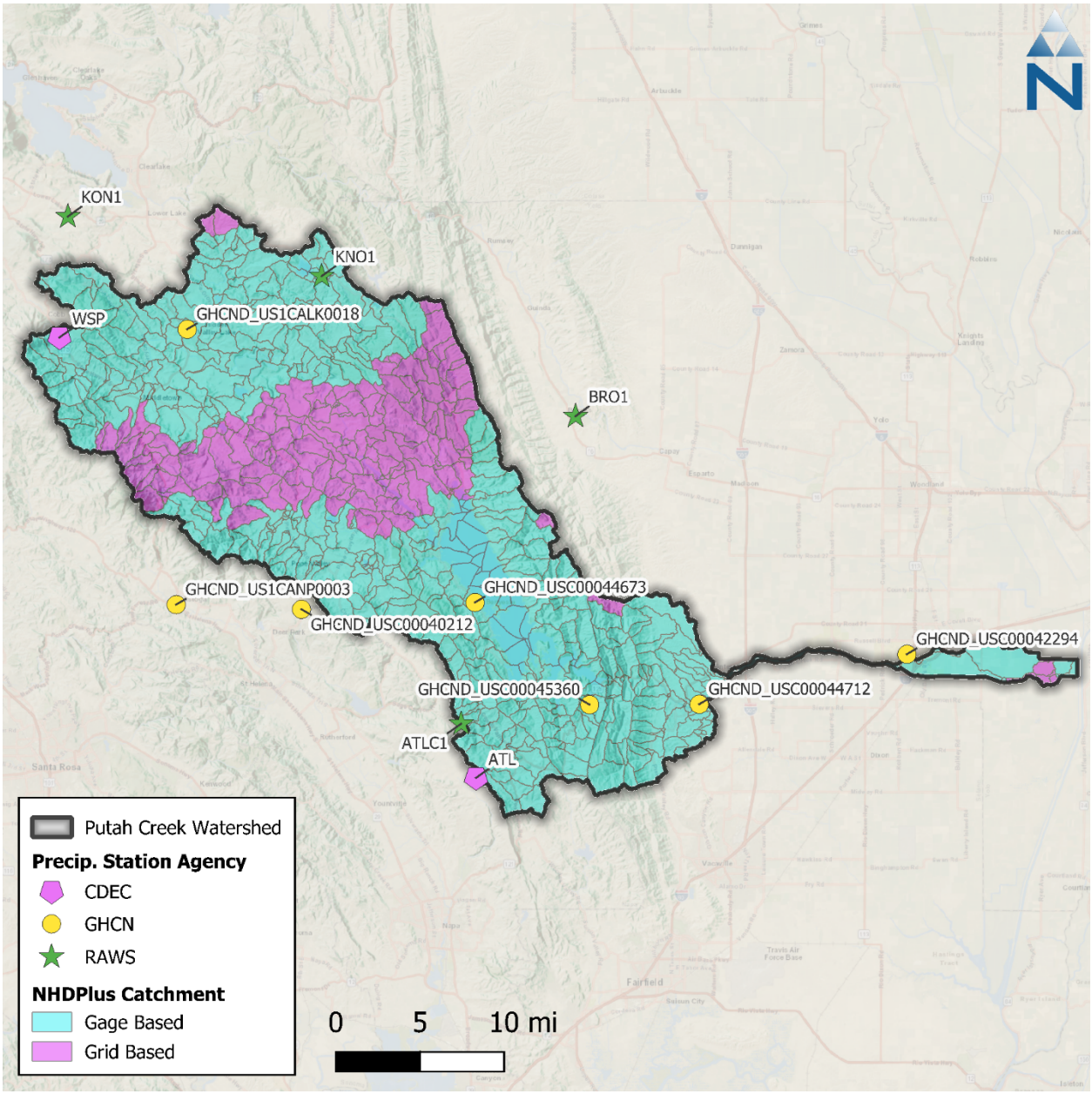

Figure 4-4. Final spatial coverage of precipitation time series by catchment.

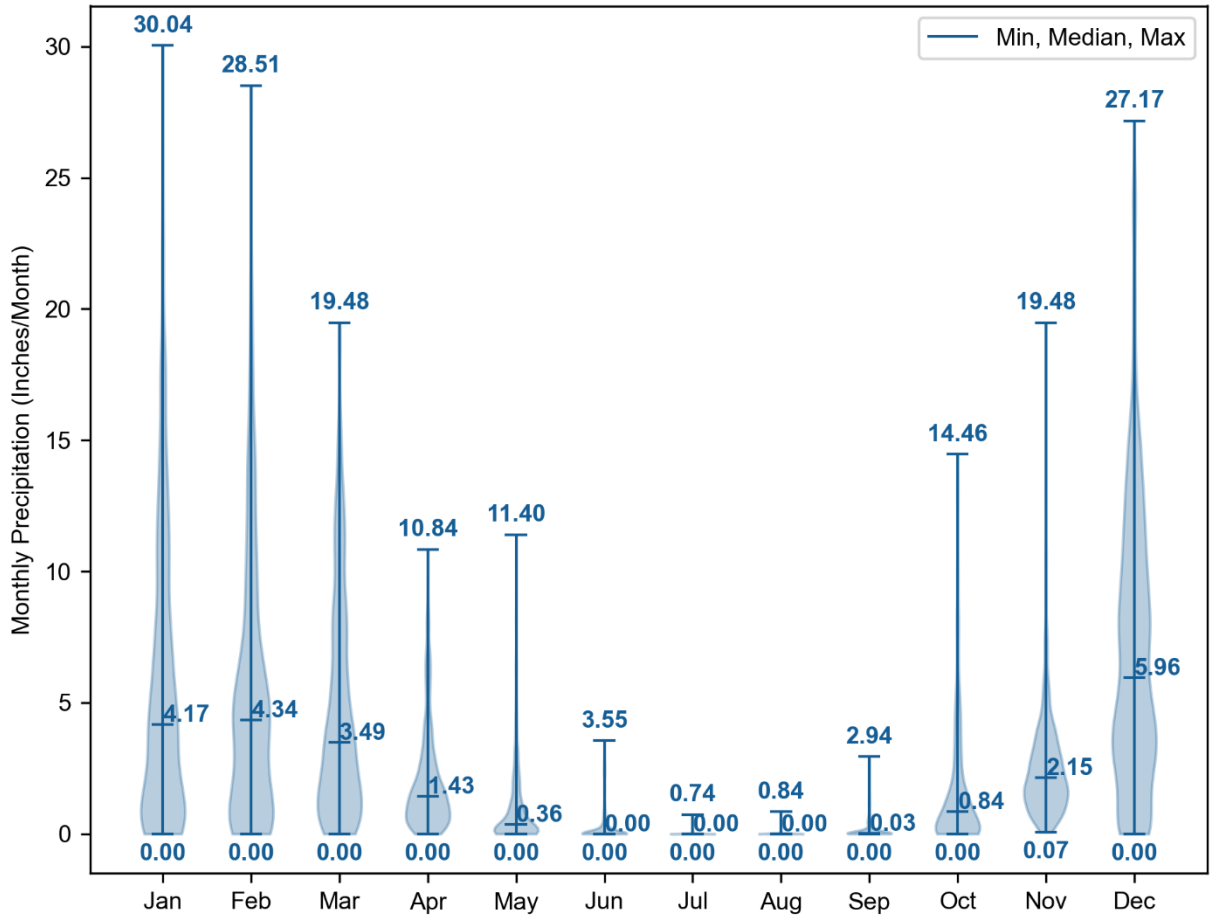

Figure 4-5. Distribution of monthly total precipitation across all hybrid time series within the Putah Creek watershed for Water Years 2004-2023.

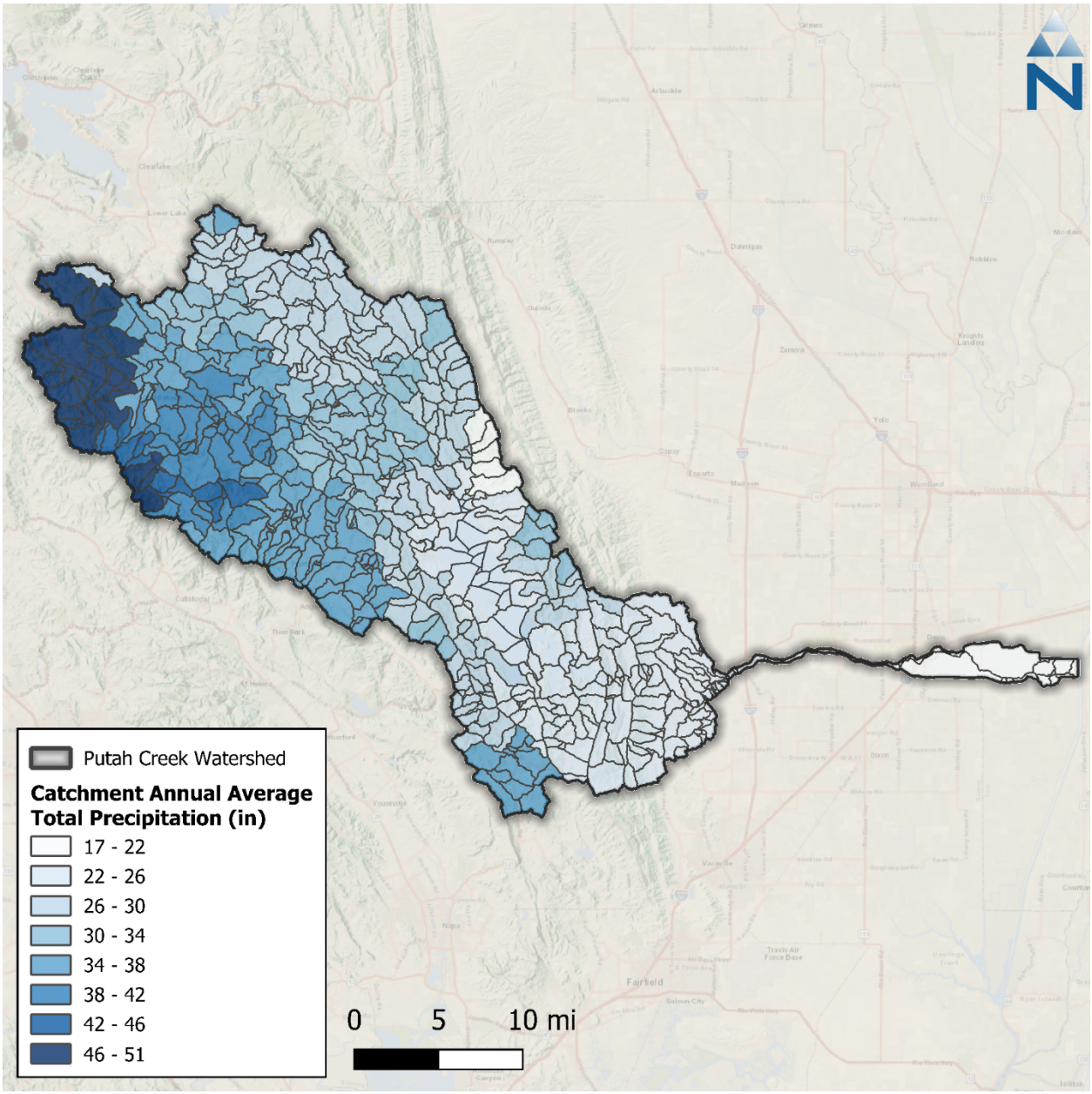

Figure 4-6. Annual average hybrid precipitation totals by catchment from Water Years 2004-2023.

4.2 Potential Evapotranspiration

In addition to precipitation, potential evapotranspiration forcing input time series were created and assigned to each catchment. Daily total reference evapotranspiration (ET_o) from the California Irrigation Management Information System (CIMIS) Spatial dataset was downscaled to hourly using the NLDAS hourly solar radiation. CIMIS Spatial expresses daily ET_o estimates calculated at a statewide 2-km spatial resolution using the American Society of Civil Engineers version of the Penman-Monteith equation (ASCE-PM). This product provides a consistent spatial estimate of ET_o that is California-specific, implicitly captures macro-scale spatial variability and orographic influences, is available from 2004 through the Present, and is routinely updated. Within each catchment, actual ET is calculated for each Hydrologic Response Unit (HRU) during the model simulation as a function of parameters representing differences in vegetation (type, height, and

density) and soil conditions. Figure 4-7 shows the distribution of monthly total ET_o across all grid points within the watershed. Figure 4-8 shows the spatial distribution of CIMIS annual average total ET_o across the watershed.

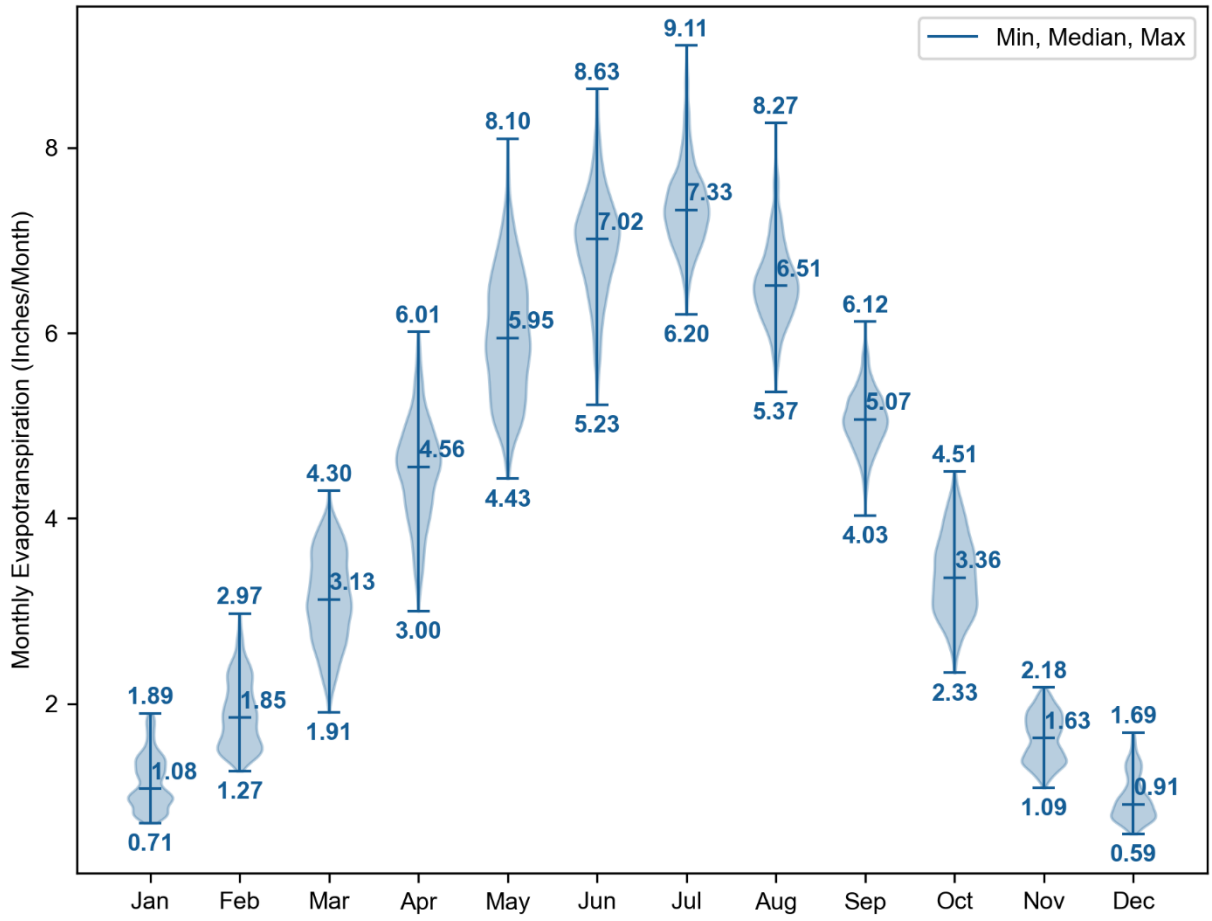

Figure 4-7. Distribution of monthly total ETo across all CIMIS spatial grid points within the Putah Creek watershed from Water Years 2004-2023.

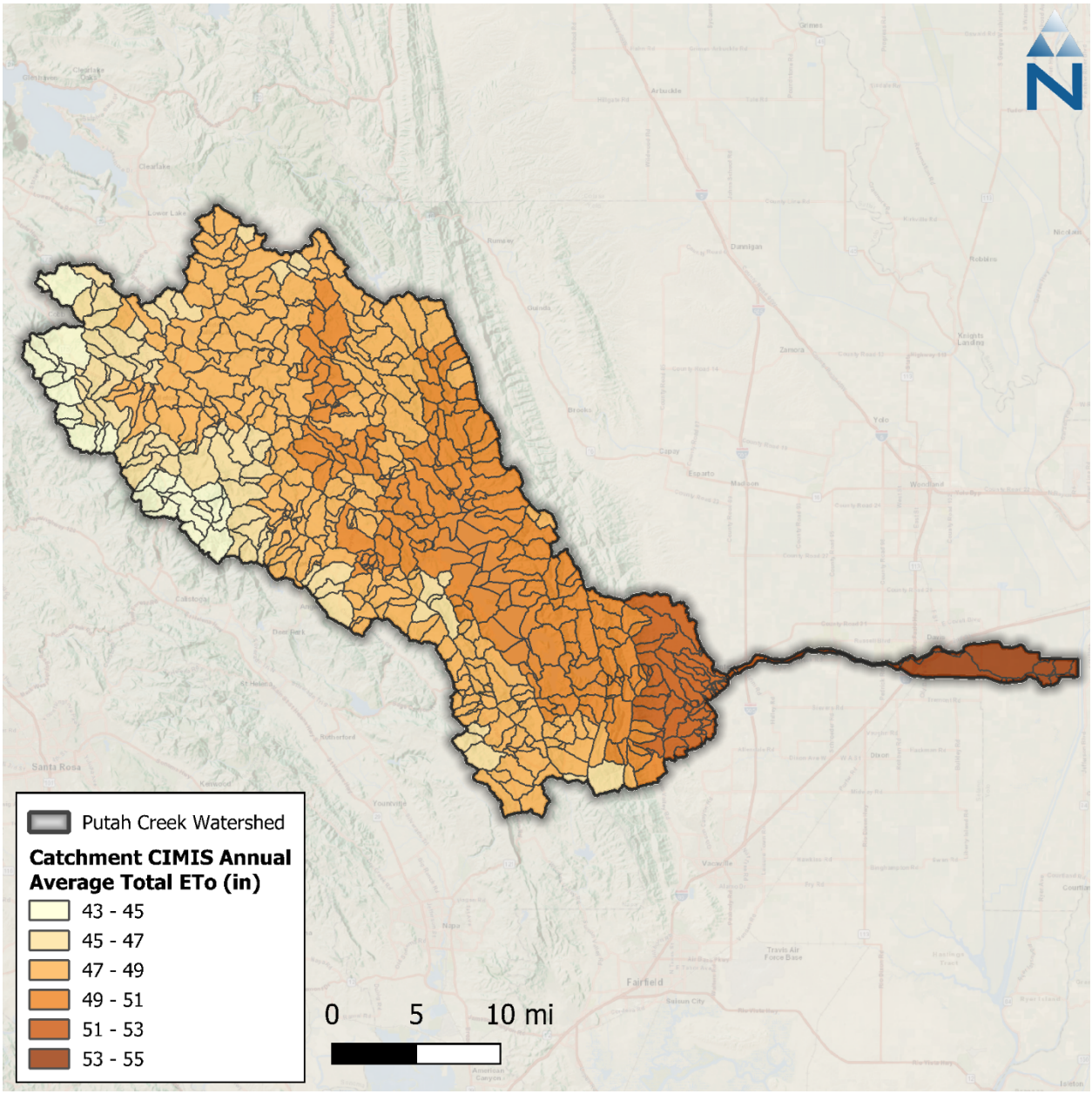

Figure 4-8. CIMIS annual average total ET_o by catchment within the Putah Creek watershed.

5 SURFACE WATER WITHDRAWALS

Datasets related to water rights, points of diversion (PODs), and water use were identified through the Water Board's eWRIMS database and a University of California Cooperative Extension (UCCE) study assessing agricultural water needs in the nearby Navarro River and Russian River watersheds (McGourty et al., 2020). These data were used to represent diversions and withdrawals in the watershed model. Monthly data from 809 active water rights within the Putah Creek watershed from 2017 to 2023 were received from the Board's Supply and Demand Unit staff. Of these, 704 had reported withdrawals; surface water withdrawals from these active water rights occur from 932 PODs as illustrated in Figure 5-1. By count, water usage is roughly evenly split between Irrigation (40%) and Other (42%) (Figure 5-2). Here, the 'Other' category groups the dust control, stock-watering, and fish and wildlife preservation and enhancement primary uses. By volume however, the Municipal category accounts for more than two-thirds of usage (70%) with Other and Irrigation making up much of the remainder (26% and 3%, respectively).

For the non-irrigated water demand, the received monthly data in acre-feet are summed by catchment and then converted to a flow rate for withdraw from the appropriate catchment's modeled reach segment. Irrigation demand is similarly converted from monthly volume into a withdraw rate by application number. These water demand data are added to the LSPC model as surface water withdraws from the appropriate reach segments based on the following considerations.

- Diversions were classified based on primary usage (irrigation, municipal, industrial, recreational, etc.) as well as by allocation type (direct and storage).
- During simulations, diverted streamflow was routed out of the system to represent the different usages (i.e. irrigation).
- For instances where PODs in different catchments share the same application/permit number, water demand was proportionally distributed based on the magnitude of upstream drainage area.

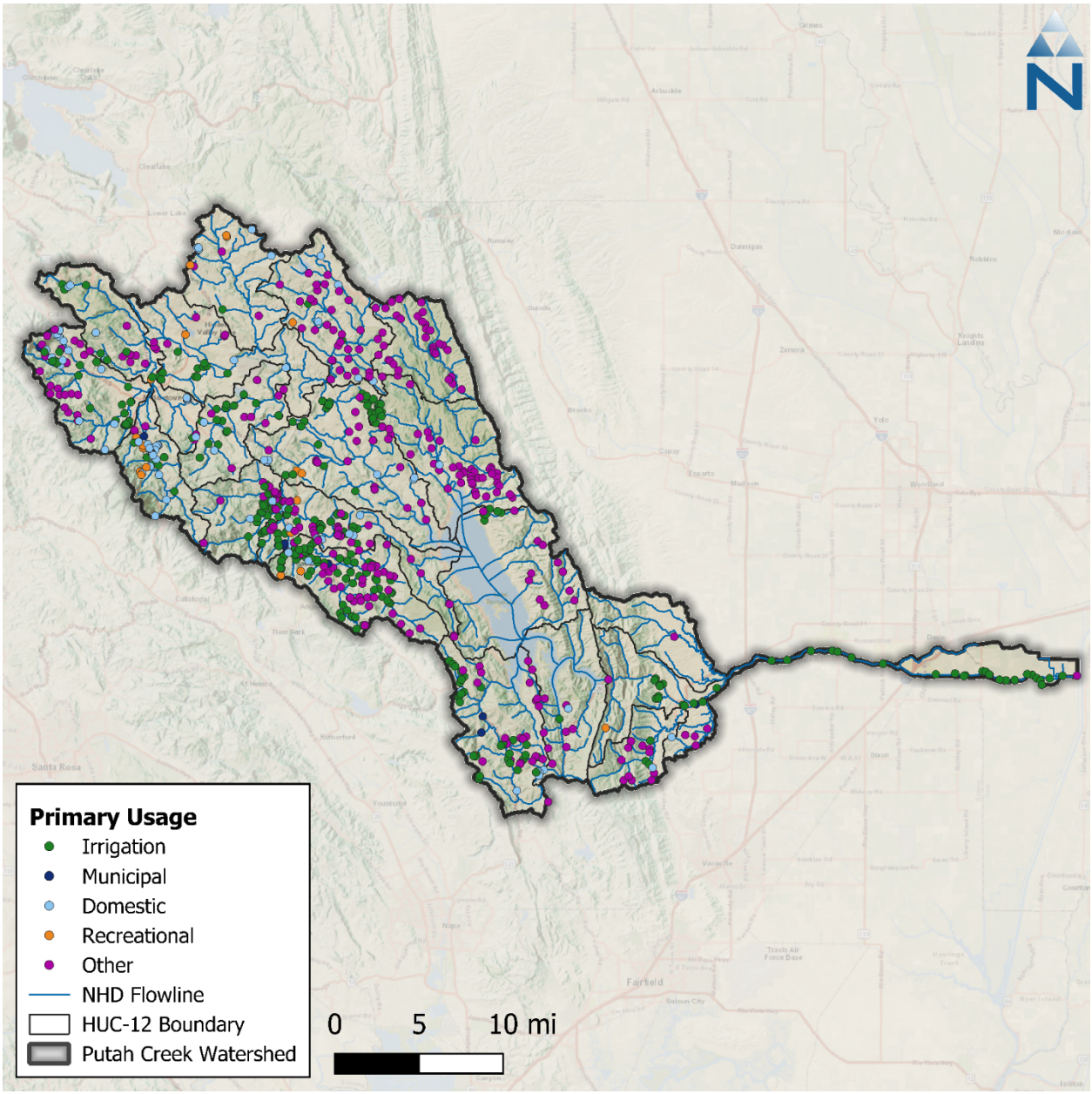

Figure 5-1. Points of diversion within the Putah Creek watershed.

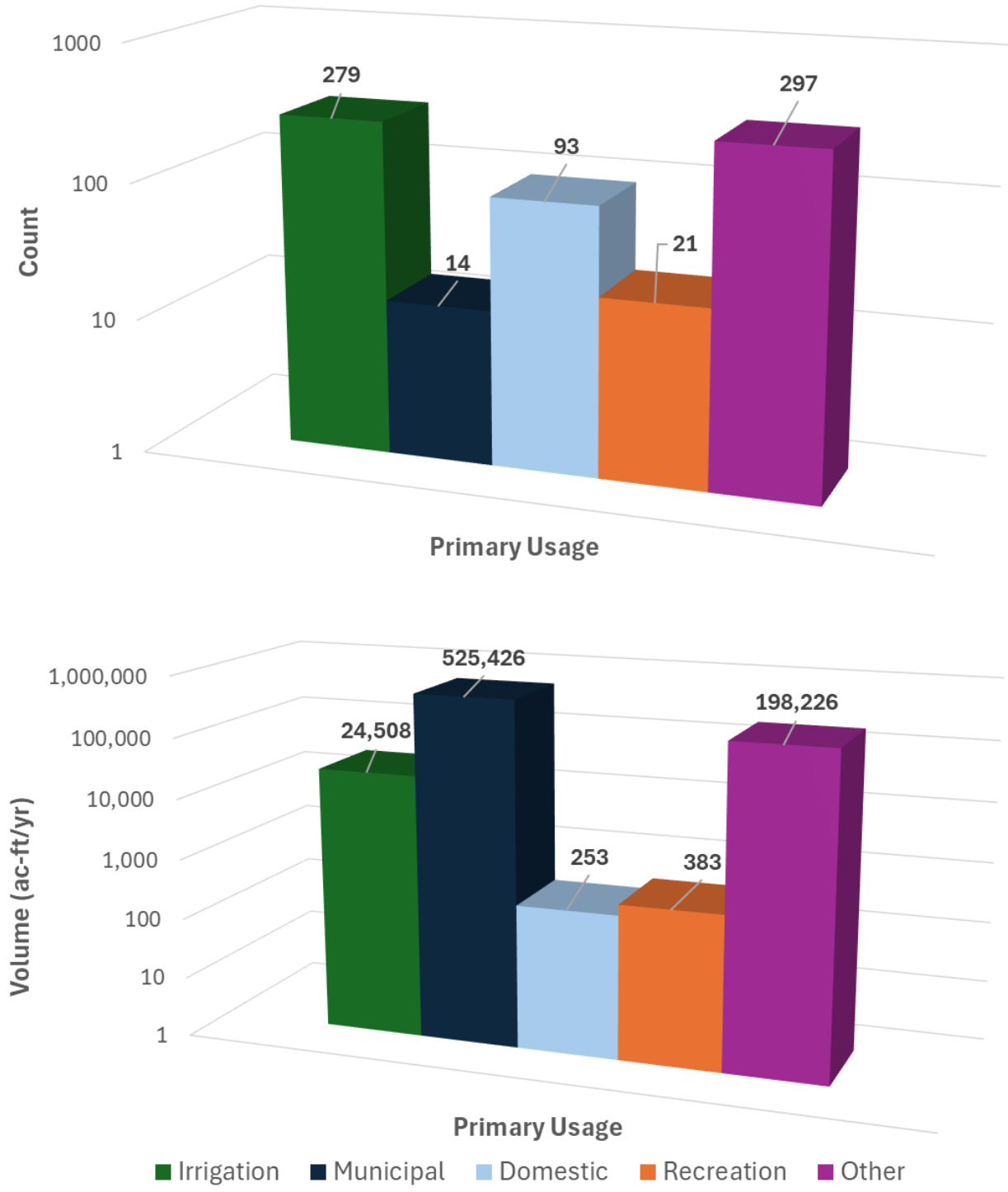

Figure 5-2. Primary water usage for points of diversion within the Putah Creek watershed. Note that these are presented on a log scale.

5.1 Irrigation

The LSPC irrigation module is designed to streamline the spatial and temporal representation of water demand, irrigation application, and associated return flows. In practice, irrigation demand is estimated as the deficit of precipitation from the product of a crop-specific evaporative coefficient (ET_c) and reference evapotranspiration (PEVT). This LSPC configuration uses a similar approach but instead works backwards to estimate the monthly crop coefficients for agricultural HRUs by using observed irrigation demand and climate data. Those crop coefficients are then used with observed climate data to calculate irrigation application rates during LSPC simulations. The equation used to calculate monthly evaporative crop coefficients for agricultural HRUs is shown as Equation 2:

$$V_{irr} = (PET \times ET_c - PREC) \times A_{irr} \qquad \text{Equation 2}$$

where (V_{irr}) is the volume of irrigation demand in acre-feet, (A_{irr}) is the cropland being irrigated in acres, (PET) is the reference evapotranspiration depth in feet, ET_c is the crop-specific evaporative coefficient, and ($PREC$) is the observed precipitation depth in feet. As mentioned above, irrigation demand was inferred from stream diversion records for each catchment. Because the exact location of irrigated vs. non-irrigated parcels was unknown, it was assumed that agricultural land located in catchments immediately draining to reach segments with irrigation PODs were irrigated.

The process for representing irrigation in the Putah Creek watershed is summarized by the following steps:

1. Estimate irrigation demand.
2. Define irrigated hydrologic response units.
3. Calculate crop evaporative coefficients.

5.1.1 Estimation of Irrigation Demand

Irrigation demand was inferred from eWRIMS stream diversion data for records between 2017 and 2023. For each LSPC catchment, the total monthly irrigation demand was estimated as the sum of all irrigation-associated stream diversions. As mentioned above, stream diversions were either directly used for the application or routed to a storage facility for later use. Due to data limitations, it was unknown exactly when and how stored streamflow was used for irrigation; however, because direct diversion is higher during the growing season and closely follows PEVT, it was assumed that irrigation of stored water would also follow a similar pattern that scales in proportion to evaporative demand, which is higher during the warmer and drier growing season. Figure 5-3 shows average monthly diversion volumes vs. potential evapotranspiration.

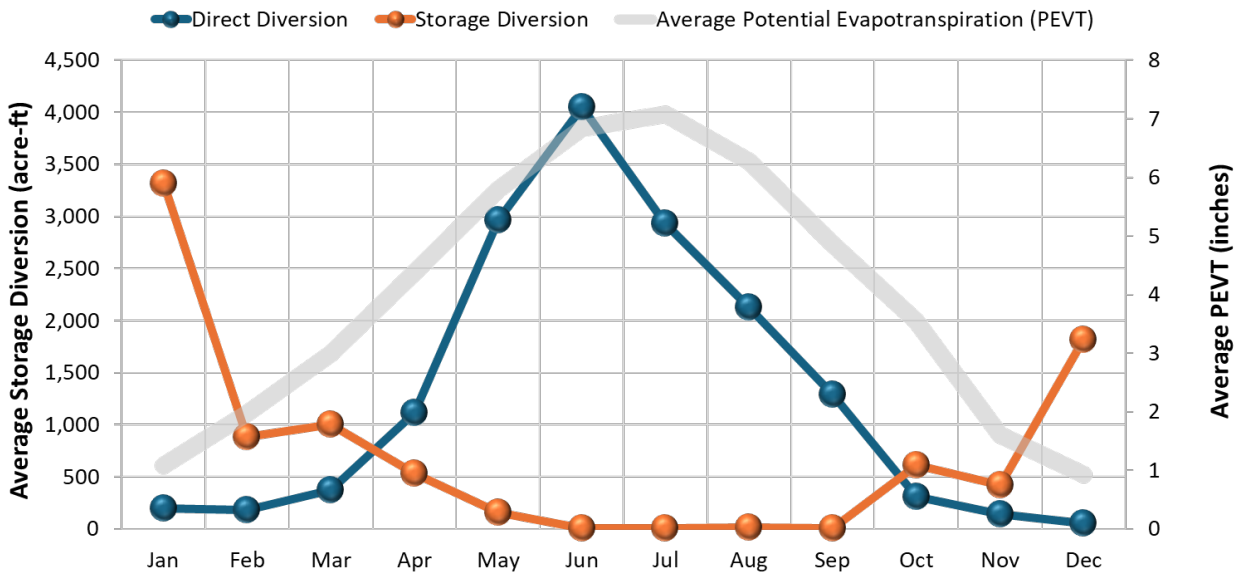

Figure 5-3. Total reported direct and storage diversions vs. average potential evapotranspiration.

5.1.2 Defining Irrigated Hydrologic Response Units

The LSPC model simulates irrigation on a unit-area basis. Agricultural and Pasture HRUs were partitioned into irrigated and non-irrigated HRU counterparts, as previously described in Section 3.6. Because the exact location of irrigated vs. non-irrigated parcels was unknown, it was assumed that agricultural and pastural land located in catchments immediately draining to reach segments with irrigation PODs were irrigated; 120 out of the 669 catchments were irrigated.

As shown in Figure 5-4, the sum of all croplands, pasture, and grassland areas represents nearly two-thirds (63%) of the watershed and could potentially be irrigated. Of that area, 20% is within the catchments with irrigation. The "Irrigated" area, where the modeled unit-area response is applied, is nearly 28,000 acres—about 6.7% of the Putah Creek watershed, as shown in Figure 5-5. For the unit-area model representation, it was assumed that 50 percent of irrigation water was applied as sprinkler and 50 percent as flood irrigation. Sprinkler irrigation enters the model at the same layer as precipitation, making it subject to interception storage and associated evaporation. Flood irrigation enters the model below interception storage and is only subject to surface ponding and infiltration.

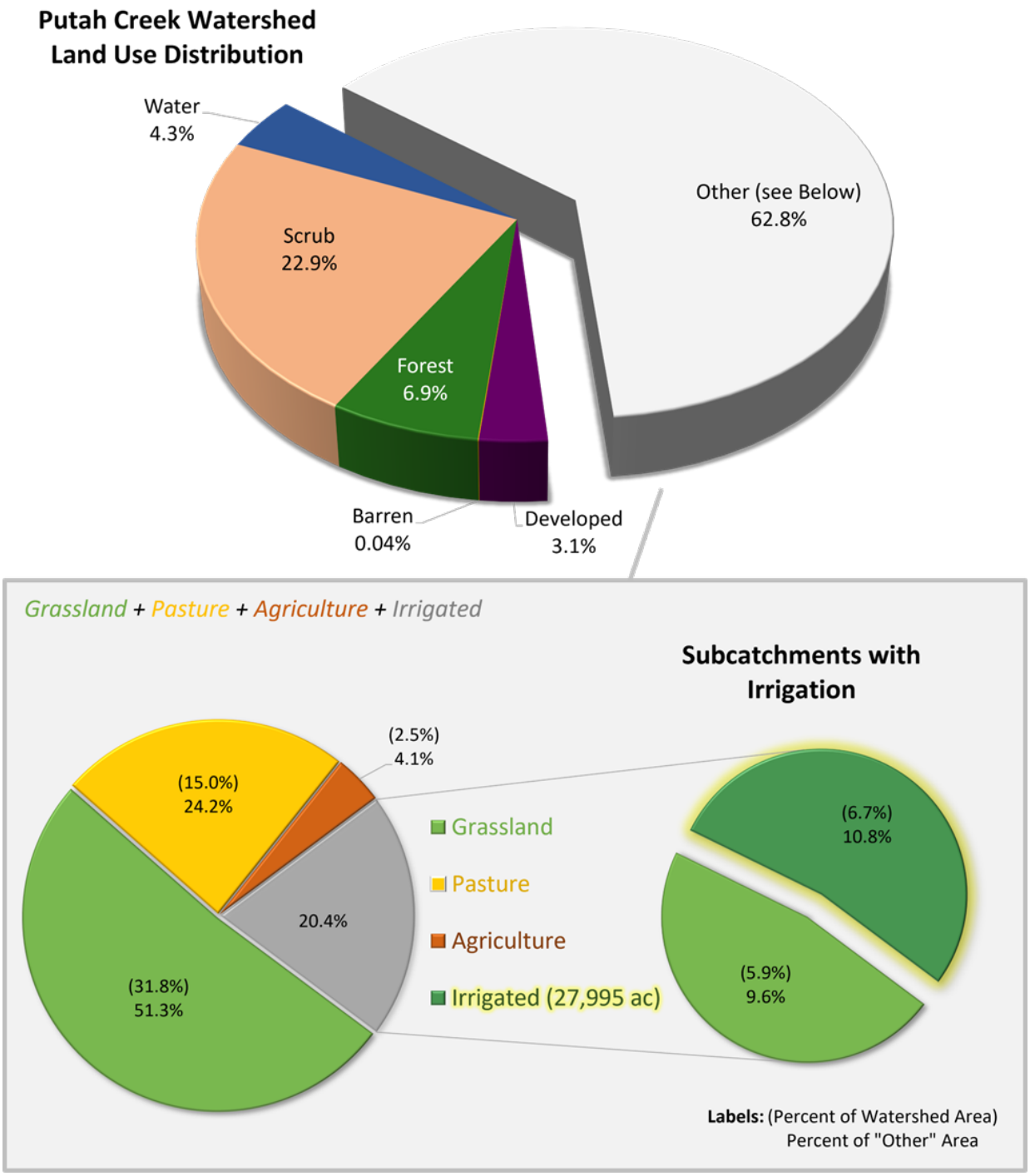

Figure 5-4. Irrigated area as a subset of the Putah Creek watershed.

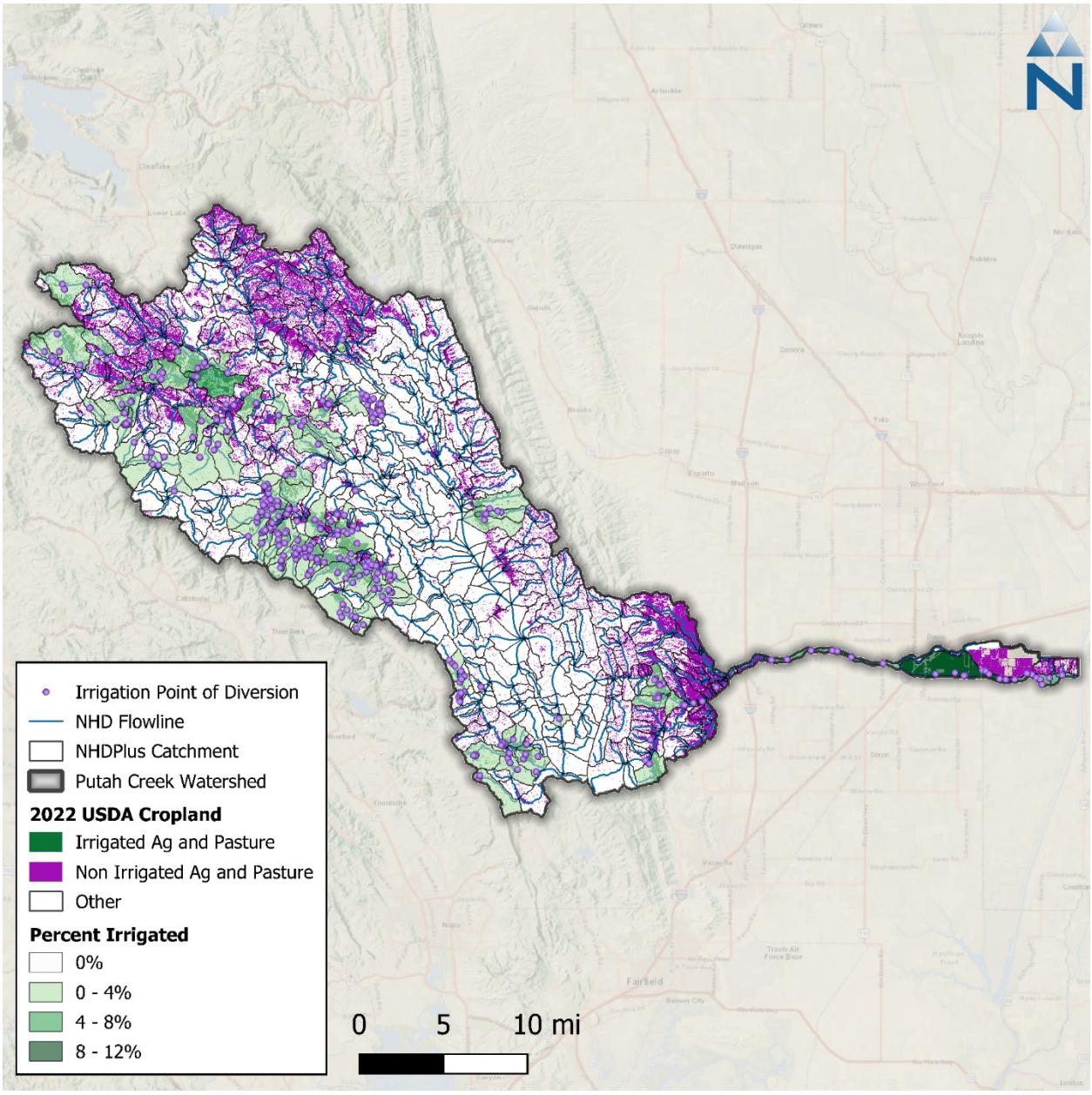

Figure 5-5. Irrigated and non-irrigated agriculture and pasture areas within the Putah Creek watershed.

5.1.3 Calculation of Crop Evaporative Coefficients

Crop evaporative coefficients (ET_c) are used to adjust reference evapotranspiration rates to better represent an evaporative demand for a specific vegetation type. In the absence of high-resolution irrigation data, this crop-specific evaporative demand can be used with observed precipitation and PEVT data to predict irrigation demand. For this LSPC model instance, distinct crop types were not represented in hydrologic response units; therefore, one value of crop evaporative coefficient per calendar month was used to represent all irrigated areas. Storage occurs in the wetter winter/spring months. Direct diversion is higher during the growing season and closely follows PEVT.

The coefficients used in the model were derived by optimizing ET_c in Equation 2 using Microsoft Excel solver to match total irrigation demand volume (V_{irr}) with the total withdrawal volume for

irrigation use. Initial estimates for these coefficients are provided in Table 5-1. Storage diversion and management were not explicitly modeled. By using these coefficients, it was assumed that the same total water diverted for irrigation (storage + direct diversion) was eventually irrigated in proportion to monthly potential evapotranspiration. However, these estimates are subject to change during streamflow calibration to improve the water balance.

Table 5-1. Estimated crop evaporative coefficients (ET_c) by month

Jan	Feb	Mar	Apr	May	Jun	Jul	Aug	Sep	Oct	Nov	Dec
0.481	0.113	0.090	0.121	0.229	0.317	0.372	0.380	0.360	0.370	0.295	0.393

6 RESERVOIR OPERATIONS

Much of the Putah Creek watershed drains into Lake Berryessa, which controls most flows out of the watershed. Lake Berryessa, the seventh largest reservoir in California, is an important source of water in the region and is managed by the Solano County Water Agency (SCWA) and its partners. The primary source of outflow from the lake is water used for hydroelectric power generation, irrigation by water rights holders, and to sustain environmental flows downstream of Monticello Dam (Figure 6-1). When the lake level reaches approximately 440 feet NGVD29 (National Geodetic Vertical Datum of 1929), water also flows over the spillway and outfalls below the dam (Figure 6-2). As described in Section 5, there are also some PODs from Lake Berryessa; these are modeled as surface water withdrawals.

Within LSPC, outflow from Lake Berryessa is represented by two components: (1) a functional table (F-table) and (2) a "Reach Operations" table. The F-table relates reservoir depth to surface area, storage volume, and outflow and is modeled at the most downstream catchment of the lake (ID 8016105), which corresponds with the dam. The depth-area-storage relationship shown in Figure 6-3 is from a bathymetric study of the lake (SCWA 2009). There are 18 outlets represented in the F-table. The first outlet represents spillway overflow based on the relationship between observed lake level and outflow derived from daily observations when the spillway is active as measured at the CDEC Lake Berryessa station (BER) from January 1, 2000 to February 11, 2025. The remaining 17 outlets are used to represent the 'non-spillway' observed daily outflow from the dam. These outlets are constant outflow values that are toggled between open and closed using the Reach Operations table. The outlet flow rates were stratified between 600 and 0.1 cfs so that the maximum observed outflow was achieved by turning on all the outlets, while the minimum flow rate was achieved by turning on only the smallest outlet. The best-fit combination of F-table outflows was then optimized to fit the observed reservoir releases by turning on different combinations of the 17 outlets. The Reach Operations table allows outlets to be toggled uniquely for each day in the simulation—the average daily release rates shown in Figure 6-4 were used for days missing observed outflow (0.6% of all days between January 2000 – February 2025 and only 1 day within the simulation period [WY 2004 – 2023]). The average daily release rates can also be used for extending intervals before and after available observed data.

Figure 6-1. Face of Monticello Dam and outflow (photo taken June 4, 2025).

Figure 6-2. Lake Berryessa spillway (photo taken June 4, 2025).

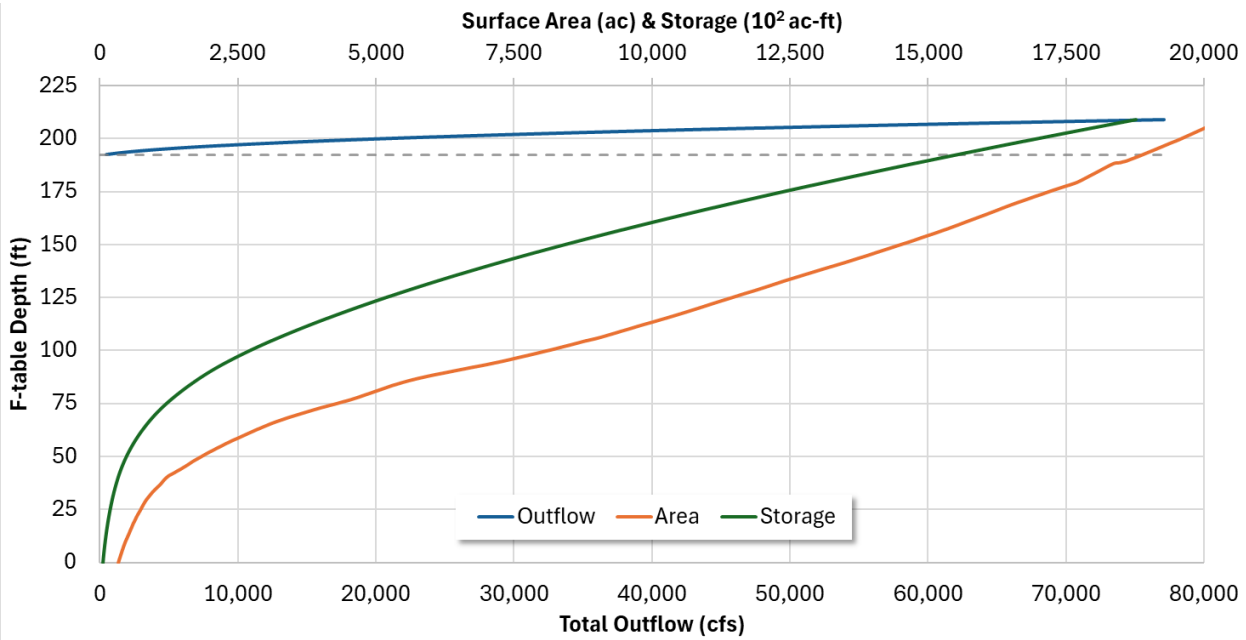

Figure 6-3. F-table data representing depth - surface area – storage relationship for Lake Berryessa with total spillway outflow estimated from observations. Note that outflow for lake levels below the spillway are represented in conjunction with the Reach Operations table.

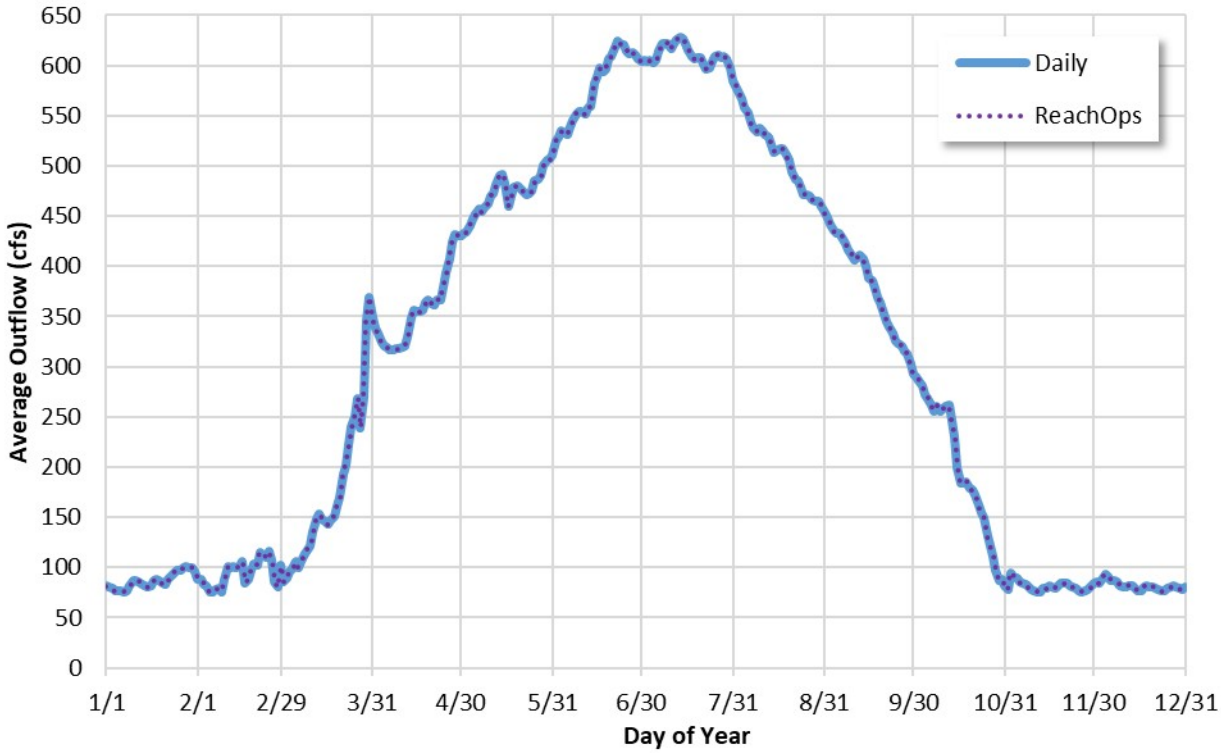

Figure 6-4. Daily average observed outflow from Lake Berryessa, excluding days with spillway flow, and outflows simulated with the Reach Operations table.

A total of 69 catchments intersect the lake boundary as defined by the NHD waterbodies data set (NHDPlus Hydrography, 2022), as shown in Figure 6-5. Within these catchments, "Water" HRU area is not simulated in the model and reach length is set to zero, but routing is preserved. The F-table supplies the lake surface area over which LSPC simulates direct rainfall and evaporation; therefore, these processes are not simulated at the catchment-HRU level. Routing through the lake is simulated using a representative length calculated by summing the NHDPlus reach segments from the top of the lake where Eticuera Creek enters to the dam (approximately 17.5 mi).

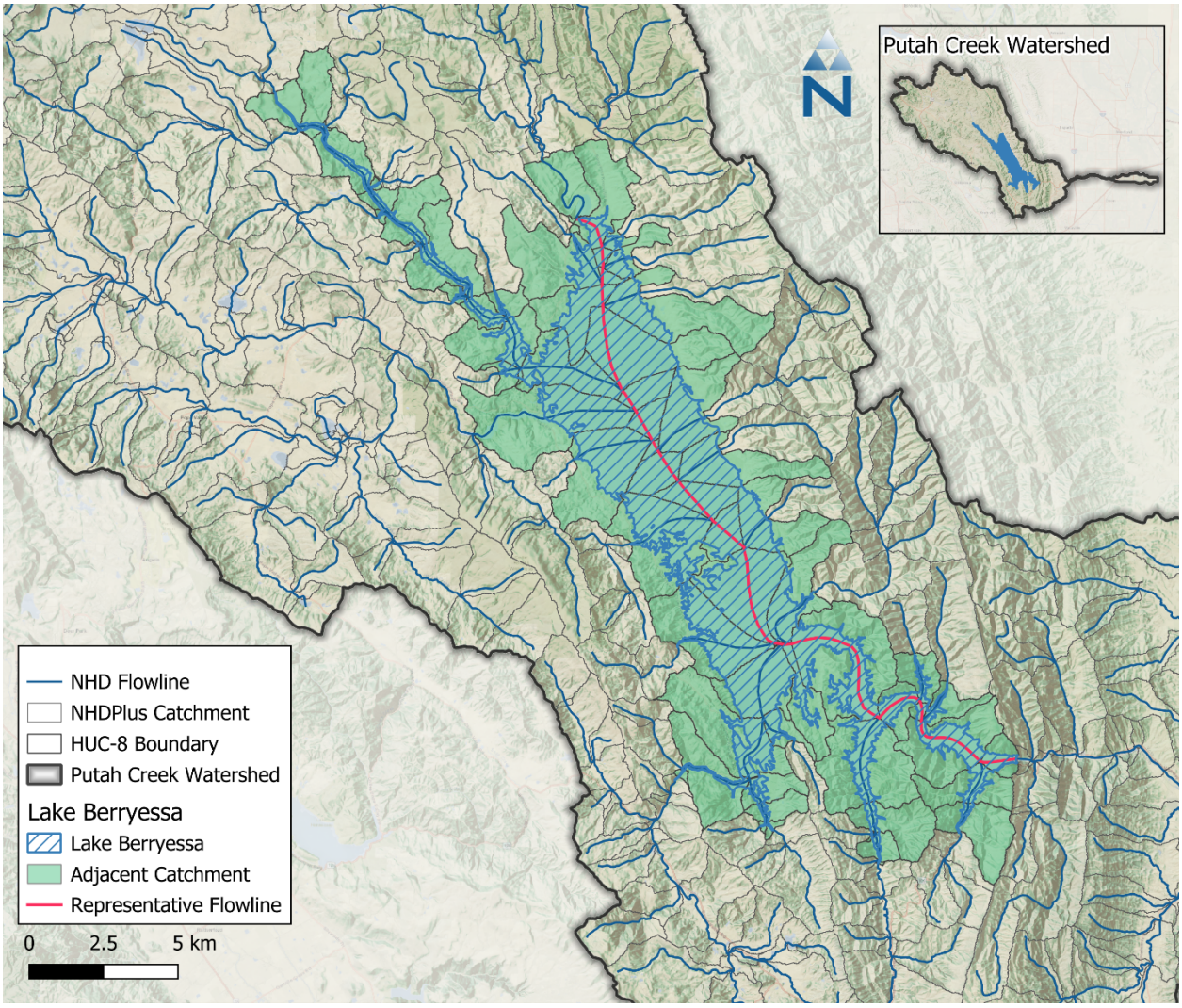

Figure 6-5. Lake Berryessa catchments within the Putah Creek Watershed.

7 OBSERVED WATER BALANCE

A water balance analysis was conducted using the primary observed data to explore the hydrological behavior of the Putah Creek watershed. For this analysis, precipitation (as described in Section 4.1) is assumed to be the primary source of water while potential evapotranspiration (as described in Section 4.2) and streamflow are the primary sinks. Streamflow is retrieved from two USGS stations: Putah Creek near Guenoc (USGS 11453500) and Putah Creek near Winters (USGS 11454000). These stations are detailed in Table 7-1 and shown in Figure 7-1. The Guenoc station is nested within the drainage area of the Winters station and represents one-fifth of its area (20%). The Winters station is below Lake Berryessa, which controls essentially all flows to this station.

The water balance components are spatially and temporally aggregated over each station's drainage area for the 20-year period from October 2003 through September 2023. The water year total volumes for this period are shown in Table 7-2 and Table 7-2 for the Guenoc and Winters stations, respectively. These tables include the percentile ranking of each WY by precipitation total, which helps illustrate the long-term pattern of wet and dry years. Because PET is based on the CIMIS reference ET, these tables also include an estimated actual ET value, which is calculated as the difference between precipitation and streamflow; note that this value can include other unknown storages and losses.

For the Guenoc station, streamflow makes up 52% of outflow on average, while estimated ET and other storages/losses account for the remainder. For the Winters station, the storage change and streamflow, which is essentially all outflow from Lake Berryessa, were used to estimate lake evaporation and other losses. ET from the remainder of the Winters station drainage area, excluding Lake Berryessa, was estimated as Precipitation – Lake Evaporation – Streamflow. Assuming that precipitation represents all inflow to the watershed, outflows consist of streamflow (29%), lake surface evaporation (28%), and land ET (43%). These values are reasonable, given that streamflow is mostly controlled discharge from the lake and that land ET at the Guenoc station upstream of the lake is similar (48%).

Monthly average water balances for both the Guenoc (Figure 7-2) and Winters (Figure 7-3) stations were also created to illustrate the intra-annual hydrological patterns. These charts are normalized by drainage area to allow consistent comparison in terms of depth. The Guenoc station shows the expected seasonal pattern of high precipitation and streamflow in the wet season (October – April) and PET peaking in the dry season (May – September); the Winters station shows the impact of the controlled outflows from Lake Berryessa.

Table 7-1. Summary of streamflow stations with observations available after 2000

Agency	Station Description	Station ID	Drainage Area (mi^2)	Start Date	End Date	Gauge Active?
USGS	PUTAH C NR WINTERS CA	11454000	574.0	6/28/1930	Present	Yes
	PUTAH C NR GUENOC CA	11453500	113.0	10/01/1904	Present	Yes

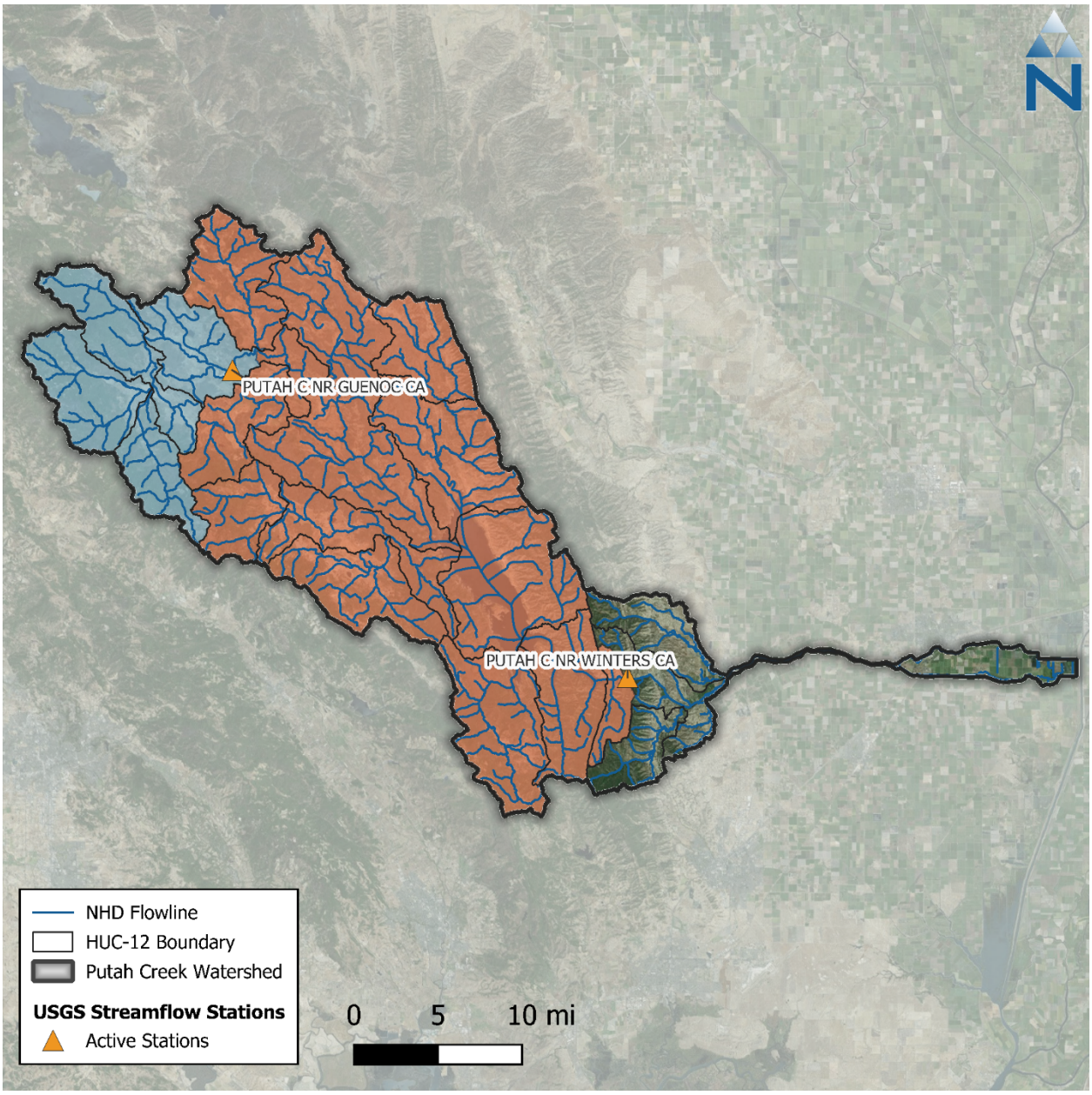

Figure 7-1. USGS streamflow stations in the Putah Creek watershed with drainage areas highlighted.

Table 7-2. Water year total volumes for observed water budget components at the PUTAH C NR GUENOC CA (11453500) station

Water Year	Precipitation Percentile Rank	Total Volume (ac-ft)				Est. ET (% PET)
		Precipitation	PET[1]	Streamflow	Est. ET & Other Losses[2]	
2004	68%	303,215	286,091	182,568	120,647	42%
2005	84%	326,002	263,036	164,746	161,256	61%
2006	89%	399,787	268,562	288,782	111,006	41%
2007	16%	180,447	289,275	55,256	125,191	43%
2008	26%	196,438	295,514	81,537	114,902	39%
2009	37%	209,581	283,094	73,100	136,481	48%
2010	63%	301,929	259,348	143,110	158,819	61%
2011	74%	319,546	258,262	175,812	143,734	56%
2012	42%	214,304	279,916	75,383	138,922	50%
2013	53%	250,367	289,347	98,330	152,037	53%
2014	5%	141,954	298,316	29,793	112,161	38%
2015	47%	224,426	292,717	85,877	138,548	47%
2016	58%	288,227	277,277	126,849	161,378	58%
2017	100%	504,615	267,942	428,286	76,329	28%
2018	32%	199,122	274,918	78,497	120,625	44%
2019	95%	406,156	276,725	275,518	130,638	47%
2020	11%	150,947	290,823	51,272	99,675	34%
2021	0%	101,554	309,133	11,293	90,261	29%
2022	21%	191,033	297,584	75,474	115,558	39%
2023	79%	324,638	271,268	217,768	106,870	39%
Average	--	**261,714**	**281,458**	**135,963**	**125,752**	**45%**
In/Out (%)	--	**100%**	--	**52%**	**48%**	--

1. Potential Evapotranspiration (PET) is based on the CIMIS reference ET, as described in Section 4.2.
2. Estimated ET is calculated as Precip. minus Streamflow and represents an approximate actual ET plus any other storages or losses.

Color Gradient: Lowest | Low | Medium | High | Highest

Table 7-3. Water year total volumes for observed water budget components at the PUTAH C NR WINTERS CA (11454000) station

Water Year	Precipitation Percentile Rank	Total Volume (ac-ft)							Est. Total ET (% PET)[4]
		Precipitation	PET[1]	Streamflow	Lake Berryessa			Est. Land ET[3]	
					Storage	Δ Storage	Est. Evap.[2]		
2004	63%	1,107,572	1,491,870	483,224	1,383,307	-62,676	420,548	203,800	42%
2005	79%	1,357,447	1,379,869	273,747	1,465,087	81,780	355,527	728,173	79%
2006	89%	1,525,691	1,413,510	802,046	1,458,170	-6,917	795,129	-71,484	51%
2007	16%	612,784	1,513,663	239,231	1,257,929	-200,241	38,990	334,563	25%
2008	26%	770,738	1,548,959	244,282	1,165,403	-92,526	151,756	374,700	34%
2009	47%	848,682	1,466,899	238,044	1,016,290	-149,113	88,931	521,707	42%
2010	68%	1,166,124	1,354,973	204,913	1,096,508	80,218	285,131	676,080	71%
2011	74%	1,339,904	1,348,853	202,727	1,315,129	218,621	421,348	715,829	84%
2012	32%	800,887	1,466,452	231,307	1,207,903	-107,225	124,082	445,498	39%
2013	53%	902,295	1,512,925	261,920	1,148,554	-59,349	202,571	437,804	42%
2014	11%	554,807	1,554,741	240,936	921,908	-226,646	14,290	299,581	20%
2015	42%	828,768	1,524,032	230,031	851,420	-70,488	159,543	439,194	39%
2016	58%	1,022,551	1,460,158	207,062	877,538	26,118	233,180	582,309	56%
2017	100%	1,876,615	1,413,677	436,529	1,408,018	530,480	967,009	473,077	102%
2018	21%	699,936	1,447,125	197,019	1,275,655	-132,362	64,657	438,260	35%
2019	95%	1,544,697	1,446,872	430,093	1,422,106	146,451	576,544	538,060	77%
2020	5%	553,509	1,521,124	235,968	1,213,307	-208,800	27,168	290,373	21%
2021	0%	385,448	1,613,852	255,283	923,711	-289,595	-34,312	164,477	8%
2022	37%	815,489	1,565,735	220,382	830,314	-93,397	126,985	468,122	38%
2023	84%	1,392,871	1,418,575	194,659	1,255,391	425,077	619,736	578,476	84%
Average	--	**1,005,341**	**1,472,210**	**291,470**	**1,174,682**	**-9,530**	**281,941**	**431,930**	**49%**
In/Out (%)	--	**100%**	--	**29%**			**28%**	**43%**	--

1. Potential Evapotranspiration (PET) is based on the CIMIS reference ET, as described in Section 4.2.
2. Estimated evaporation from Lake Berryessa is calculated as Δ Storage + Streamflow and represents an approximate evaporation plus any other losses.
3. Estimated ET from the land surface is calculated as Precipitation – Lake Evaporation – Streamflow.
4. Estimated total ET, as a percentage of CIMIS PET, is calculated as (Lake Evaporation + Land ET) / PET

Color Gradient: Lowest | Low | Medium | High | Highest

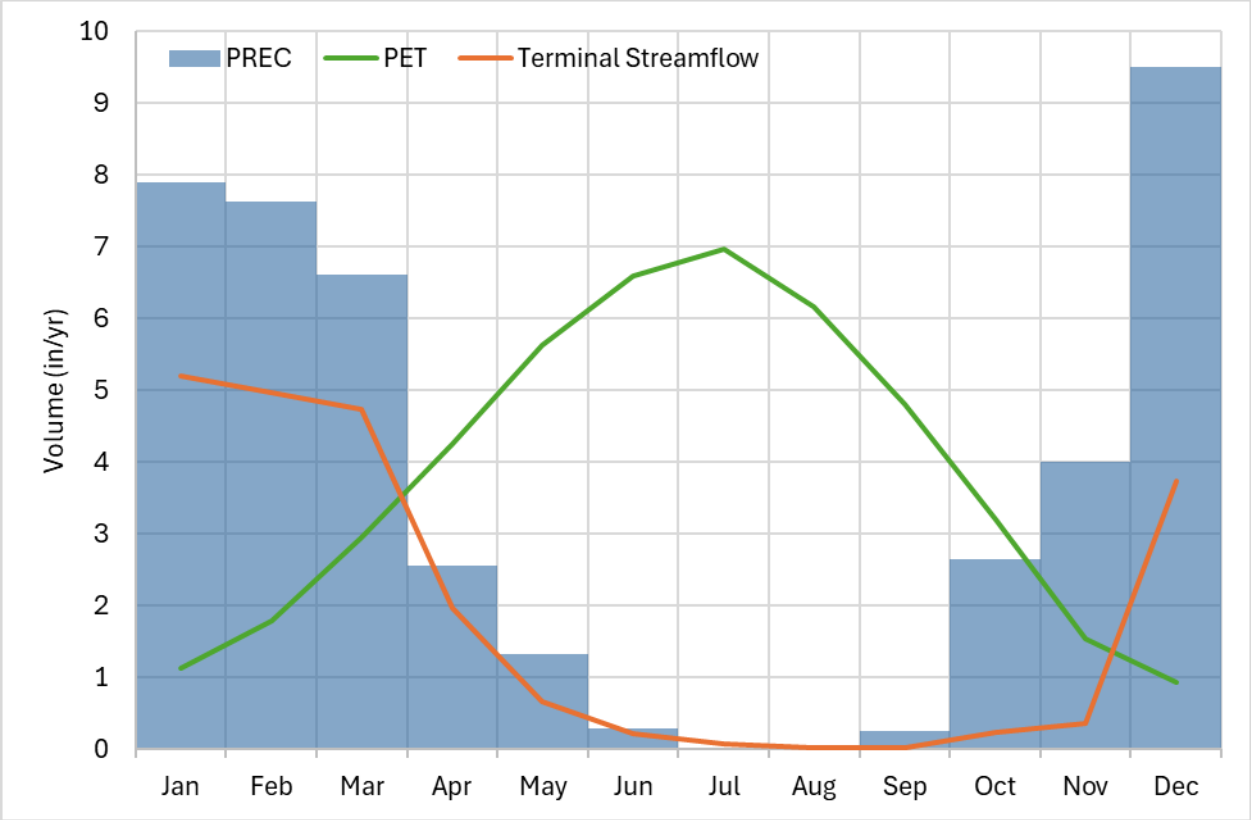

Figure 7-2. Monthly observed area-normalized average depths for the modeling period (water years 2004 -2023) at the PUTAH C NR GUENOC CA (11453500) station.

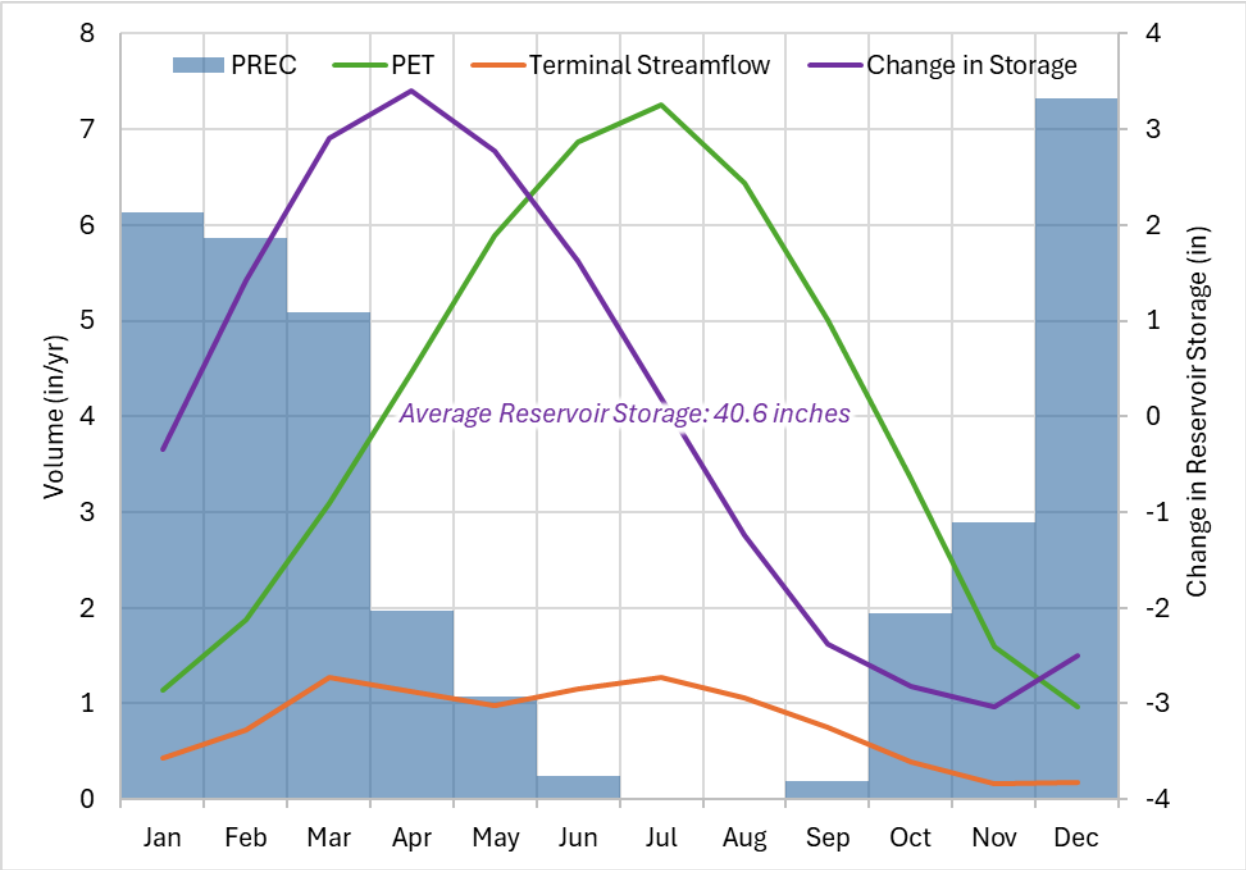

Figure 7-3. Monthly observed area-normalized average depths for the modeling period (water years 2004 -2023) at the PUTAH C NR WINTERS CA (11454000) station. Note that streamflow is controlled by outflow from Lake Berryessa.

8 MODEL CALIBRATION

The goal of the hydrology model calibration is to adjust model parameters to improve predictive performance based on comparisons to observed data. The desired outcome of the calibration process is a set of modeling parameters that characterize existing conditions for all processes in LSPC that vary by HRU (as described in Section 3), reach group, and process-based parameters group. The model development approach prioritizes model configuration over calibration by investigating and expressing known physical characteristics of the watershed wherever possible and practical, and only leaving responses that cannot be explained by physical characteristics to calibration of model parameters. The resulting model is parameterized in such a way that variability trends in the observed data are replicated relative to hydrological conditions (e.g. wet and dry streamflow conditions and rainfall magnitude). The resulting calibrated parameters are consistent by HRU with responses varying as a function of HRU distribution and weather variability minimizes spatial biases and reduces the possibility of over tuning during model calibration. A robustly calibrated model can then serve as the starting point for future watershed-specific applications and investigations and management scenarios.

Figure 8-1 shows how the model configuration and calibration components are layered in the model. LSPC makes clear distinctions between inputs that are physical characteristics and process parameters. The term "parameters" refers to the rates and constants used to represent physical

processes in the model. All other model inputs previously described such as weather data, HRU distribution, and the length and slope of overland flow for individual HRUs are generally considered physical characteristics of the watershed because they can be directly measured, assigned, or reasonably estimated from available spatial and temporal data sources. Those components are generally set during model configuration and are not varied during model calibration unless new information is received that justifies a systemwide change to those components.

Developing modeling parameters begins with specifying one set of parameters systemwide. The Putah Creek model comprises 98 possible HRUs per catchment and 179 unique combinations of meteorological boundary conditions (i.e., unique combinations of precipitation time series and potential evapotranspiration time series). As described in Section 3.4.1, LSUR and SLSUR are uniquely computed by HRU and catchment; therefore, the initial degrees of freedom are already quite broad. Consequently, using one parameter group, the model represents 15,931 unique non-zero area HRU × meteorological responses over the model domain of 669 catchments. Wherever model responses diverge from observed data in ways that the modeling parameters cannot explain, further investigation may warrant introducing a new parameter group or reach group to add more degrees of freedom to the range of model parameters. This methodical calibration sequence can also help to identify areas where additional data collection may be warranted to better characterize the physical system.

Figure 8-2 shows the model calibration sequence, a top-down data approach that began with the extensive model configuration and quality control process previously described in Section 1 through Section 6. The sequence begins with climate-forcing data, followed by edge-of-stream land hydrology and water budget estimates and representation of the stream routing network. This sequencing minimizes the propagation of uncertainty and error by distinguishing physical characteristics of the watershed that can be measured and configured from process-based parameters, which are rates and constants that can be estimated within a reasonable range of variability by HRU.

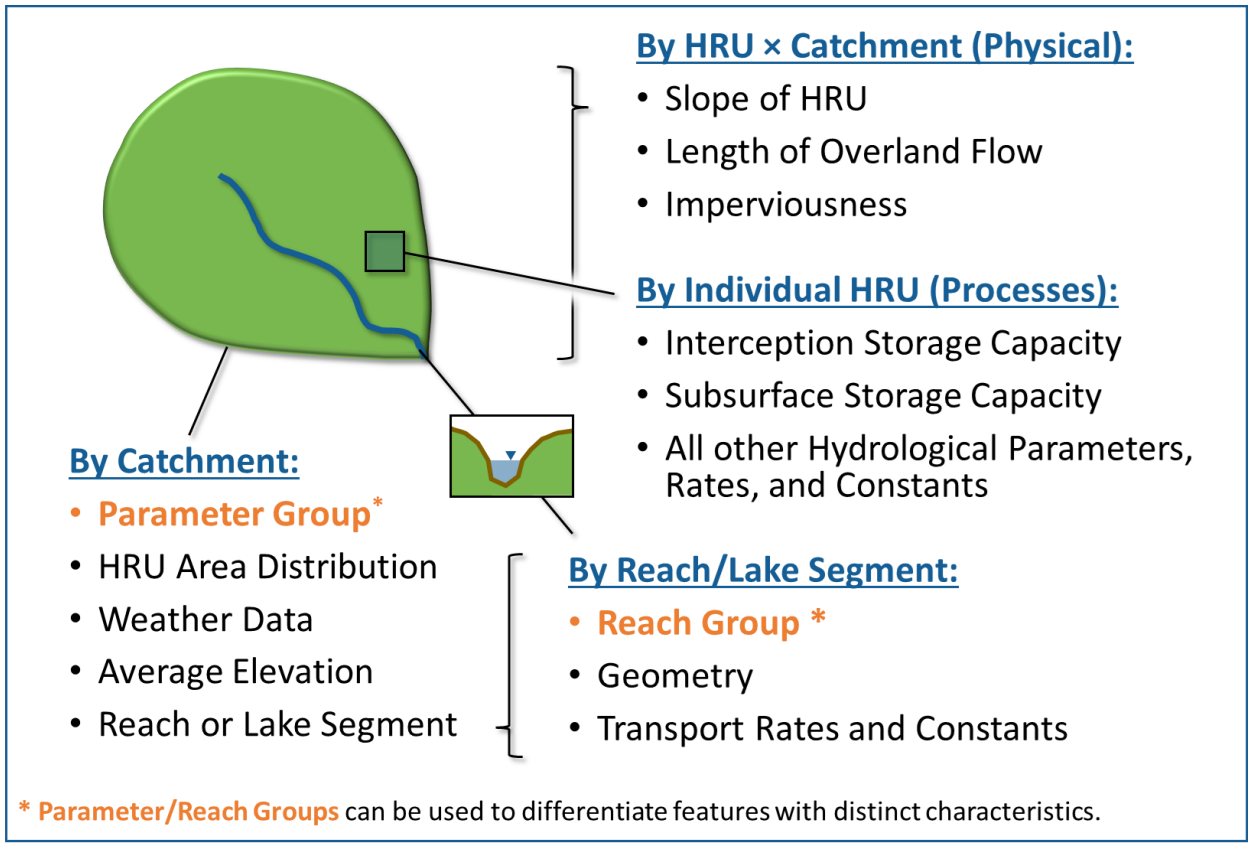

Figure 8-1. LSPC model configuration and calibration components.

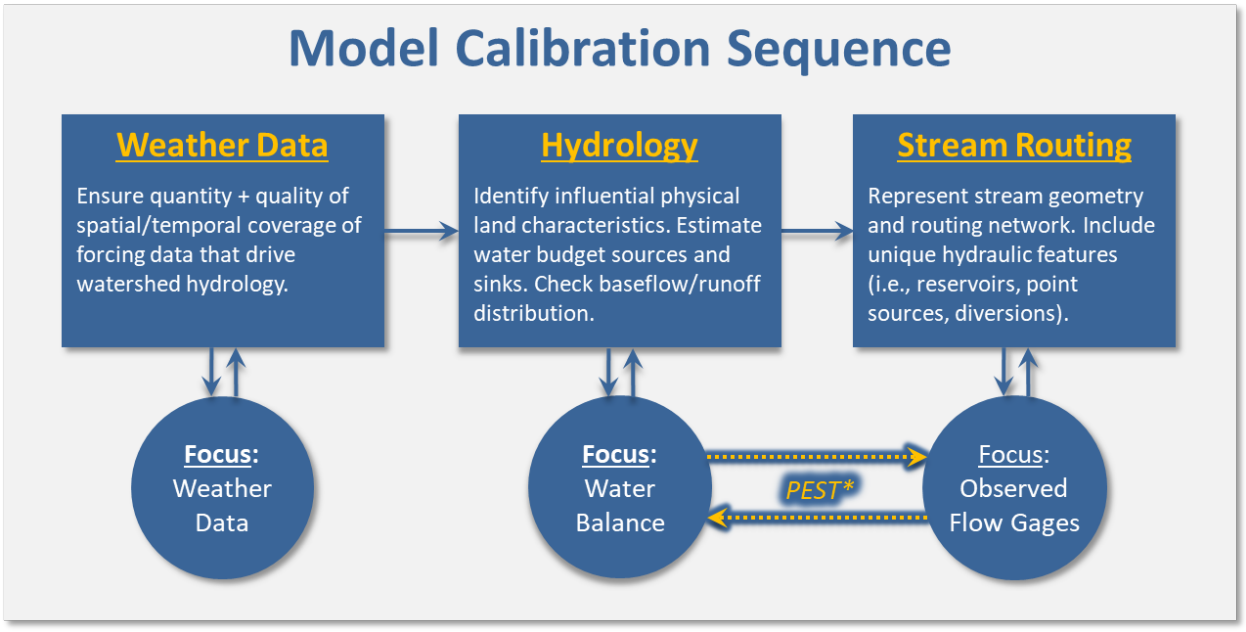

Figure 8-2. Top-down calibration sequence for hydrology model calibration.

Twenty water years of meteorological forcing data between October 2003 and September 2023 were processed to drive the Putah Creek watershed model. Consumptive use data were available for the most recent 6 among those 20 years, water years 2018 through 2023; therefore, those 6 years were selected for model calibration and Parameter Estimation (PEST)—that process is further described in Section 8.2. Calibration of hydrology parameters was primarily carried out for the Putah Creek near Guenoc USGS station (11453500) because it is not impacted by Lake Berryessa, is within the headwaters of the watershed, and has a high-quality data record (see Figure 8-4 and Table 8-1 for details).The HRU distributions for the USGS stations are summarized in Table 8-2. As shown in Figure 8-3, the 6-year calibration period included a range of wet (2019) to very dry years (2020, 2021). The 13 water years prior to the calibration period (water years 2005 through 2017) were selected for independent model validation at the Guenoc station. Additional validation was performed using the full period of record at the other stations with flow data.

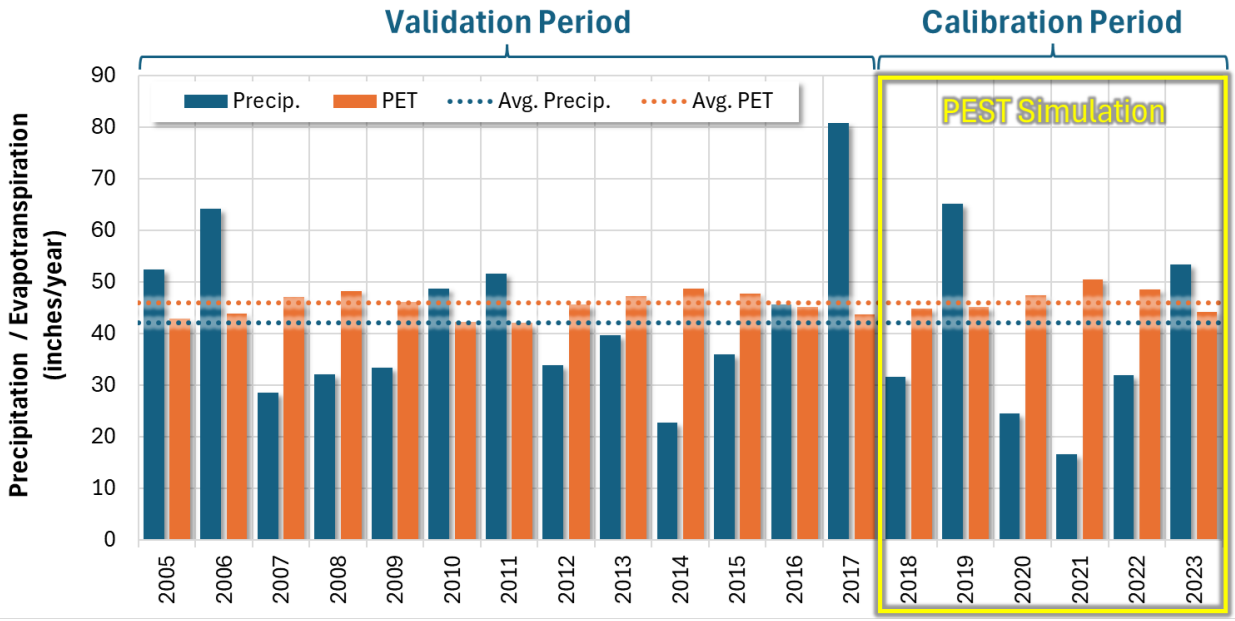

Figure 8-3. Annual average precipitation and potential evapotranspiration (PET) between water years 2004 – 2023, along with PEST simulation and hydrology calibration periods for the Putah Creek near Guenoc USGS station (11453500) drainage area.

Table 8-1. Summary of gauging stations with observations available after 2000

Agency	Gauge Description	Station ID	Drainage Area (mi²)	Start Date	End Date	Gauge Active?
USGS	PUTAH C NR GUENOC CA	11453500	113.0	10/1/1904	Present	Yes
	POPE C A WALTER SPRINGS CA	11453590	40.0	12/24/2020	Present	Yes
	PUTAH C NR WINTERS CA	11454000	574.0	6/28/1930	Present	Yes
	PUTAH SOUTH CN NR WINTERS CA	11454210	603.6	10/1/1994	Present	Yes
CDEC	Lake Berryessa	BER	566.0	10/4/1993	Present	Yes

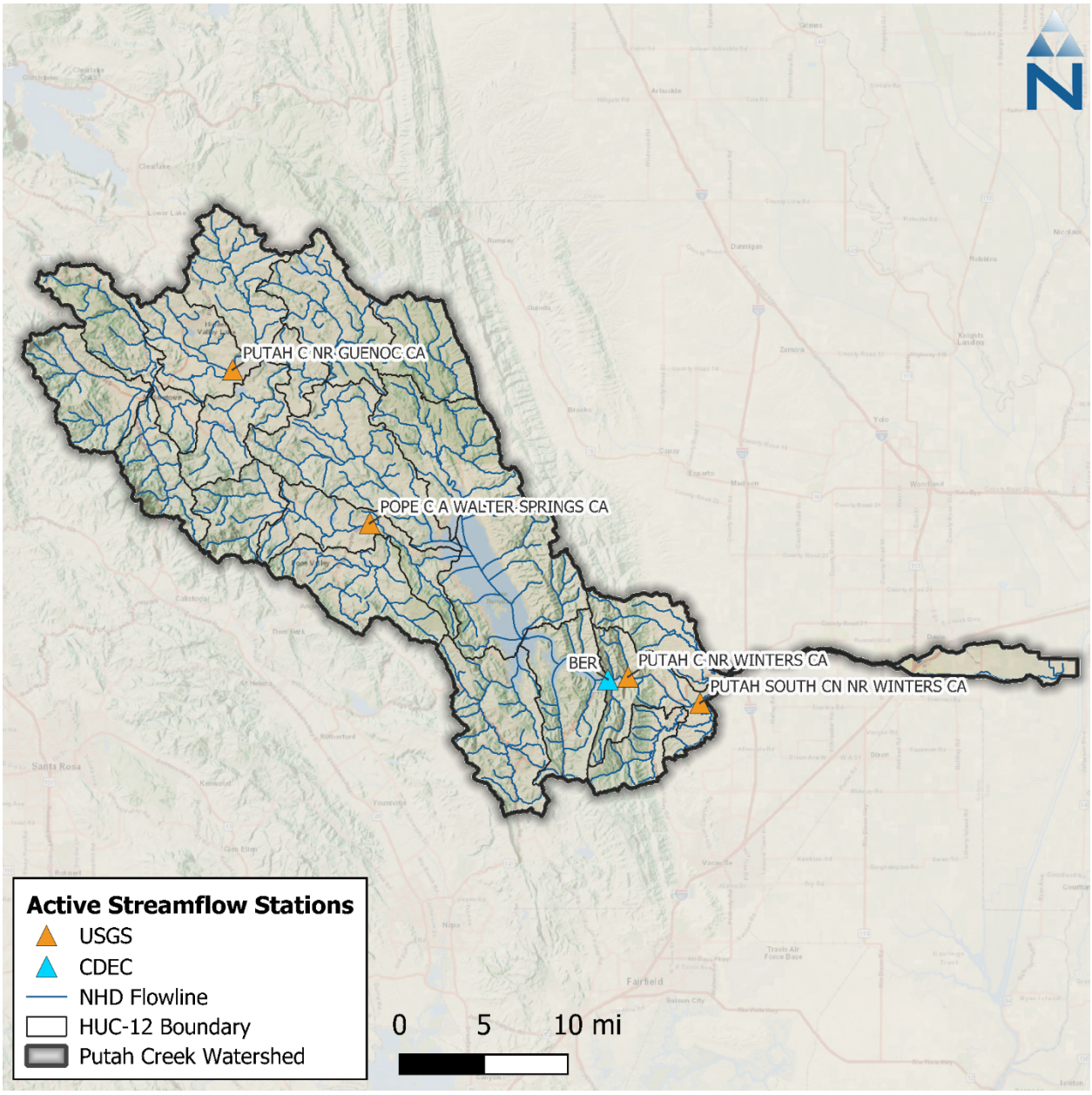

Figure 8-4. USGS streamflow stations in the Putah Creek watershed.

Table 8-2. HRU component distribution by USGS station

Station ID	Station Name	Area by Land Use/Land Cover (%)									Area by HSG (%)				Area by Slope (%)		
		Developed Impervious	Developed Pervious	Barren	Forest	Scrub	Grassland	Pasture	Agriculture	Water	A	B	C	D	Low	Med	High
11453500	PUTAH C NR GUENOC CA	1.9%	4.7%	0.1%	15.7%	27.5%	19.5%	29.1%	1.2%	0.2%	6.2%	4.5%	36.9%	52.4%	14.9%	15.6%	69.5%
11453590	POPE C A WALTER SPRINGS CA	0.3%	1.4%	0.0%	6.3%	12.4%	56.5%	17.2%	5.1%	0.9%	0.9%	3.8%	43.0%	52.3%	15.4%	18.0%	66.6%
11454000	PUTAH C NR WINTERS CA	0.9%	2.0%	0.0%	7.6%	24.8%	39.1%	19.2%	1.6%	4.8%	1.4%	2.5%	37.8%	58.3%	13.2%	15.8%	71.0%
11454210	PUTAH SOUTH CN NR WINTERS CA	0.9%	2.0%	0.0%	7.3%	23.7%	40.0%	19.7%	1.8%	4.6%	1.4%	2.5%	36.4%	59.6%	13.0%	15.7%	71.3%
Model Domain		1.0%	2.1%	0.0%	6.9%	22.9%	38.1%	20.0%	4.7%	4.3%	1.6%	3.8%	35.9%	58.7%	15.7%	15.8%	68.5%

8.1 Calibration Assessment and Metrics

A combination of visual assessments and computed numerical evaluation metrics were used to assess model performance during calibration. Model performance was assessed using graphical comparisons of simulated vs. observed data (e.g., time-series plots, flow duration curves, etc.), quantitative metrics, and qualitative thresholds recommended by Moriasi et al. (2015) and Duda et al. (2012), which are considered highly conservative. Moriasi et al. (2007 and 2015) assign narrative grades for hydrology and water quality modeling to the percent bias (PBIAS), the ratio of the root-mean-square error to the standard deviation of measured data (RSR), and the Nash-Sutcliffe model efficiency (NSE). These metrics are defined as follows:

- The percent bias (PBIAS) quantifies systematic overprediction or underprediction of observations. Positive values of PBIAS reflect a bias towards underestimation, while negative values reflect a bias towards overestimation. Low magnitude values of PBIAS indicate better fit, with a value of 0 being optimal.
- The ratio of the root-mean-square error to the standard deviation of measured data (RSR) provides a measure of error based on the root-mean-square error (RMSE), which indicates error results in the same units as the simulated and observed data but normalized based on the standard deviation of observed data. Values for RSR can be greater than or equal to 0, with a value of 0 indicating perfect fit. Moriasi et al. (2007) provides narrative grades for RSR.
- The Nash-Sutcliffe efficiency (NSE) is a normalized statistic that determines the relative magnitude of the residual variance compared to the measured data variance (Nash & Sutcliffe, 1970). NSE indicates how well the plot of observed versus simulated data fits the 1:1 line. Values for NSE can range between -∞ and 1, with NSE = 1 indicating a perfect fit.

Other metrics were computed and used to assess calibrated model performance, including the Kling-Gupta Efficiency (KGE). This metric can provide additional or complementary information on model performance to the three metrics listed above and is defined as follows:

- The Kling-Gupta Efficiency (KGE) metric is based on the Euclidean Distance between an idealized reference point and a sample's bias, standard deviation, and correlation within a three-dimensional space (Gupta et al. 2009). KGE attempts to address documented shortcomings of NSE, but the two metrics are not directly comparable. A KGE value of 1 indicates perfect fit, with agreement worsening for values less than 1. Knoben et al. (2019) have suggested a KGE value > - 0.41 as a benchmark that indicates a model has more predictive skill than using the mean observed flow. Qualitative thresholds for KGE have been used by Kouchi et al. (2017).

Both simulated time series and observed data were binned into subsets of time to highlight seasonal performance and different flow conditions. Hydrograph separation was also performed to assess stormwater runoff vs. baseflow periods to isolate model performance on stormflows and low flows.

Table 8-3 is a summary of performance metrics that will be used to evaluate the hydrology calibration. As shown in the table, "All Conditions" (i.e., annual interval) for R-squared and NSE is the primary condition typically evaluated during model calibration. For sub-annual intervals, the pattern established in the literature for PBIAS/RME when going from "All Conditions" to sub-annual intervals is to shift the qualitative assessment by one category (e.g., use the "good" range for "very good", "satisfactory" for "good", and so on). This pattern was followed for RSR and NSE qualitative assessments of sub-annual intervals.

Using hydrograph separation to classify baseflow and stormflow provides a more reliable method for assessing low-flow model performance than using the lowest 50% of flows, a metric widely used in hydrology model calibration as a convenient indicator of low-flow model performance. There are several key reasons for this:

1. **Improved Representation of Low-Flow Conditions:** The lowest 50% of flows include not only baseflow but also portions of stormflow as the hydrograph rises and falls. This can mask the true low-flow or baseflow behavior of the system, as the transitions from baseflow to stormflow can have very different physical and hydrological drivers. By using hydrograph separation, baseflow, which is primarily driven by groundwater contributions, can be isolated from storm flows, which are influenced by rainfall (Smakhtin 2001). This provides a clearer, more consistent metric for assessing low-flow conditions during model calibration and performance evaluation.
2. **Reduction in Variability of Metrics:** Because the rising and falling limbs of the hydrograph are affected by factors such as precipitation intensity, antecedent moisture conditions, and catchment characteristics, including portions of these limbs in the low-flow metric can lead to high variability in model performance metrics. This variability can obscure the modeler's ability to accurately assess low-flow performance. Hydrograph separation, on the other hand, offers a cleaner classification, resulting in lower variability and a more stable and reliable assessment of baseflow model performance.
3. **Better Calibration for Baseflow-Driven Processes:** In many hydrological studies, low flows are important for understanding groundwater-surface water interactions, sustaining streamflow during dry periods, and supporting aquatic habitats. Hydrograph separation allows for the explicit calibration of baseflow processes, providing a better assessment of groundwater dynamics and groundwater-fed contributions to the stream network. Without separating baseflow and stormflow, calibration based on the lowest 50% of flows may inadvertently skew model performance statistics by over-emphasizing short-term stormflow events and recession behavior, rather than the sustained low flow processes crucial to many hydrological applications.
4. **Alignment with Process-Based Hydrology:** Hydrograph separation aligns with a process-based understanding of hydrology, where distinct processes govern baseflow and stormflow. This approach respects the inherent differences in generation mechanisms: baseflow is usually a slower, more consistent groundwater-driven process, while stormflow is a quicker response to precipitation events. This distinction is essential for accurately simulating hydrological systems and ensuring model results that are realistic and representative of different flow conditions. Models that capture these distinct flow components are better suited for making predictions about changes in land use, climate, or other factors affecting baseflow and stormflow differently.
5. **Widely Accepted in Hydrological Modeling:** Hydrograph separation techniques are well-established and widely used in hydrological research and practice, offering a consistent framework for distinguishing between baseflow and stormflow (Arnold et al. 1995; Nathan and McMahon 1990). Techniques like those used in the United States Geological Survey (USGS) Hydrograph SEParation (HySEP) methodology provide different options for empirically parsing baseflow time series from storm flows (Sloto and Crouse 1996). The sliding interval method was used to separate both observed and simulated hydrographs at a daily timestep. This provides a consistent approach for the rollup and comparison of hydrograph components. This method is robust because they can be directly applicable to time series data as a function of the upstream drainage area.

Table 8-3. Summary of qualitative thresholds for performance metrics used to evaluate hydrology calibration

Performance Metric	Hydrological Condition	Performance Threshold for Hydrology Simulation			
		Very Good	Good	Fair	Poor
Percent Bias (PBIAS)	All Conditions [1]	<5%	5% - 10%	10% - 15%	>15%
	Seasonal Flows [2]	<10%	10% - 15%	15% - 25%	>25%
	Highest 10% of Daily Flow Rates [3]				
	Days Categorized as Storm Flow [4]				
	Days Categorized as Baseflow [4]				
RMSE – Std. Dev. Ratio (RSR)	All Conditions [1]	≤0.50	0.50 - 0.60	0.60 - 0.70	>0.70
	Seasonal Flows [2]	≤0.60	0.60 - 0.70	0.70 - 0.80	>0.80
Nash-Sutcliffe Efficiency (NSE)	All Conditions [1]	>0.80	0.70 - 0.80	0.50 - 0.70	≤0.50
	Seasonal Flows [2]	>0.70	0.50 - 0.70	0.40 - 0.50	≤0.40
Kling-Gupta Efficiency (KGE)	Monthly Aggregated [5]	≥0.90	0.90 - 0.75	0.75 - 0. 50	<0.50

1. All Flows considers all daily time steps in the model time series.
2. Seasonal Flows consider daily flows during a predefined, seasonal period (e.g., Wet Season and Dry Season). The Wet Season includes the months of October through April. The Dry Season includes the months of May through September.
3. Highest 10% of Flows considers the top 10% of daily flows by magnitude as determined from the observed flow duration curve.
4. Baseflows and Storm flows were determined from analyzing the daily model time series by applying the USGS hydrograph separation approach (Sloto and Crouse 1996).
5. KGE evaluated using thresholds for monthly aggregated time series (Kouchi et al. 2017).

8.2 Parameter Estimation

The model-independent Parameter ESTimation tool (PEST) is a powerful tool used for model parameter estimation, sensitivity analysis, and uncertainty analysis (Doherty 2015). It automates adjusting a specific set of model parameters within a reasonably constrained range of variability, with the objective of minimizing the differences between observed and simulated data. PEST seeks to minimize the sum of Squared Errors (SSE) across all specified observations that can be customized as needed to evaluate complete flow time series or other temporal categorizations such as flow duration intervals, monthly volumes, wet and dry periods, etc. A supervised PEST simulation helps to ensure that recommended outcomes are realistic and representative of the natural system being modeled. PEST is versatile and can be integrated with a wide range of environmental and hydrological models, including LSPC.

Sections 1 through 6 above describe model configuration and quality control methods used to represent physical characteristics of the watershed that are either directly measurable or can be reasonably estimated from available spatial or temporal data. On the other hand, parameters associated with subsurface geology represent one of the areas of uncertainty in the model where

optimization of model parameters can improve performance. PEST was used in conjunction with model parameterization guidance documentation (BASINS Technical Note 6 [EPA 2000]) to vary six parameters associated with subsurface geology: the infiltration index parameter (INFILT), the lower zone nominal storage parameter (LZSN), the upper zone nominal storage parameter (UZSN), the active groundwater recession coefficient (AGWRC), and the interflow recession coefficient (IRC).

The infiltration index parameter (INFILT) is one of the parameters optimized by PEST. Within a given hydrological soil group, TN6 guidance suggests that INFILT typically varies within minimum and maximum values shown in Table 8-4. Some model parameters are codependent. For example, TN6 recommends that the upper zone nominal storage parameter (UZSN) should first be estimated as a percentage of the lower zone nominal storage parameter (LZSN), taking into consideration other physical characteristics such as slope, vegetation cover, and depression storage, and then calibrated. Table 8-5 shows recommended initial values for UZSN as a percentage of LZSN and other physical characteristics. The active groundwater recession coefficient (AGWRC), the ratio of current groundwater discharge to that of the previous day, was the fourth parameter optimized by PEST. TN6 notes that "the overall watershed recession rate is a complex function of watershed conditions, including climate, topography, soils, and land use" that can be estimated from observed time series, and then adjusted during calibration (EPA 2000). Interflow recession coefficient (IRC), the ratio of the current daily interflow discharge to the interflow discharge on the previous day, affects the rate that interflow is discharged from storage and, therefore, the shape of the hydrograph receding limb after storm events. Model guidance and previous experience suggest that these parameters are both uncertain and very sensitive; therefore, using PEST to explore their impact and optimize performance is worthwhile and beneficial.

Table 8-4. Typical ranges by hydrological soil group for the infiltration index model parameter, INFILT

Hydrological Soil Group	INFILT Typical Ranges (in./hr)		Runoff Potential
	Low	High	
A	0.40	1.00	Low
B	0.10	0.40	Moderate
C	0.05	0.10	Moderate to High
D	0.01	0.05	High

Source: BASINS Technical Note 6 (EPA 2000)

Table 8-5. Recommended initial values for upper zone nominal storage (UZSN) as a percentage of lower zone nominal storage (LZSN) and other physical characteristics

Slope	Vegetation Cover	Depression Storage	UZSN (% of LZSN)
Very Mild	Heavy/Forest	High	14%
Moderate	Moderate	Moderate	8%
Steep	Moderate	Moderate	6%

Source: BASINS Technical Note 6 (EPA 2000)

PEST could have optimized model parameters at the HRU level (up to 97 possible degrees of freedom per parameter for previous HRUs); however, to better manage the search space, those degrees of freedom were constrained to 12 combinations of hydrological soil group (4 types) × slope (3 categories). Figure 8-5 is a schematic of HRU-level LSPC hydrology parameters with the six PEST-optimized parameters and process pathways highlighted. Table 8-6 shows the minimum and maximum parameter value ranges used to constrain PEST optimization by hydrological soil group

and slope. Table 8-7 shows the initial and final PEST-optimized estimates for subsurface process parameters, summarized by hydrological soil group and slope—the data bars show the relative magnitude of the initial and estimated parameter value within the PEST min/max range (a full cell indicates the maximum value while an empty cell indicates the minimum value). Note that initial parameter values were based on final calibrated values from the nearby Navarro River watershed model (SWRCB 2025).

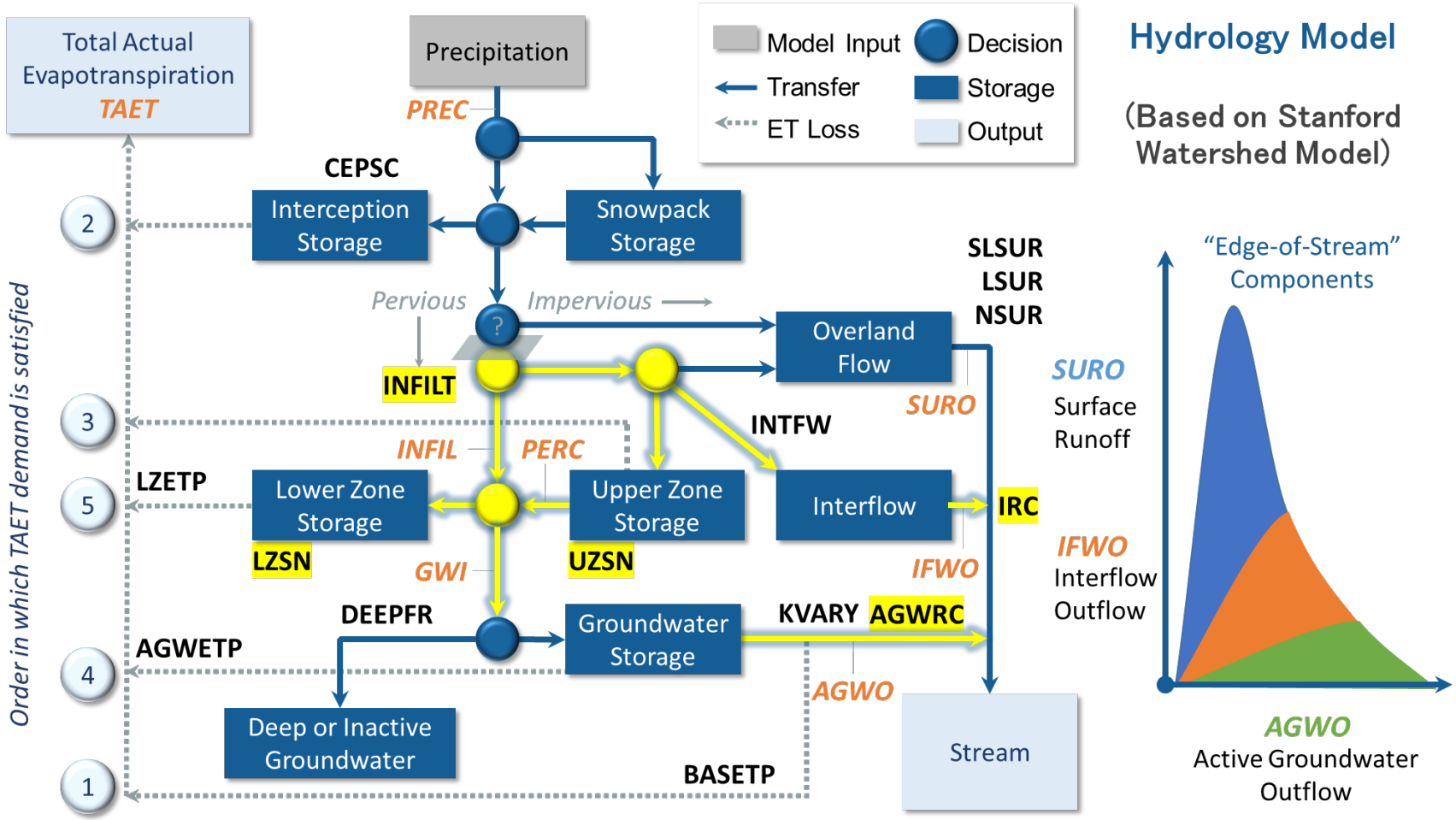

Figure 8-5. HRU-level LSPC hydrology parameters with PEST-optimized parameters and process pathways highlighted.

Table 8-6. Minimum and maximum parameter value ranges used to constrain PEST optimization, by hydrological soil group and slope

HSG	Slope	Area (ac)	Area (%)	LZSN		INFILT		AGWRC		UZSN (% LZSN)		IRC	
				Min	Max	Min	Max	Min	Max	Min	Max	Min	Max
A	Low	2,368.5	3.2%	2	15	0.4	1	0.85	0.999	10	17	0.3	0.85
A	Med	302.9	0.4%	2	15	0.4	1	0.85	0.999	6	12	0.3	0.85
A	High	1,822.9	2.5%	2	15	0.4	1	0.85	0.999	4	8	0.3	0.85
B	Low	862.0	1.2%	2	15	0.1	0.4	0.85	0.999	10	17	0.3	0.85
B	Med	328.0	0.4%	2	15	0.1	0.4	0.85	0.999	6	12	0.3	0.85
B	High	1,964.1	2.7%	2	15	0.1	0.4	0.85	0.999	4	8	0.3	0.85
C	Low	5,012.4	6.9%	2	15	0.05	0.1	0.85	0.999	10	17	0.3	0.85
C	Med	6,610.5	9.1%	2	15	0.05	0.1	0.85	0.999	6	12	0.3	0.85
C	High	15,318.0	21.0%	2	15	0.05	0.1	0.85	0.999	4	8	0.3	0.85
D	Low	2,356.7	3.2%	2	15	0.001	0.05	0.85	0.999	10	17	0.3	0.85
D	Med	4,102.0	5.6%	2	15	0.001	0.05	0.85	0.999	6	12	0.3	0.85
D	High	31,959.2	43.8%	2	15	0.001	0.05	0.85	0.999	4	8	0.3	0.85
PEST Subtotal[1]		**73,007.2**	**99.3%**	--	--	--	--	--	--	--	--	--	--

1. PEST subtotal based on area draining to the Putah Creek near Guenoc USGS station (11453500) and excludes Water and Developed Impervious HRUs.

Color Gradient: Lowest | Low | Med | High | Highest

Table 8-7. Initial and final PEST optimized estimates for subsurface process parameters, summarized by hydrological soil group and slope

HSG	Slope	Area (ac)	Area (%)	LZSN (in)		INFILT (in/hr)		AGWRC		UZSN (% LZSN)[1]		UZSN (in)		IRC	
				Initial	Est.	Initial	Est.	Initial	Est.	Initial[2]	Est.	Initial[2]	Est.	Initial	Est.
A	Low	2,368.50	3.2%	10.18	4.47	0.400	1.000	0.85	0.949	14.24	10.00	1.45	0.45	0.65	0.85
A	Med	302.9	0.4%	10.18	4.47	0.400	1.000	0.85	0.949	8.15	6.00	0.83	0.27	0.65	0.85
A	High	1,822.90	2.5%	10.18	4.47	0.400	1.000	0.85	0.949	6.09	4.00	0.62	0.18	0.65	0.85
B	Low	862	1.2%	12.50	2.60	0.100	0.400	0.95	0.957	17.52	10.00	2.19	0.26	0.58	0.85
B	Med	328	0.4%	12.50	2.60	0.100	0.400	0.95	0.957	10.00	12.00	1.25	0.31	0.58	0.85
B	High	1,964.10	2.7%	12.50	2.60	0.100	0.400	0.95	0.957	7.52	8.00	0.94	0.21	0.58	0.85
C	Low	5,012.40	6.8%	15.00	7.94	0.050	0.100	0.97	0.965	20.00	17.00	3.00	1.35	0.57	0.64
C	Med	6,610.50	9.0%	15.00	7.94	0.050	0.100	0.97	0.965	12.00	12.00	1.80	0.95	0.57	0.64
C	High	15,318.00	20.8%	15.00	7.94	0.050	0.100	0.97	0.965	9.00	8.00	1.35	0.64	0.57	0.64
D	Low	2,356.70	3.2%	15.00	15.00	0.007	0.007	0.85	0.973	20.00	13.33	3.00	2.00	0.35	0.53
D	Med	4,102.00	5.6%	15.00	15.00	0.007	0.007	0.85	0.973	12.00	12.00	1.80	1.80	0.35	0.53
D	High	31,959.20	43.4%	15.00	15.00	0.007	0.007	0.85	0.973	9.00	8.00	1.35	1.20	0.35	0.53
PEST Subtotal		**73,007.2**	**99.3%**	--	--	--	--			--	--	--	--	--	--

1. UZSN is estimated as a percentage of LZSN based on guidance from BASINS Technical Note 6 (EPA 2000).
2. Note that the UZSN ranges were updated compared to the initial values adopted from the Navarro River watershed model.

Data Bars Show the relative magnitude of the parameter values within the PEST min/max ranges (See Table 8-6).

Color Gradient: Lowest | Low | Med | High | Highest

8.2.1 Additional Parameter Adjustments

The second phase of calibration included applying the PEST estimated parameters model-wide, evaluating initial model performance, and then making additional parameter adjustments as needed. The PEST estimated parameter values provide a high degree of correspondence between simulated and observed flow at the Guenoc station during the calibration period. Using these parameters for the larger Lake Berryessa drainage area, however, may contribute more inflow to the lake as discussed in Section 9.3. Therefore, several additional parameters were fine-tuned to reduce lake inflows while minimizing any impact to the Guenoc calibration as described below:

1. **Interception storage and ET**: Grassland, Pasture, Agriculture, and Irrigation HRUs were updated to use the highest typical value of Interception Storage Capacity (CEPSC) and Lower Zone Evapotranspiration Index (LZETP) from BASINS Technical Note 6 (EPA 2000). CEPSC — which controls the amount of rainfall which is retained by vegetation, never reaches the land surface, and is eventually evaporated — was increased from 0.1 in to 0.25 in for Agriculture and Irrigation HRUs (see Table 8-8). LZETP controls ET from the lower soil zone and is primarily a function of vegetation (see Table 8-9). Grassland and Pasture HRUs used the "Grassland" value; Agriculture and Irrigation HRUs used the "Row Crops" value.

Table 8-8. Typical ranges for the interception storage capacity parameter, CEPSC

TN6 Land Use/Land Cover	Typical Maximum CEPSC (in)	HRU Land Use/Land Cover	Modeled CEPSC (in)
Grassland	0.1	Grassland	0.1
		Pasture	0.1
Cropland	0.10 – 0.25	Agriculture	0.25
		Irrigation	0.25
Forest Cover, Light	0.15	Scrub	0.15
Forest Cover, Heavy	0.2	Forest	0.2

Source: BASINS Technical Note 6 (EPA 2000)

Table 8-9. Typical and modeled ranges for the lower zone evapotranspiration parameter, LZETP

TN6 Land Use/Land Cover	Typical LZETP Range (coefficient)	HRU Land Use/Land Cover	Modeled LZETP (coefficient)
Forest	0.6 - 0.8	Forest	0.6
Grassland	0.4 - 0.6	Grassland	0.6
		Pasture	0.6
		Scrub	0.4
Row crops	0.5 - 0.7	Agriculture	0.7
		Irrigation	0.7
Barren	0.1 - 0.4	Barren	0.4
Wetlands	0.6 - 0.9	--	--

Source: BASINS Technical Note 6 (EPA 2000)

2. **Riparian Evapotranspiration (Riparian ET)**: Riparian ET was estimated to represent the ET losses from riparian corridors. Examination of the NLCD land cover data indicated that the Putah Creek watershed has over 3,000 ac of wetlands where riparian ET is expected to be high (Table 8-10). Wetlands are not explicitly represented by an HRU; therefore, riparian ET was proportionally configured for stream segments in catchments with NLCD wetland area. In

these catchments, it was assumed that wetlands are always along the edge of the stream segment. Riparian width (RIPWID) and fraction of Riparian Cover (RIPCOV) were back-calculated from wetland area and stream length (LEN) using this equation: wetland area = LEN×RIPWID×RIPCOV with RIPCOV ranging from 0-1. Figure 8-6 is a distribution plot of wetland area along modeled stream length, which was used to model riparian ET. About 35% of total stream length had nearby wetland area ranging from 0.2 acres to 228 acres.

Table 8-10. Comparison of NLCD wetland classes between selected drainage areas

Drainage Area Name	Woody Wetlands (ac)	Emergent Herbaceous Wetlands (ac)	Total Wetlands (ac)	Drainage Area (%)
POPE C A WALTER SPRINGS CA (11453590)	63.2	83.0	146.1	0.6%
PUTAH C NR GUENOC CA (11453500)	152.8	131.7	284.4	0.4%
Lake Berryessa (BER) (excluding Pope and Guenoc)	302.0	1,844.5	2,146.5	0.8%
Below Lake Berryessa	362.3	116.5	478.8	0.9%
Total	880.2	2,175.7	3,055.9	0.7%

Color Gradient: Lowest | Low | Med | High | Highest

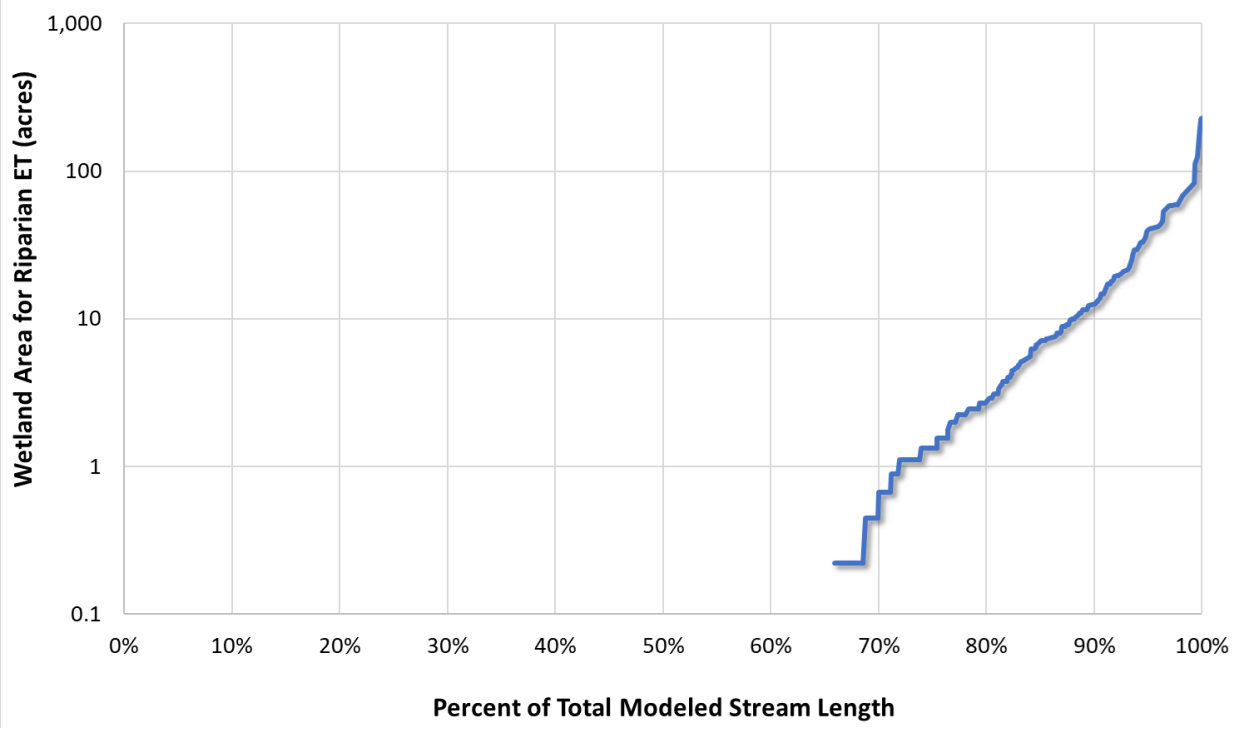

Figure 8-6. Distribution of wetland area along modeled stream length used for riparian ET.

8.3 Calibration Results

Using the PEST estimated parameters, the model was run for water years 2018 through 2023 and calibration performance was evaluated. Note that all results presented below exclude observed flows < 1 cfs, where there may be more uncertainty in gauge readings. As shown in Table 8-11,

performance across the calibration period was "Good" for PBIAS with simulated flow volumes slightly underpredicted by 9.5%. Wet season was "Very Good" with 9.3% and the dry season was "Good" underpredicting by 14.1%. RSR and NSE performance was "Very Good" across the entire calibration period and seasons. KGE (calculated with monthly flow values) was "Good" across the entire calibration period and seasons. These metric values indicate the model is performing well at capturing the observed volume (PBIAS) and trends in wet and dry season flow (RSR, NSE, KGE). Table 8-12 is a summary of model calibration performance metrics computed using monthly time series, as recommended by Moriasi et al. (2015). As expected, PBIAS is not impacted by the time step change, however, RSR and NSE both show notable improvement in performance compared to using daily average time series.

Examination of daily and normalized monthly streamflow (Figure 8-7 and Figure 8-8, respectively) shows that, as indicated by the metrics, the most extreme peaks are slightly underestimated, but general rising/falling patterns in the hydrographs are well captured. Figure 8-9 and Figure 8-10 present the interquartile ranges and averages, respectively, of monthly normalized flow—both show a high degree of correspondence between observed and simulated values. The highest flows at the beginning of the Wet season (November – February) are somewhat overpredicted but the highest spring flows at the end of the Wet season are somewhat underpredicted. The flow duration curve (FDC) shown in Figure 8-11 indicates that observed flow regime trends are generally well matched by the model. Below the 55th percentile, modeled flows are lower than observed, with increased underprediction below the 25th percentile; it should be noted that modeled and observed FDCs are calculated independently and flows of the same percentile do not necessarily occur at the same time.

Table 8-11. Summary of daily calibration performance metrics

Hydrology Monitoring Locations	Performance Metrics (10/01/2017 - 09/30/2023)														
	PBIAS						RSR			NSE			KGE[1]		
	All	Wet Season	Dry Season	>10th %ile Flows	Storm Flows	Baseflow	All	Wet Season	Dry Season	All	Wet Season	Dry Season	All	Wet Season	Dry Season
PUTAH C NR GUENOC CA	9.5%	9.3%	14.1%	15.2%	7.8%	11.8%	0.37	0.38	0.38	0.86	0.86	0.85	0.85	0.84	0.85

[1] Monthly, as specified in Table 8-3.

Very Good | Good | Fair | Poor

\- Overpredicts | + Underpredicts

Table 8-12. Summary of calibration performance metrics using monthly total volume at PUTAH C NR GUENOC CA (11453500)

Calibration Metrics for Monthly Flow (10/01/2017 - 09/30/2023)	Hydrological Condition		
	All (n = 60)	Wet Season (n = 38)	Dry Season (n = 22)
Percent Bias (PBIAS)	9.50%	9.30%	14.10%
Nash-Sutcliffe Efficiency (E)	0.97	0.97	0.98
RMSE-Std. Dev. Ratio (RSR)	0.17	0.18	0.14
Kling–Gupta Efficiency (KGE)	0.85	0.84	0.85

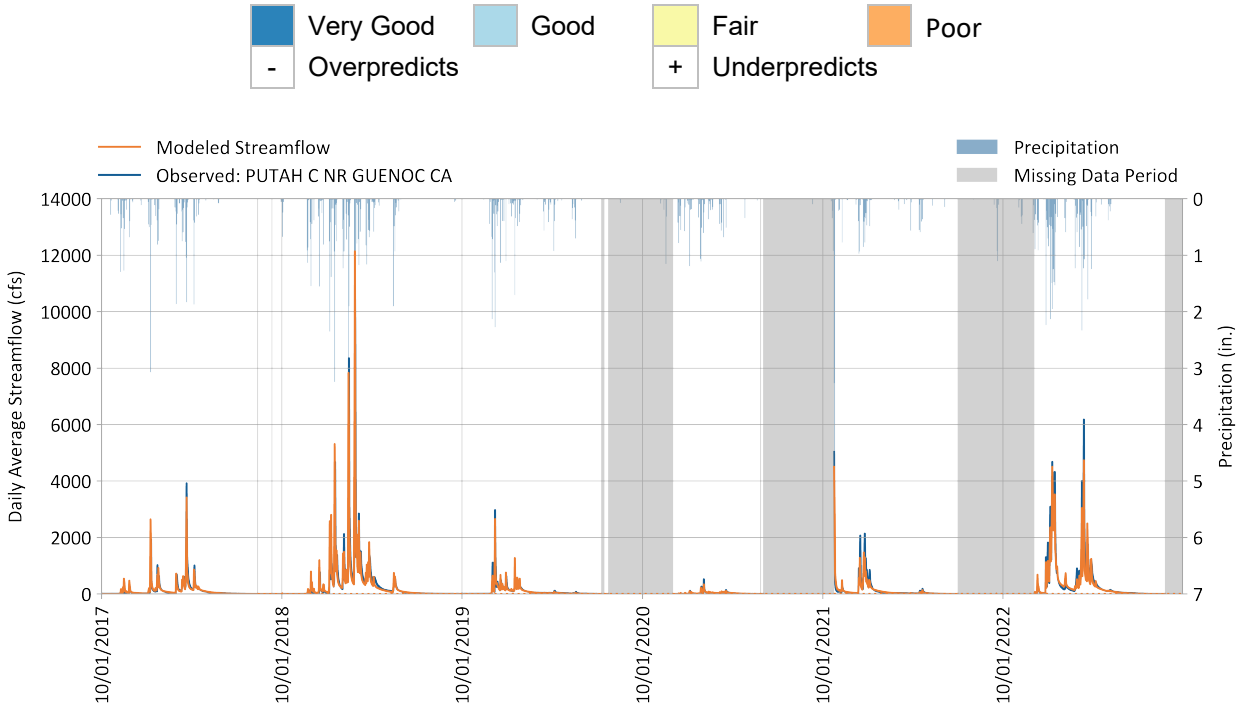

Figure 8-7. Daily simulated vs. observed streamflow for PUTAH C NR GUENOC CA (11453500).

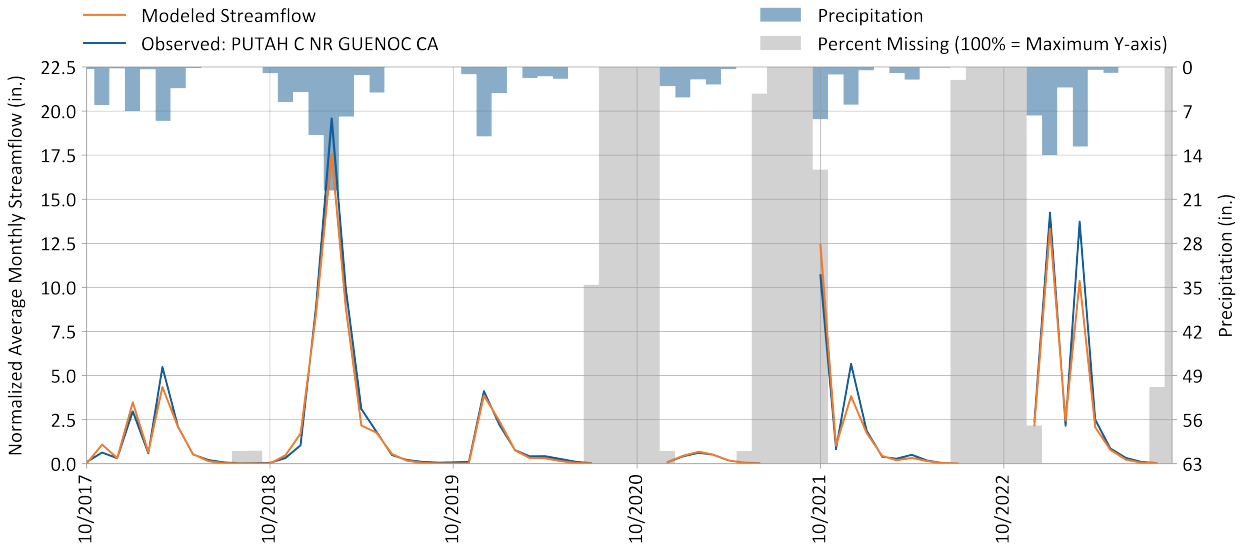

Figure 8-8. Monthly simulated vs. observed streamflow for PUTAH C NR GUENOC CA (11453500).

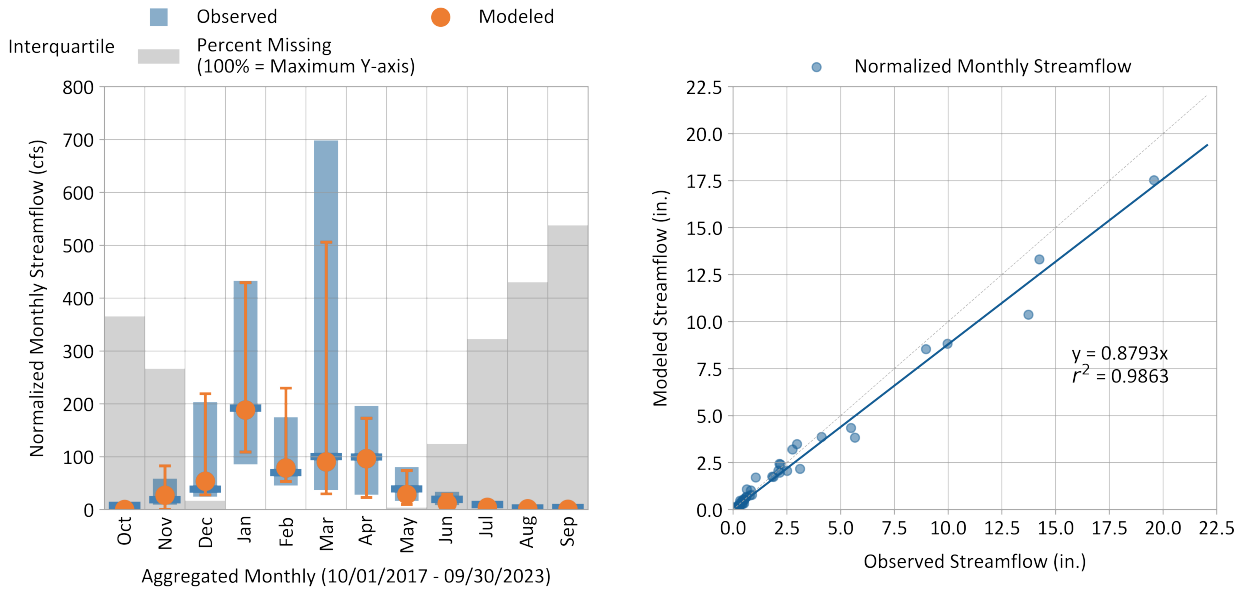

Figure 8-9. Monthly normalized simulated vs. observed streamflow for PUTAH C NR GUENOC CA (11453500).

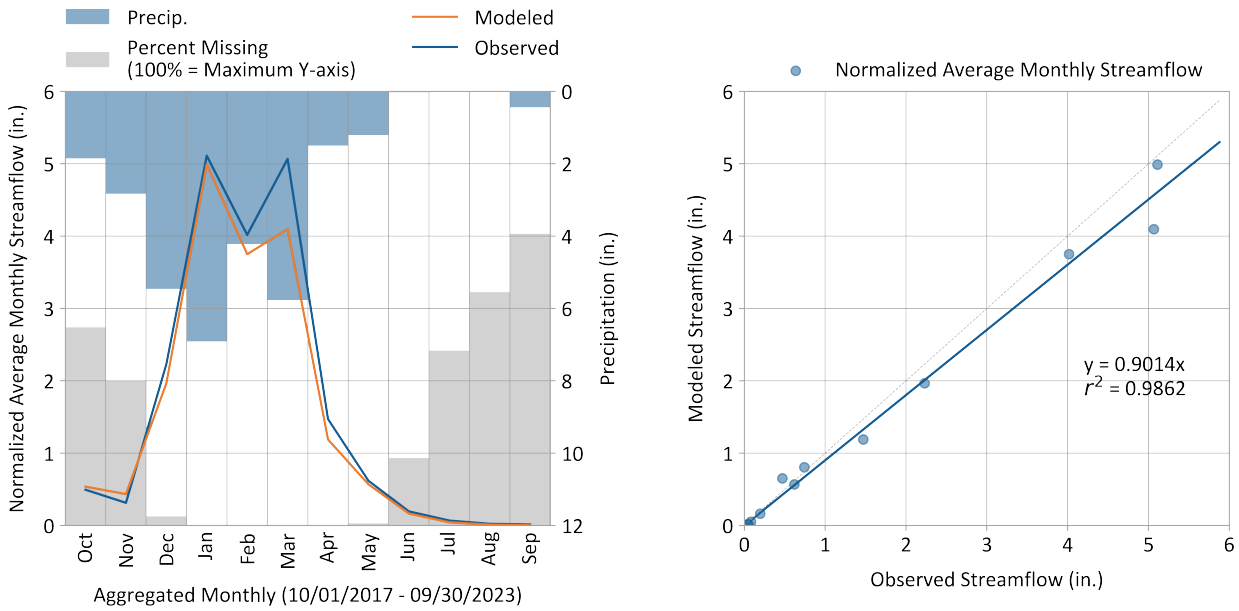

Figure 8-10. Average monthly simulated vs. observed streamflow for PUTAH C NR GUENOC CA (11453500).

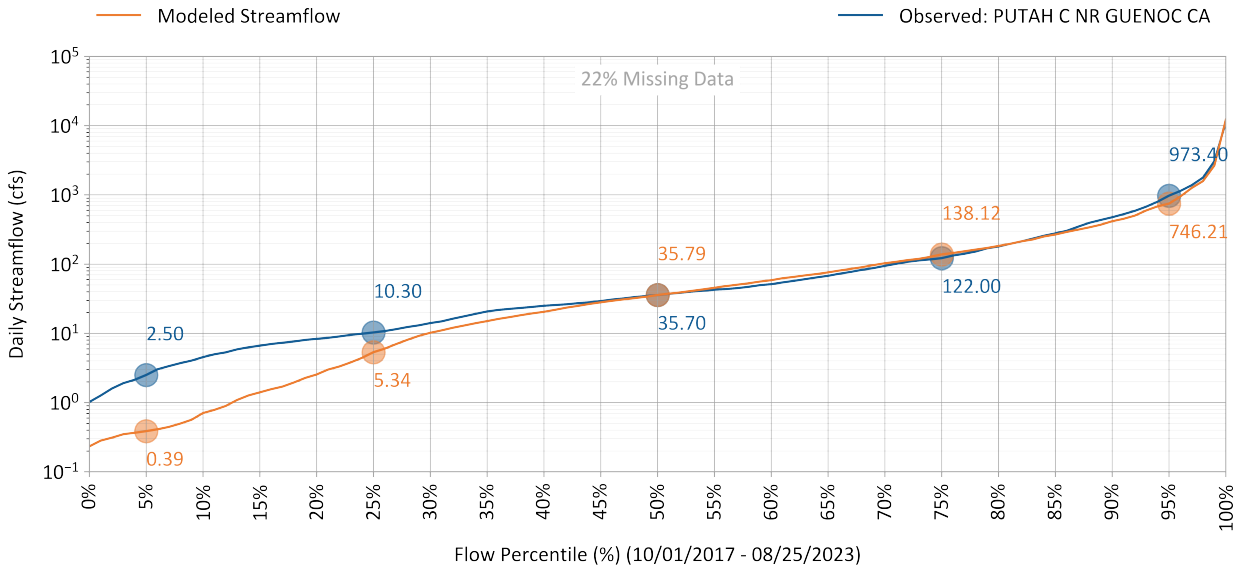

Figure 8-11. Simulated vs. observed flow duration curve for PUTAH C NR GUENOC CA (11453500).

PBIAS, NSE, and RSR performance values by season and flow regime are shown in Table 8-13, Table 8-14, and Table 8-15, respectively. The "Days Categorized as Baseflow" metric, which is derived from hydrograph separation, consistently shows "Good" model performance across all conditions and all metrics. The only metrics outside of the "Good" to "Very Good" range are for the Highest 10% of Daily Flows during the wet season and Days Categorized as Storm Flow during the dry season. These values are "Fair" for PBIAS and overpredicted by 15.2% and 20.5%, respectively.

Table 8-13. Simulated vs. observed daily streamflow PBIAS at PUTAH C NR GUENOC CA (11453500)

Calibration Metrics for Daily Flow (10/01/2017 - 09/30/2023)	Percent Bias (PBIAS)		
	All Seasons	Wet Season	Dry Season
All Conditions	9.5%	9.3%	14.1%
Highest 10% of Daily Flow Rates	15.2%	15.3%	N/A
Days Categorized as Storm Flow	7.8%	7.5%	20.5%
Days Categorized as Baseflow	11.8%	11.7%	12.1%

Table 8-14. Simulated vs. observed daily streamflow NSE at PUTAH C NR GUENOC CA (11453500)

Calibration Metrics for Daily Flow (10/01/2017 - 09/30/2023)	Nash-Sutcliffe Efficiency (NSE)		
	All Seasons	Wet Season	Dry Season
All Conditions	0.86	0.86	0.85
Highest 10% of Daily Flow Rates	0.76	0.76	N/A
Days Categorized as Storm Flow	0.85	0.84	0.87
Days Categorized as Baseflow	0.89	0.89	0.83

Table 8-15. Simulated vs. observed daily streamflow RSR at PUTAH C NR GUENOC CA (11453500)

Calibration Metrics for Daily Flow (10/01/2017 - 09/30/2023)	RMSE-Std. Dev. Ratio (RSR)		
	All Seasons	Wet Season	Dry Season
All Conditions	0.37	0.38	0.38
Highest 10% of Daily Flow Rates	0.48	0.49	N/A
Days Categorized as Storm Flow	0.39	0.4	0.36
Days Categorized as Baseflow	0.33	0.34	0.41

Very Good | Good | Fair | Poor

\- Overpredicts | + Underpredicts

Table 8-16. Daily streamflow metric data count for Calibration period Wet and Dry seasons for at PUTAH C NR GUENOC CA (11453500)

Counts used for calibration Metrics (10/01/2017 - 09/30/2023)	Data Count		
	All Seasons	Wet Season	Dry Season
All Conditions	1,717	1,124	593
Highest 10% of Daily Flow Rates	172	170	2
Days Categorized as Storm Flow	604	421	183
Days Categorized as Baseflow	1,113	703	410

The current calibrated model underpredicts streamflow during low flow conditions, as indicated by the FDC (Figure 8-11), which is conservative for management scenarios focused on maintaining minimal flows. Examination of seasonal simulated vs. observed daily hydrograph plots led to the following observations:

- There appears to be an increasing flow trend at the beginning of some water years that the model is not currently representing. Figure 8-12 provides an example of this where, after the first small storm in October, there is no more precipitation, but the observed flow increases by several cfs until the first large storm in mid-November. The USGS has documented that the Putah Creek near Guenoc gauge has "some regulation by Hartmann Dam on Coyote Creek since 1969 … diversions and ground-water withdrawals for domestic use and irrigation of about 1,600 acres above station"[1]. This waterbody, Hidden Valley Lake, is not currently represented in the model.
- The timing for surface water withdrawals does not provide the temporal resolution to capture intra-monthly withdrawals. For example, in late July through the end of the dry period in Figure 8-13, observed flow has rapid declines and then recovers even though there is no rainfall. This seems indicative of surface water diversions being turned on and off.

[1] Station Manuscript page:
https://waterdata.usgs.gov/nwis/wys_rpt/?site_no=11453500&agency_cd=USGS#adr

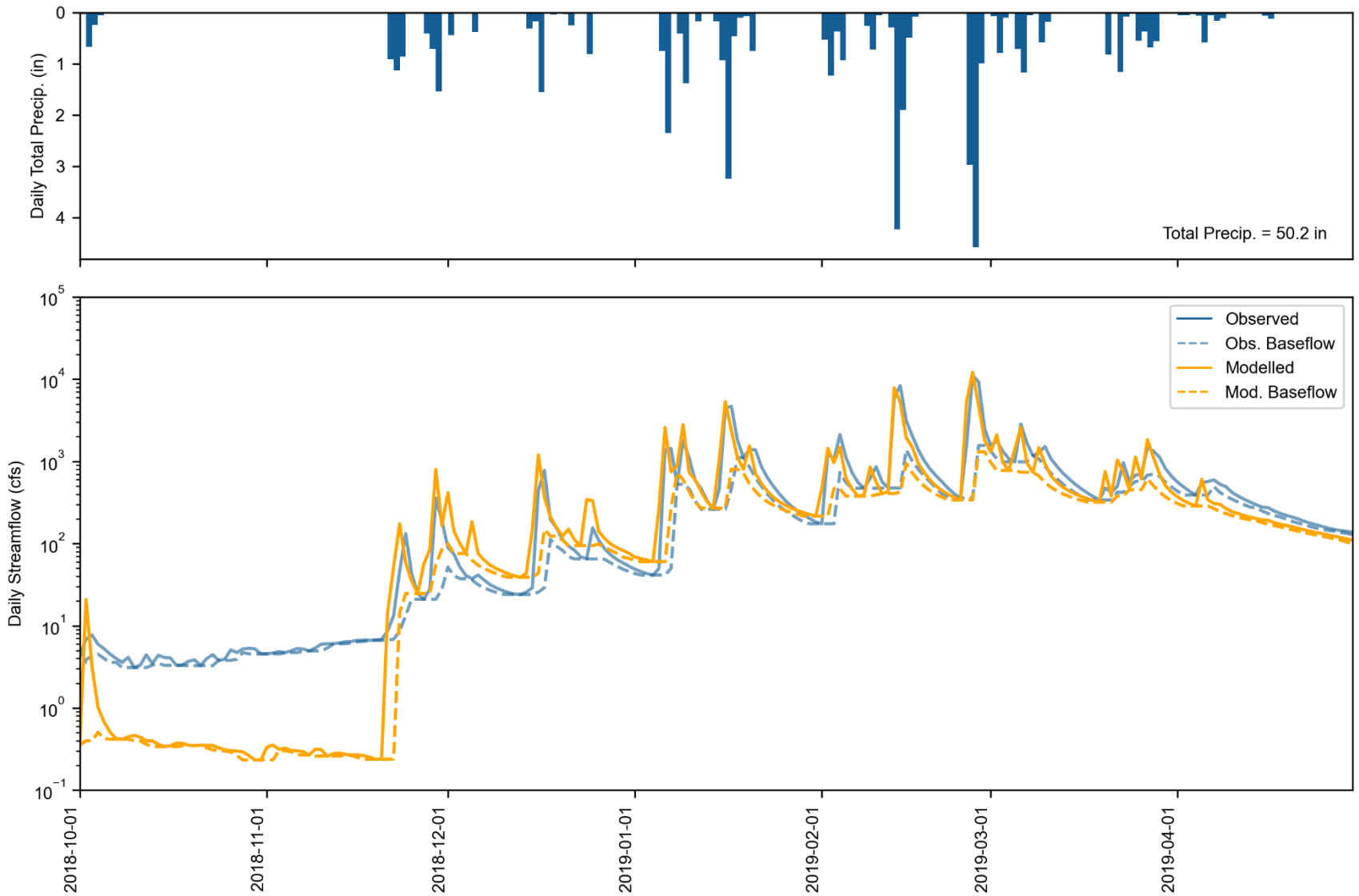

Figure 8-12. Water Year 2019 Wet season daily total precipitation (top) and streamflow (bottom) at PUTAH C NR GUENOC CA (11453500). Observed and simulated baseflow are calculated with HYSEP.

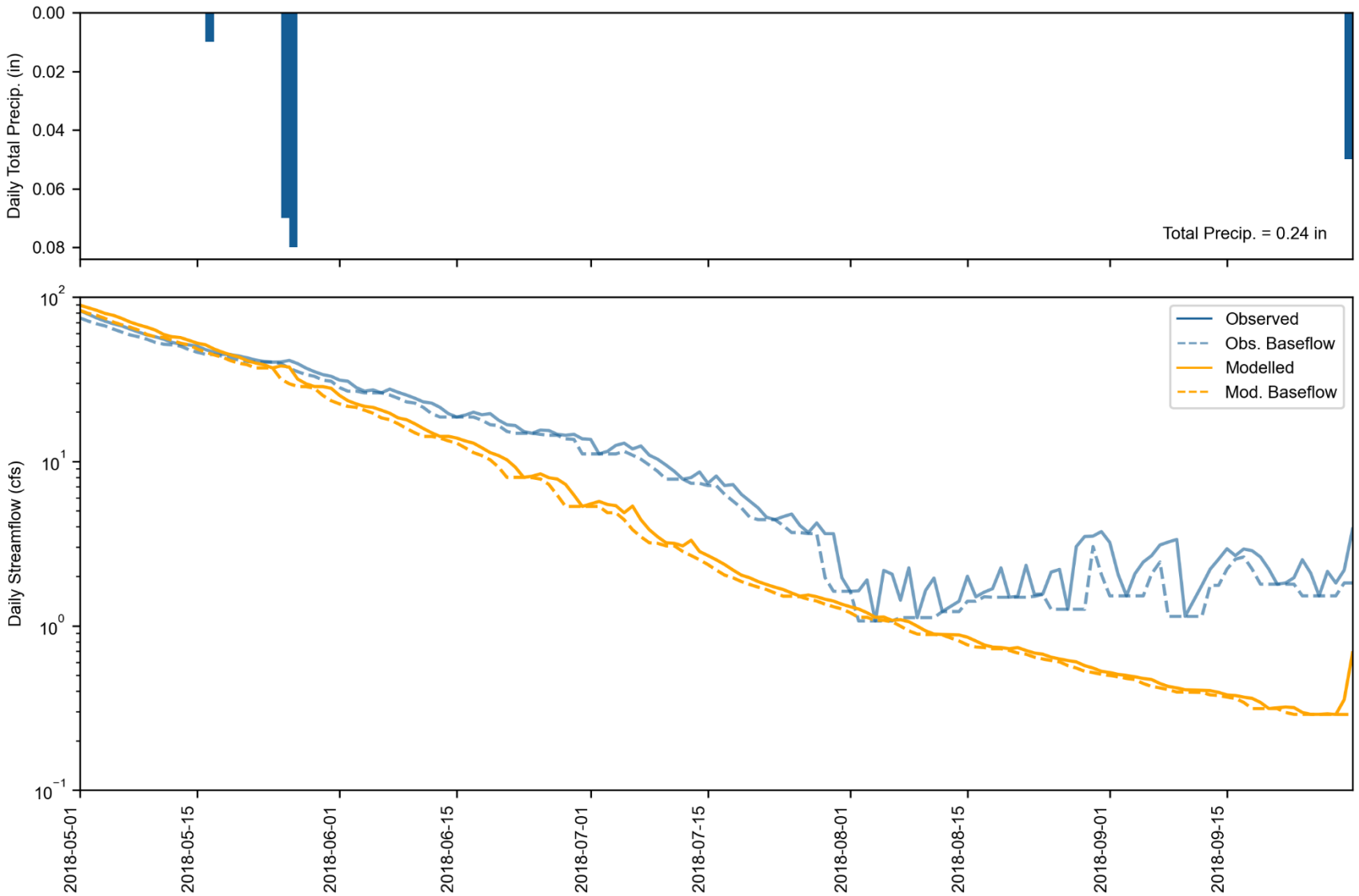

Figure 8-13. Water Year 2018 Dry season daily total precipitation (top) and streamflow (bottom) at PUTAH C NR GUENOC CA (11453500). Observed and simulated baseflow are calculated with HYSEP.

9 MODEL VALIDATION

The model was calibrated for water years 2018-2023 (6 years) and validated for water years 2004-2017 (previous 13 years) at the Putah Creek near Guenoc gauge. Spatial validation was carried out using the full period of record overlapping the simulation period for other gauges listed in Table 8-1 First, a water budget analysis was conducted for the period 2018-2023 because reported diversion estimates were only available for that period. Next, the irrigation water budget was confirmed by normalizing associated inputs and outputs by total irrigated area. This validation check was to confirm that applied irrigation water and withdrawals as represented using the coefficients, rates, and methods described in Section 5.1 produced a reasonable and representative average monthly distribution relative to the precipitation and evapotranspiration meteorological forcing data. Irrigation was simulated for the full period from 2004-2023. This section presents results for the water budget analysis (Section 9.1), the validation period performance at gauges upstream and downstream of Lake Berryessa (Section 9.2 and 9.4, respectively), and a detailed examination of the simulated representation of Lake Berryessa (Section 9.3).

9.1 Water Budget

A water budget analysis was conducted to validate a match between the sum of model inputs and outputs. Water inputs include precipitation (both to land segments and water body surfaces) and applied irrigation water. Water outputs include terminal outflow at the Putah Creek near Guenoc gauge, total actual evapotranspiration (from land segments + direct evaporation from water bodies), and total withdrawals (i.e., irrigation and non-irrigation diversion). The water budget was calculated from October 2004 through September 2023. The water budget validation showed a close match between all model inputs and outputs—there is a 0.06 % difference between inflow and outflow, which represents net volume to/from system storage over the 20-year simulation period; this is an expected difference for water balances at the watershed scale. Figure 9-1 shows the simulated water balance expressed as total volumes and area-normalized annual average depths for water years 2004-2023 at the Putah Creek near Guenoc; these values are within +/-4% of the observed values over the same time period, as described in Section 7. Figure 9-2 shows monthly average area-normalized simulated water balance components for the same period. In both figures, intermediate values for edge-of-stream outflows prior to stream routing (i.e., surface runoff + interflow outflow + active groundwater outflow) and inflow to active groundwater storage are presented to illustrate the relative scale of those components. The monthly summary also illustrates the expected system lag of approximately 5 months between peak rainfall (Dec-Jan) and peak evapotranspiration (Apr-May).

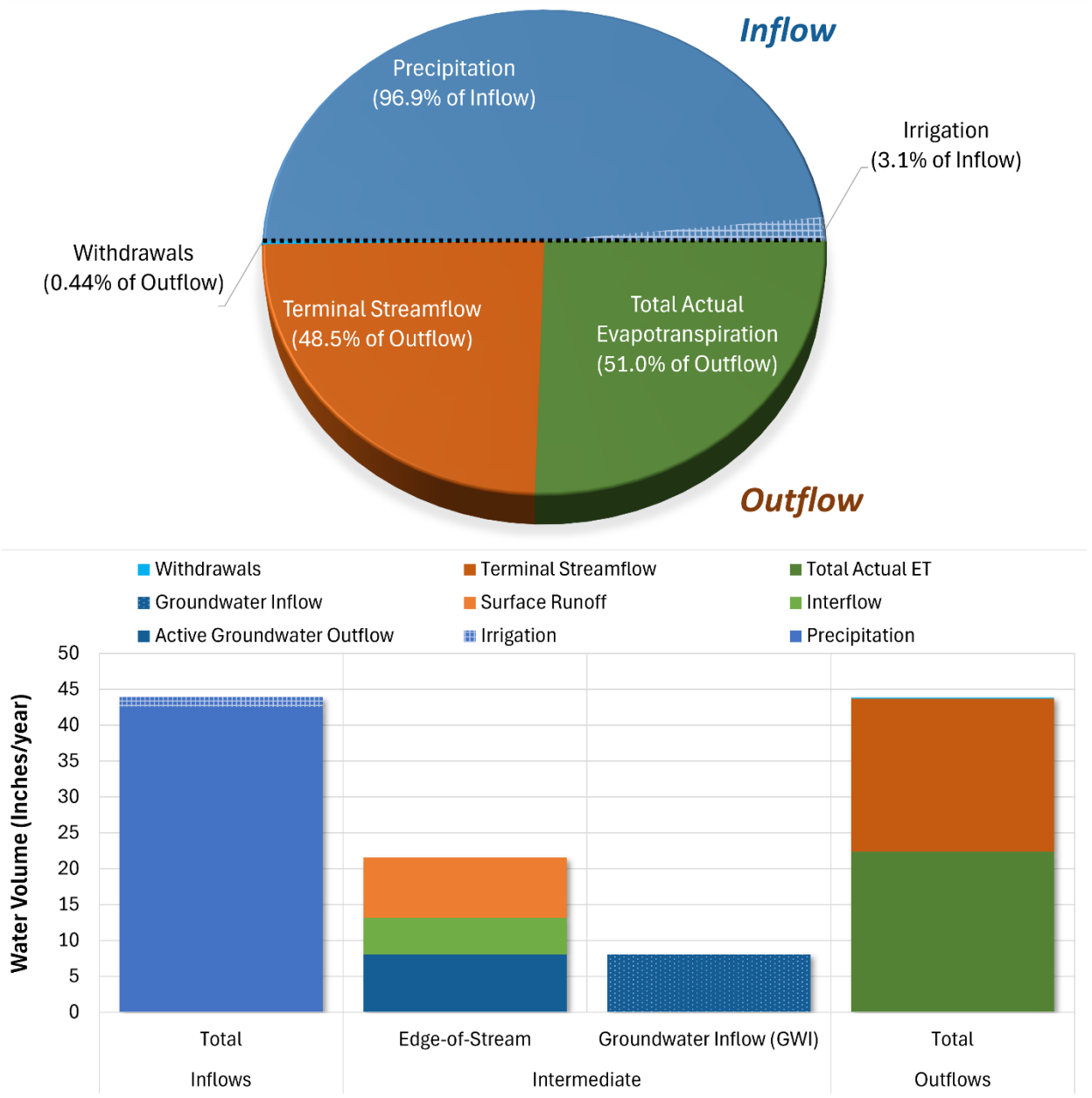

Figure 9-1. Simulated water balance expressed as total volumes and area-normalized annual average depths for the calibration period (water years 2004-2023) at the PUTAH C NR GUENOC CA (11453500) gauge.

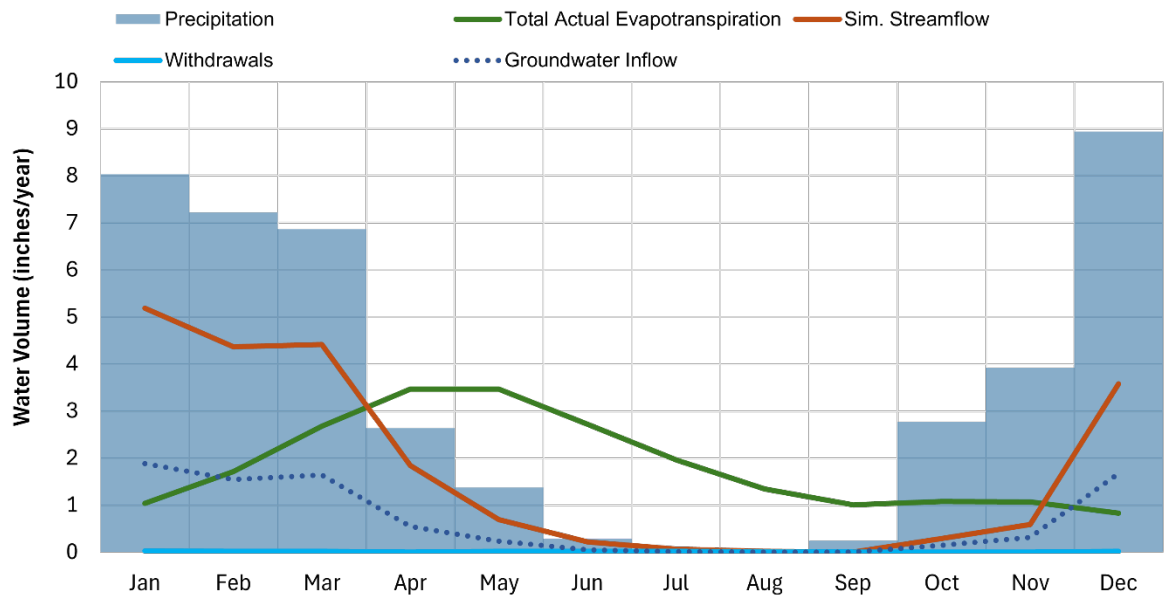

Figure 9-2. Monthly average area-normalized simulated water balance components for water years 2004-2023 at the PUTAH C NR GUENOC CA (11453500) gauge. Note that withdrawals are a minor portion of the total water balance within this drainage area.

The water budget for applied irrigation volume was also summarized from calibrated model outputs. On average, a total of 8,461 acre-feet of irrigation water per year was applied on 7,880 acres of land in the Guenoc drainage area; this equates to just under 13 inches. Irrigation volume was temporally distributed with monthly evaporative coefficients (described in 5.1.3) so that more irrigation occurred during the drier months, as shown in Figure 9-3. The total reported volume of surface water withdrawn in this drainage area is negligible.

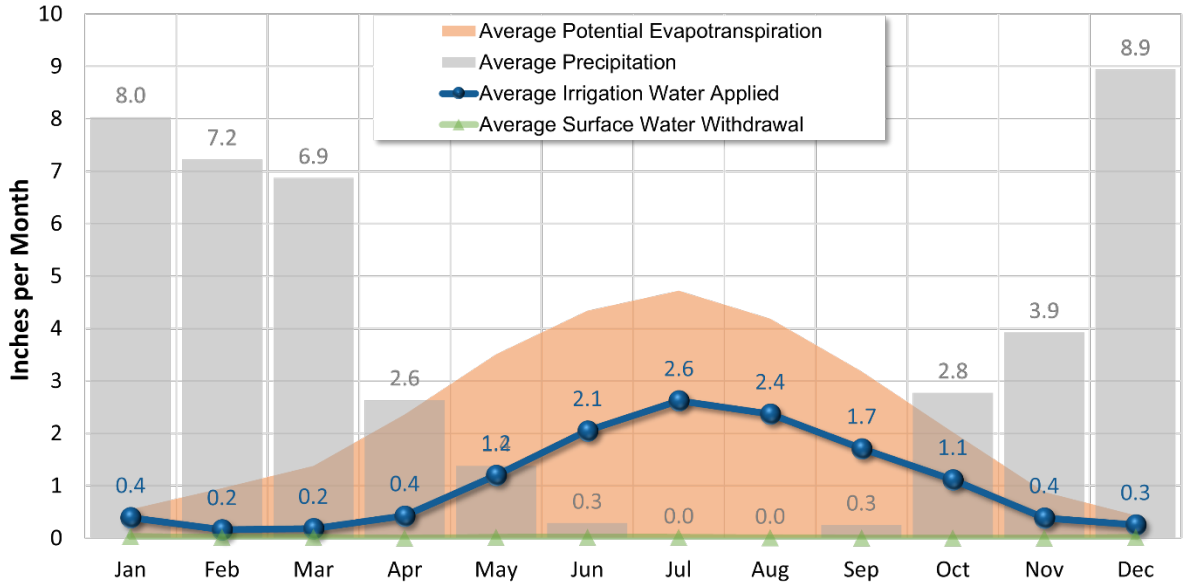

Figure 9-3. Monthly average area-normalized irrigation water balance for irrigated HRUs in the Putah Creek near Guenoc drainage area (average precipitation in this area is also plotted for reference).

9.2 Headwater Hydrology

There are two stations upstream of Lake Berryessa as shown in Figure 8-4 and Table 8-1. The validation performance of these stations is discussed here.

9.2.1 Putah Creek near Guenoc

Across the validation period (water years 2005 to 2017) hydrologic performance at Putah Creek near Guenoc was generally slightly overpredicted, as opposed to the calibration period where flows were generally slightly underpredicted. Note that all results below exclude observed average daily flows < 1 cfs, where there may be more uncertainty in gauge readings. Over the long-term simulation, PBIAS is "Very Good" and slightly overpredicted (Table 9-1); seasonal PBIAS values were also "Very Good". All calibration statistics so far, including those in Table 9-1, were computed using daily average time series and included higher resolution flow-regime metrics like the highest 10% of flows, storm flows, and baseflow. Table 9-2 is a summary of model calibration vs. validation performance metrics computed using monthly time series, as recommended by Moriasi et al. (2015). As expected, PBIAS is not impacted by the time step change, however, RSR and NSE both show notable improvement in performance compared to using daily average time series.

As with the calibration period, flow time series plots, monthly aggregate figures, and FDC were also created for the validation period, and are shown in Figure 9-4 to Figure 9-8. PBIAS, NSE, and RSR performance values by season and flow regime are shown in Table 9-3, Table 9-4, and Table 9-5 respectively. The wet and dry season daily hydrographs exhibit similar responses as were seen for the calibration period (Figure 9-9 and Figure 9-10). On average, the performance assessments demonstrate that the model performs very well across both wet and dry conditions and is a robust predictor of hydrological conditions in the Putah Creek near Guenoc drainage area and the transition periods between both individual storms and wet/dry seasons.

Table 9-1. Summary of daily validation performance metrics for PUTAH C NR GUENOC CA (11453500)

Hydrology Monitoring Locations	Performance Metrics (10/01/2004 - 09/30/2017)														
	PBIAS						RSR			NSE			KGE[1]		
	All	Wet Season	Dry Season	>10th %ile Flows	Storm Flows	Baseflow	All	Wet Season	Dry Season	All	Wet Season	Dry Season	All	Wet Season	Dry Season
PUTAH C NR GUENOC CA	-0.5%	-0.4%	-2.2%	9.8%	-2.8%	2.8%	0.37	0.38	0.55	0.87	0.86	0.7	0.9	0.88	0.97

[1] Monthly, as specified in Table 8-3.

Very Good | Good | Fair | Poor

\- Overpredicts | + Underpredicts

Table 9-2. Summary of calibration performance metrics using monthly averages at PUTAH C NR GUENOC CA (11453500)

Calibration Metrics for Monthly Flow (10/01/2004 - 09/30/2017)	Hydrological Condition		
	All (n = 139)	Wet Season (n = 84)	Dry Season (n = 55)
Percent Bias (PBIAS)	-0.5%	-0.4%	-2.2%
Nash-Sutcliffe Efficiency (NSE)	0.96	0.95	0.97
RMSE-Std. Dev. Ratio (RSR)	0.21	0.22	0.18
Kling–Gupta Efficiency (KGE)	0.9	0.88	0.97

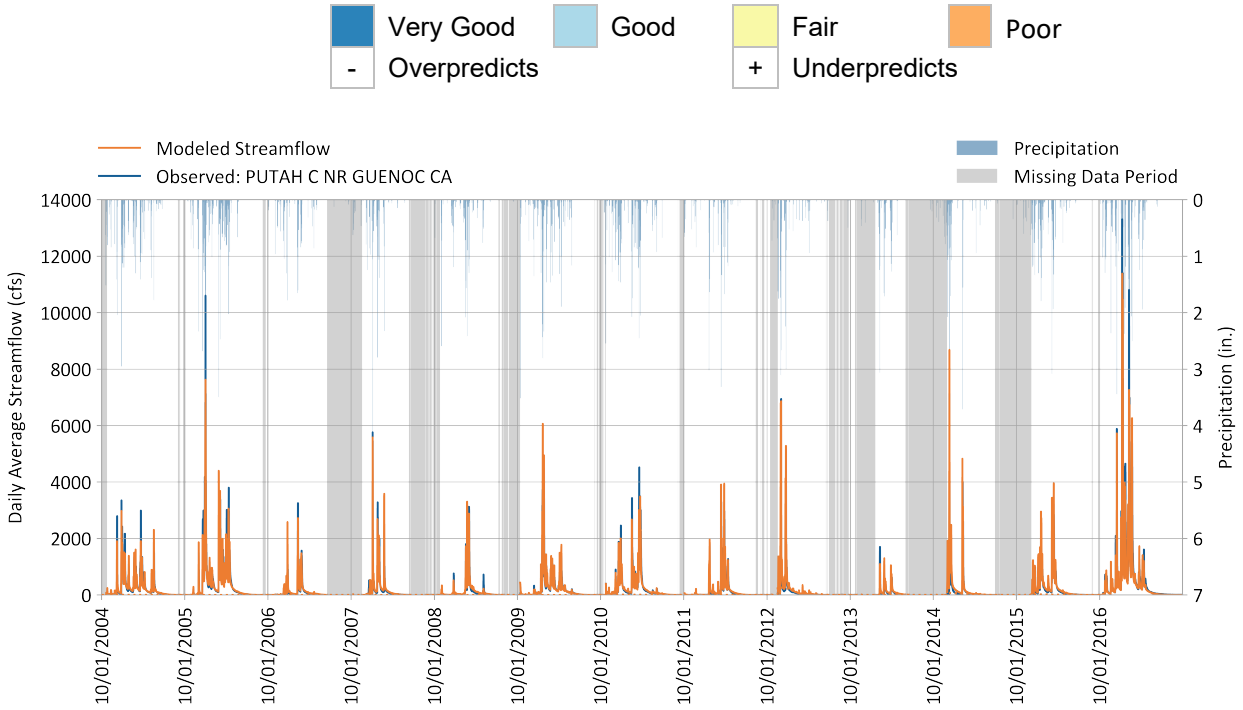

Figure 9-4. Daily simulated vs. observed streamflow for PUTAH C NR GUENOC CA (11453500).

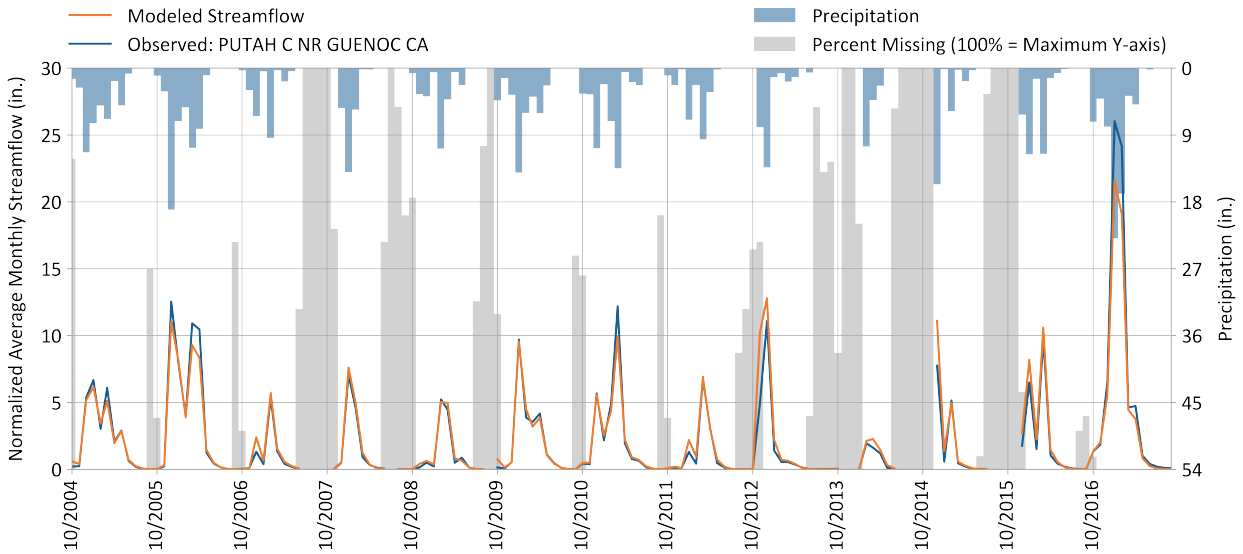

Figure 9-5. Monthly simulated vs. observed streamflow for PUTAH C NR GUENOC CA (11453500).

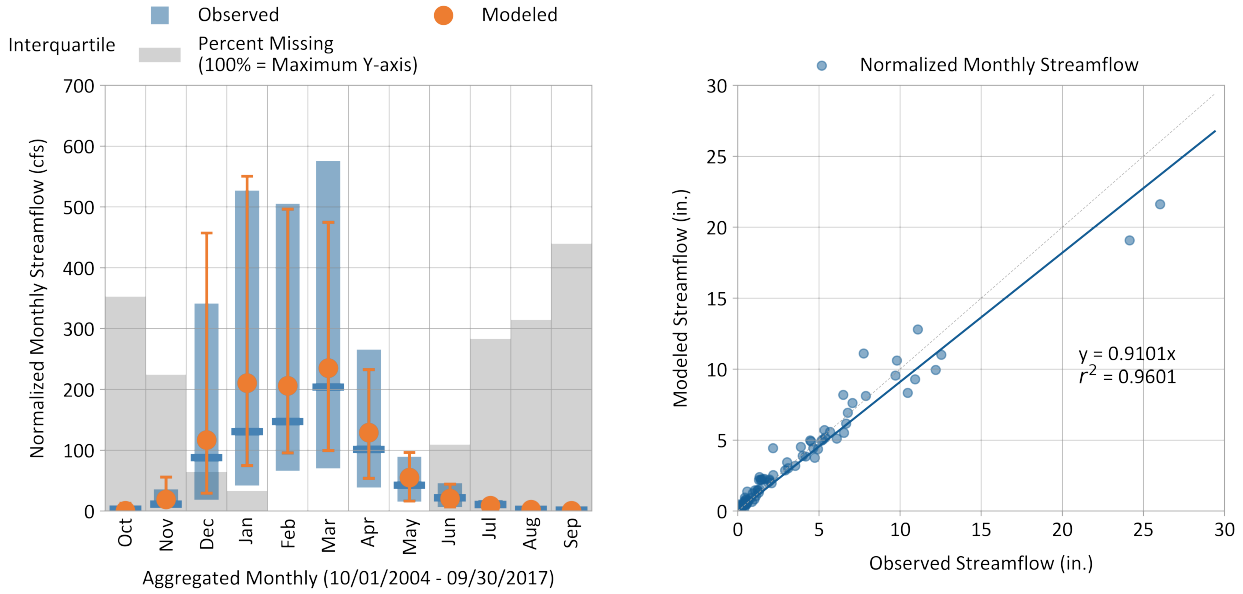

Figure 9-6. Monthly normalized simulated vs. observed streamflow for PUTAH C NR GUENOC CA (11453500).

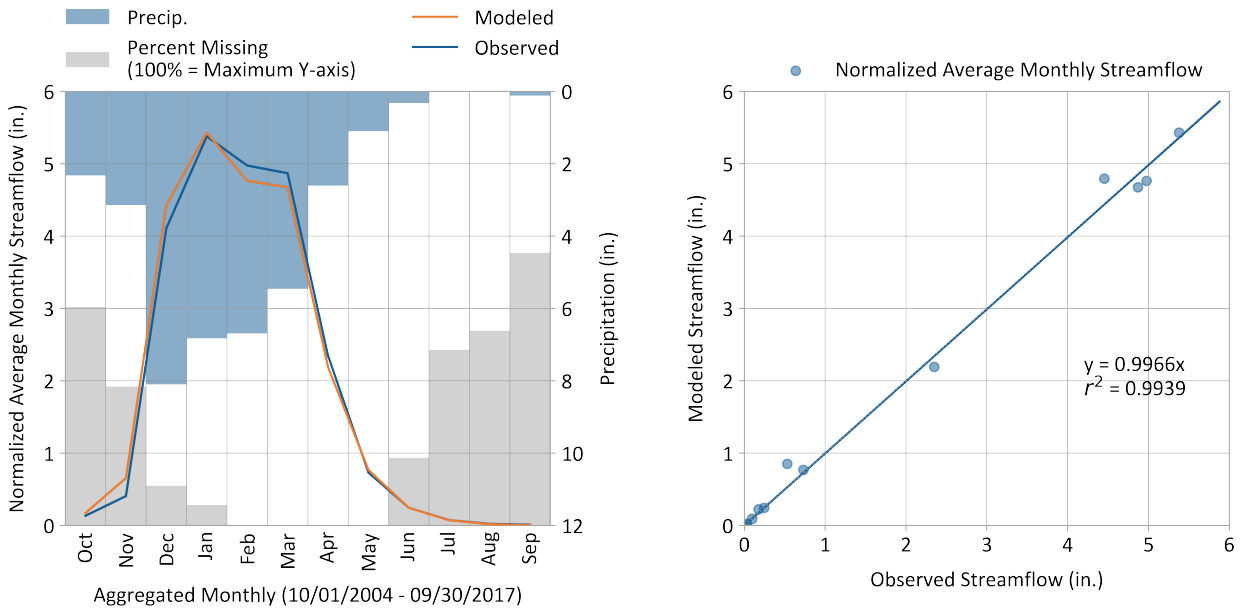

Figure 9-7. Average monthly simulated vs. observed streamflow for PUTAH C NR GUENOC CA (11453500).

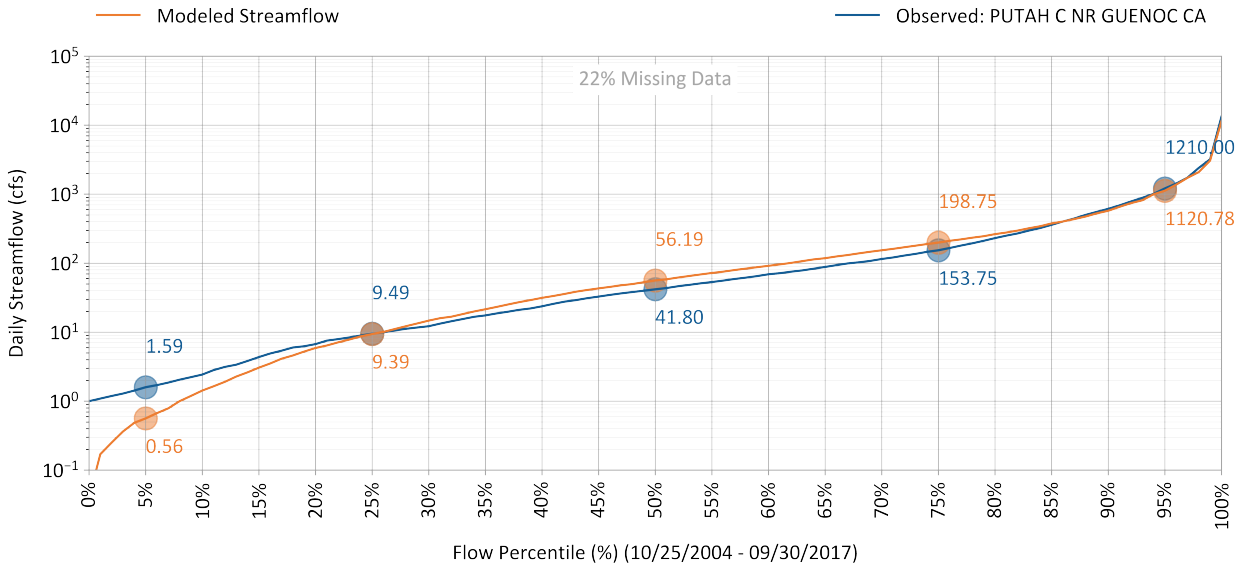

Figure 9-8. Simulated vs. observed flow duration curve for PUTAH C NR GUENOC CA (11453500).

Table 9-3. Simulated vs. observed daily streamflow PBIAS at PUTAH C NR GUENOC CA (11453500)

Calibration Metrics for Daily Flow (10/01/2004 - 09/30/2017)	Percent Bias (PBIAS)		
	All Seasons	Wet Season	Dry Season
All Conditions	-0.5%	-0.4%	-2.2%
Highest 10% of Daily Flow Rates	9.8%	9.7%	23.4%
Days Categorized as Storm Flow	-2.8%	-3.1%	5.7%
Days Categorized as Baseflow	2.8%	3.5%	-5.5%

Table 9-4. Simulated vs. observed daily streamflow NSE at PUTAH C NR GUENOC CA (11453500)

Calibration Metrics for Daily Flow (10/01/2004 - 09/30/2017)	Nash-Sutcliffe Efficiency (NSE)		
	All Seasons	Wet Season	Dry Season
All Conditions	0.87	0.86	0.7
Highest 10% of Daily Flow Rates	0.76	0.76	-1.08
Days Categorized as Storm Flow	0.86	0.86	0.65
Days Categorized as Baseflow	0.85	0.84	0.9

Table 9-5. Simulated vs. observed daily streamflow RSR at PUTAH C NR GUENOC CA (11453500)

Calibration Metrics for Daily Flow (10/01/2004 - 09/30/2017)	RMSE-Std. Dev. Ratio (RSR)		
	All Seasons	Wet Season	Dry Season
All Conditions	0.37	0.38	0.55
Highest 10% of Daily Flow Rates	0.49	0.49	1.44
Days Categorized as Storm Flow	0.37	0.38	0.59
Days Categorized as Baseflow	0.39	0.4	0.31

Very Good | Good | Fair | Poor

\- Overpredicts | + Underpredicts

Table 9-6. Daily streamflow metric data count for validation period Wet and Dry seasons for at PUTAH C NR GUENOC CA (11453500)

Counts used for calibration Metrics (10/01/2004 - 09/30/2017)	Data Count		
	All Seasons	Wet Season	Dry Season
All Conditions	3714	2375	1339
Highest 10% of Daily Flow Rates	372	367	5
Days Categorized as Storm Flow	1298	908	390
Days Categorized as Baseflow	2416	1467	949

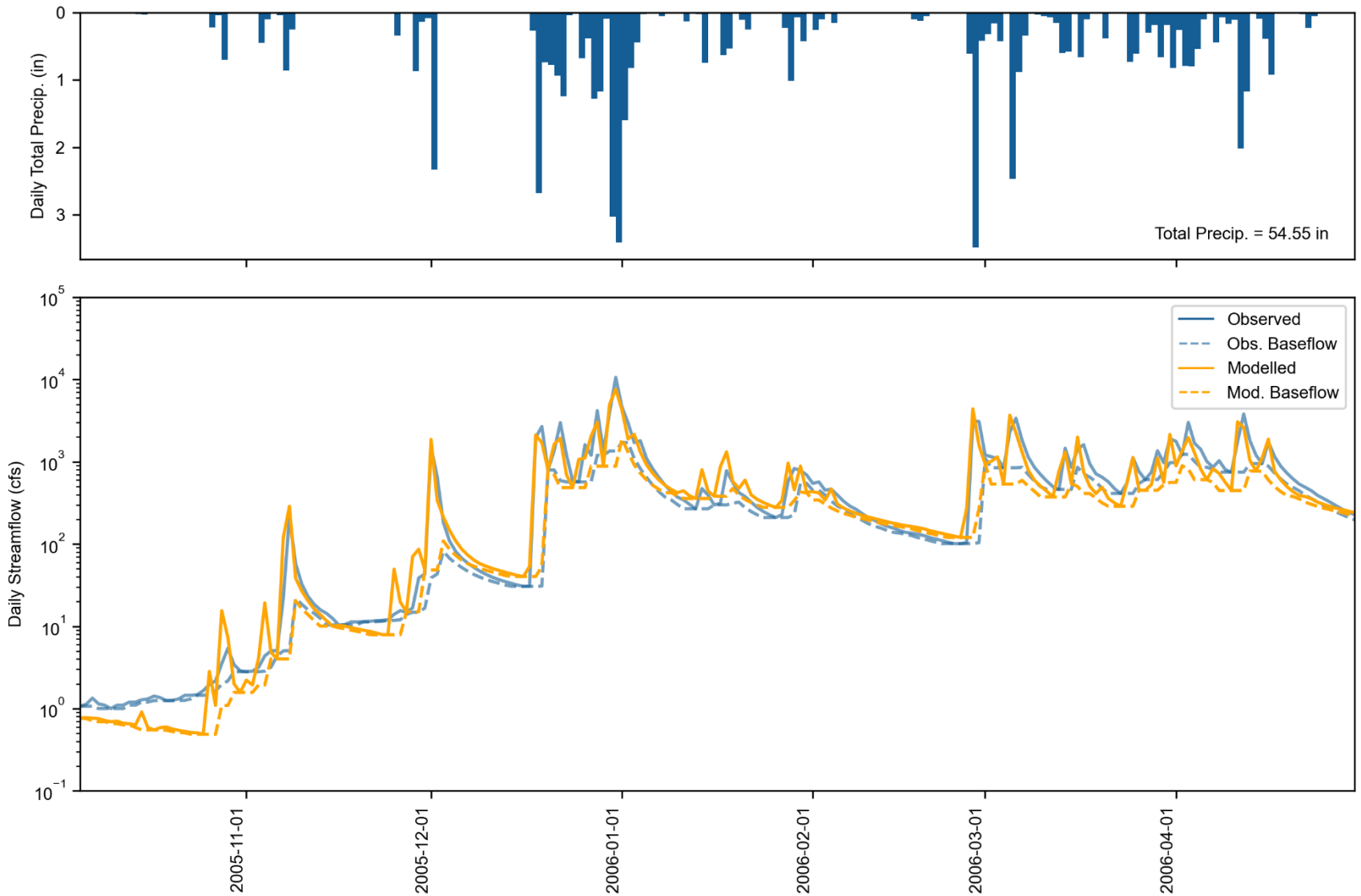

Figure 9-9. Water Year 2006 Wet season daily total precipitation (top) and streamflow (bottom) at PUTAH C NR GUENOC CA (11453500). Observed and simulated baseflow are calculated with HYSEP.

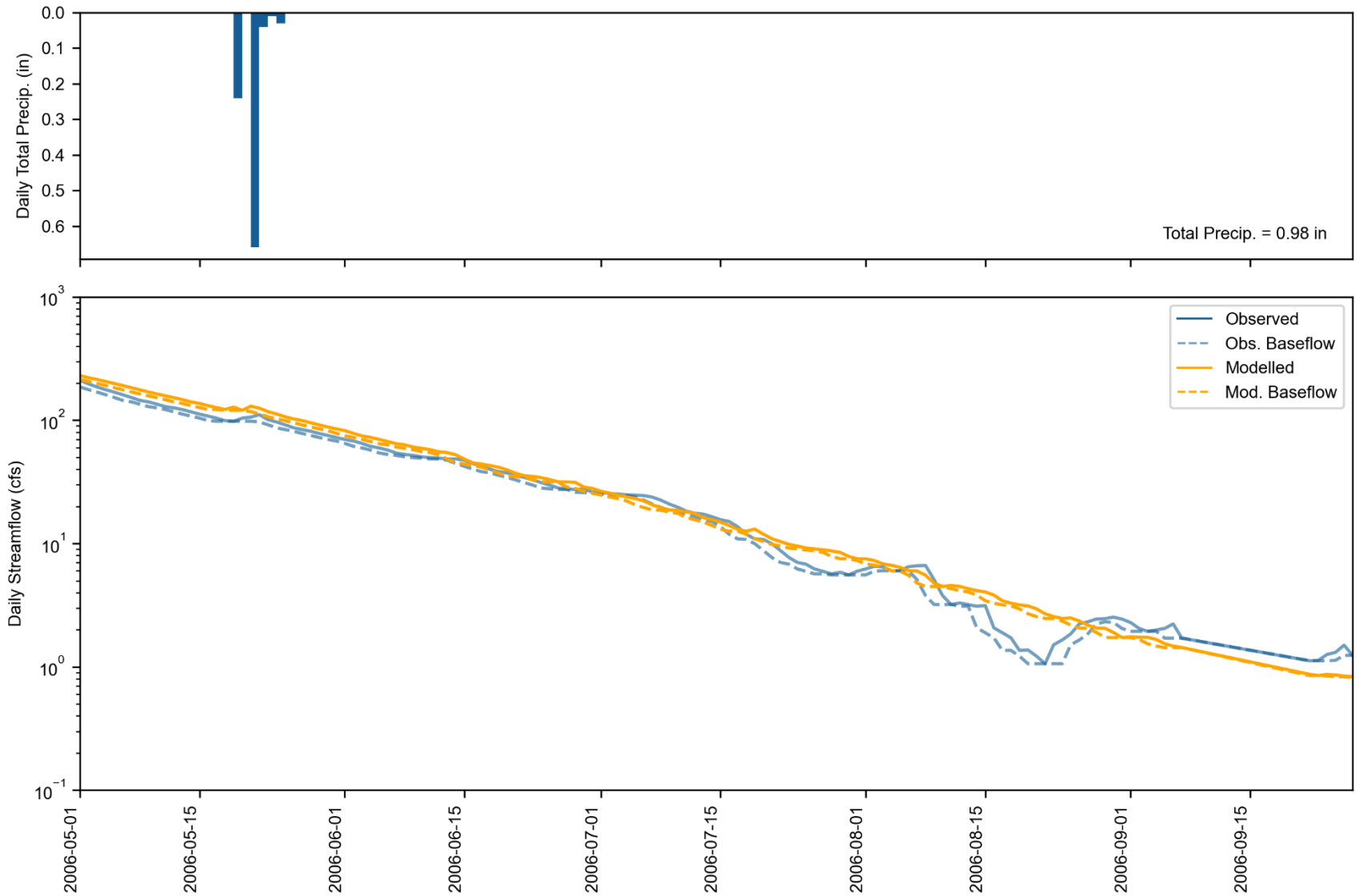

Figure 9-10. Water Year 2006 Dry season daily total precipitation (top) and streamflow (bottom) at PUTAH C NR GUENOC CA (11453500). Observed and simulated baseflow are calculated with HYSEP.

9.2.2 Pope Creek at Walter Springs

Three years of wet season observed flow data for Pope Creek at Walter Springs were available, part of which occurred during a severe drought. Only 8 percent of observed flows exceed the 1 cubic foot per second threshold required for inclusion in performance metrics—which substantially limits the station's usefulness as a validation location until a longer period of record is established—therefore all available data were used. Due to the limited number of viable observations, performance evaluation focused on R-squared results only (Table 9-7). The R-squared metric measures the degree of linear relationship in the variability of observed and simulated data, describing how well the model predicts the timing of streamflow. Values for R-squared range from 0 to 1, with 1 indicating a perfect fit; values greater than 0.85 indicate a very good fit while values ≤ 0.6 indicate a poor match of simulated and observed values (Donigian 2000). For daily flows, R-squared is 0.62, indicating "Fair" correspondence between simulated and observed variability. Monthly flows yield a similar value of 0.63.

A key takeaway from the model's performance at the Pope Creek station is that there may be fundamental differences in hydrologic responses in this drainage area as opposed to the Putah Creek near Guenoc drainage area. Examination of the daily hydrograph during WY 2021 (Figure 9-11) shows that the observed flow is very flashy with peaks that rapidly recede and may go to zero during the dry season; this is not currently captured by the model. Overall, despite the limited and drought-influenced record, the model reproduces variability and storm-driven dynamics reasonably well, with reduced agreement during baseflow conditions. A longer period of observed streamflow data is needed for further analyses or model adjustment in this drainage area. Some additional discussion of the processes potentially impacting Pope Creek, as they relate to Lake Berryessa, is provided in Section 9.3. A photo depicting the landscape in Pope Valley near the gauge is presented in Figure 9-12.

Table 9-7. Summary of R-Squared performance metrics for POPE C A WALTER SPRINGS CA (11453590)

Hydrology Monitoring Location	Performance Metrics (12/24/2020 - 04/30/2023)	
	R-Squared	
	Daily (n = 212)	Monthly (n = 10)
POPE C A WALTER SPRINGS CA	0.62	0.63

Very Good - Overpredicts | Good | Fair + Underpredicts | Poor

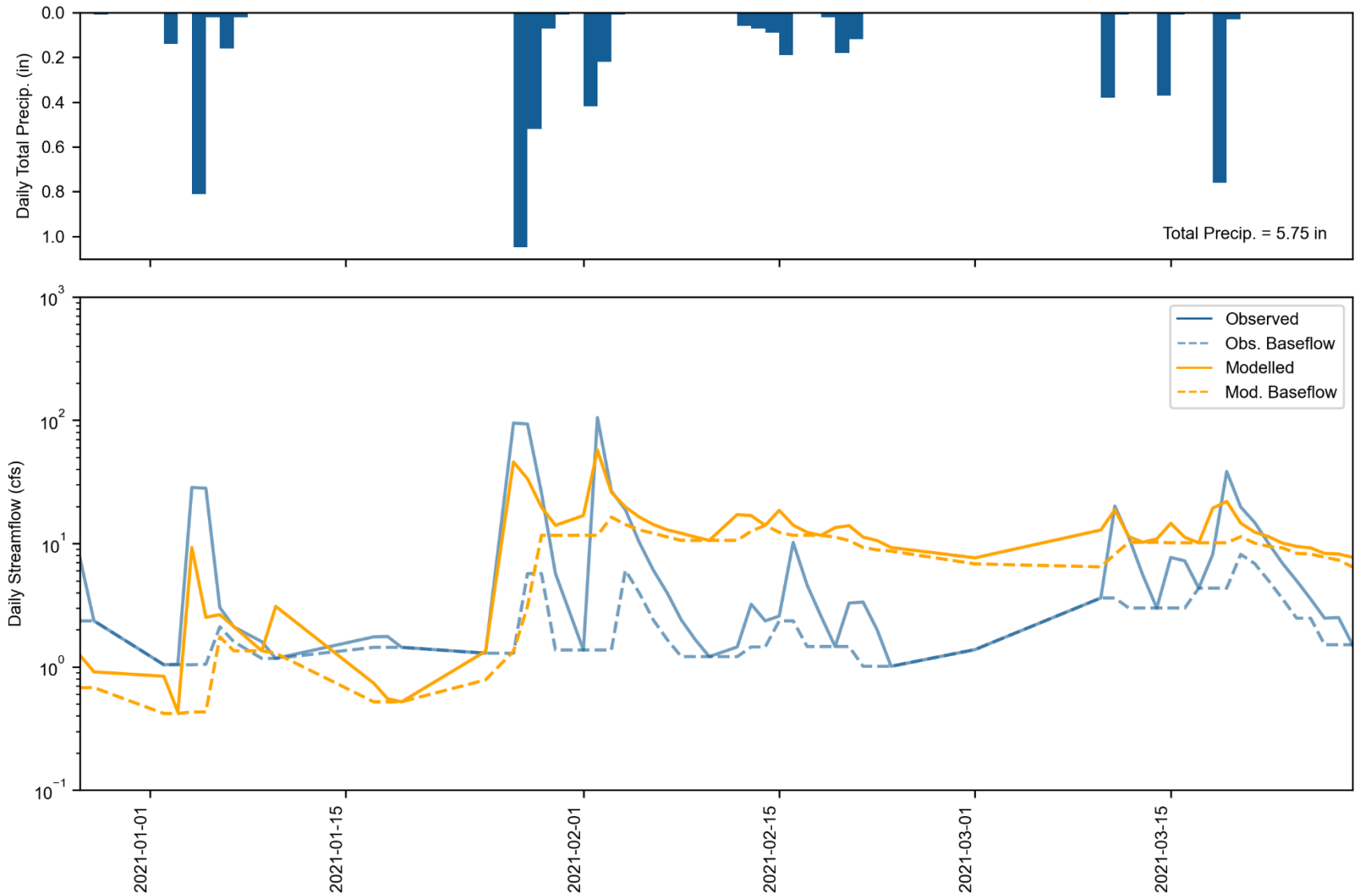

Figure 9-11. Water Year 2021 Wet season daily total precipitation (top) and streamflow (bottom) at POPE C A WALTER SPRINGS CA (11453590). Observed and simulated baseflow are calculated with HYSEP.

Figure 9-12. Pope Creek near the USGS station (photo taken June 4, 2025).

9.3 Lake Berryessa

The modeled representation of Lake Berryessa (discussed in Section 6) was evaluated against lake water balance data at the CDEC station; CDEC partners with the U.S. Bureau of Reclamation (USBR) to monitor the lake. CDEC and USBR monitor daily lake elevation, evaporation, and outflow. CDEC and USBR calculate other parameters from these observations, including storage volume based on the lake's depth-volume-area relationship and total inflow, which is estimated as a change in storage, releases, and evaporation. The modeled lake representation was evaluated by comparing modeled vs. observed water surface elevations, storage volume, evaporation, and outflow.

Initial evaluation of modeled lake elevation and storage showed that it was accumulating too much water compared to the observed data ("Simulated" in Figure 9-15 and Figure 9-16, respectively). This caused more frequent spillway overflow events than observed and led to an overprediction of wet-season storage and flows (i.e., February, March, April). Potential causes for the overprediction were investigated as follows:

- **Evaporation**: Evaporation from the lake, along with outflow from the dam, is a primary pathway for water loss. Evaporation is monitored by USBR using a Class A evaporation pan. This station has been moved several times and has been thought to underpredict. In a study of the lake evaporation, Jensen et al. (2005) compared the USBR pan measurements to evaporation calculations using energy-balance approaches (i.e., Penman-Monteith, Priestly-Taylor) and found that pan measurements were lower than energy-balance values (even when adjusted with a factor of 0.95 to account for shading). For WY 2004, Jensen, et al. estimated 57 inches of evaporation using the shade-adjusted Penman-Monteith equation, while the USBR pan measurements were 40 inches. This suggests that the USBR pan measurements are too low and not representative of actual lake surface evaporation. Water year 2004 was used as a simulation spin-up period and therefore was not compared to the Jensen value; however, the simulated values for 2005 and 2006 were 55 in and 56 in, respectively (Figure 9-13). Across the modeling period, simulated lake evaporation was 58 in/yr on average, which corresponds well with Jensen's Penman-Monteith estimates.
- **Groundwater Interactions and Geology**: As noted in the Putah Creek Modeling Work Plan[2], the watershed contains several groundwater basins, including Collayomi Valley, Coyote Valley, and Pope Valley upstream of Lake Berryessa that have active pumping. This pumping likely influences fluxes to and from the lake. Other areas of the watershed are largely composed of marine sedimentary rock, "generally considered to be non-water-bearing, but it does provide water through fractures" (DWR 2020). The geology in the watershed also includes two distinct groups with low and high potential for loss of near-surface water to deeper groundwater, largely divided by a northwest-southeast fault bisecting the watershed; a USGS report documents the regional hydrogeologic context (Thomasson et al. 1960). The northwestern portions of the watershed above Lake Berryessa have Franciscan mélange, ultramafics, and blueschist that likely have less subsurface loss and thus, may generate more surface flow. The areas southeast of the central fault are mostly Quaternary and Tertiary volcanic rocks and alluvium, which may have higher subsurface loss potential. Most reach segments of Putah Creek below Lake Solano are known to lose flow to groundwater and are within the Sacramento Valley groundwater basin (SCWA 2026).

[2] See Section 4, https://www.waterboards.ca.gov/waterrights/water_issues/programs/supply-and-demand/docs/putah-creek-workplan.pdf

The hydrogeology within the Putah Creek watershed may play a larger role in Lake Berryessa's water balance than expected; however, these detailed subsurface interactions are currently not explicitly represented in the model.

- **Upstream Inflow**: HRU hydrology was calibrated for the Putah Creek near Guenoc USGS station. Model performance at this station is generally "Good" to "Very Good" with slight underprediction during the calibration period (see Section 8.2.1) and slight overprediction during the validation period (see Section 9.2.1). Flow is overpredicted at the Pope Creek at Walter Springs station; however, observed data at that station are extremely limited (see Section 9.2.2). Given the satisfactory performance at the Guenoc station and the geology considerations noted above that are not represented in the model, it is possible that the calibrated HRU parameters for the Guenoc drainage area are not representative of areas with higher subsurface loss potential and may be generating more inflow to the lake.
- **Physical Dimensions**: As noted in Section 6, the physical dimensions of the lake (depth, volume, surface area) and the relationships between them are based on a bathymetric study of the lake conducted in 2007. This study reduced the volume at spillway depth from the estimated value from surveys prior to dam construction by approximately 3%. The change from the original surveyed estimates to the bathymetric estimates can be seen in the difference between the "F-table" and "Observed" lines in Figure 9-16 prior to 2009. No matter the source of the physical dimensions of the lake, the model representation is a simplified storage/volume/discharge relationship—there is uncertainty in how the geometry behaves since Lake Berryessa is a flooded river valley with small, distributed coves and embayments at different elevations, and not a symmetrical layering of storages as modeled.
- **Precipitation Inputs**: It is possible that the precipitation inputs to the model upstream of Lake Berryessa but downstream of the Putah Creek near Guenoc calibration station (see Figure 4-4) are higher than the actual rainfall that occurs. For example, the two stations on the Napa side of the western drainage divide near Pope Creek (GHCND:US1CANP0003 and GHCND:USC00040212) may receive more precipitation than the catchments they are assigned to on the drier eastern side of the divide (see Figure 4-3 and Figure 4-4). The orographic influence can also be seen at CDEC (ATL) and RAWS (ATLC) stations to the south and north of Atlas Peak, respectively; ALT is slightly lower in elevation but receives approximately 10 in more precipitation on an annual average basis and up to 20 in more during the wettest years. Further, the interior of the watershed, between the lake and the headwaters, lacks long-term high quality station data and is driven by the gridded PRISM-based time series.
- **Wildfires**: The watershed has experienced several wildfires that have impacted hydrology in the upstream drainage area of Lake Berryessa. Some of those changes influence interception storage and evapotranspiration, which ultimately impacts the water that reaches the lake differently before and after fires. The model was developed and calibrated using the most recent inputs and outputs impacted by fires. Those reflect an altered hydrological state that, when compared to historical periods, could also result in overpredictions. Although fire impacts were not explicitly modeled, their spatial extents and potential temporal impacts are described in Section 9.5.

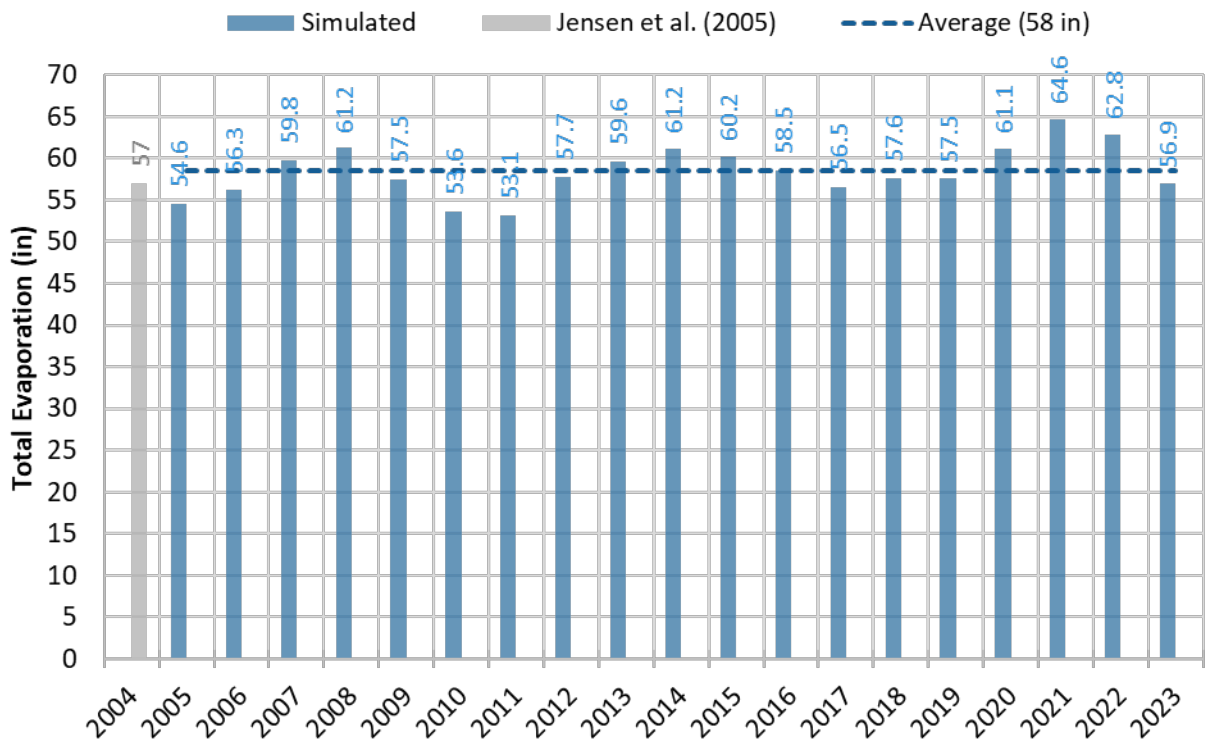

Figure 9-13. Total simulated evaporation from Lake Berryessa by water year.

The components listed above have uncertainty associated with them and likely all contribute to the high simulated accumulation in the lake. To help account for unknown losses, Jensen, et al. (2005) applied a 10 cfs seepage loss from the lake. In the absence of additional information, a logarithmic curve relating lake elevation to seepage, as shown in Figure 9-14, was applied to the current model as an initial means of accounting for all unknown losses of water from the vicinity of the lake. As shown in Figure 9-15 and Figure 9-16, the seepage greatly improves the simulated elevation and storage volume. Isolating the seepage loss estimates to the lake segment also preserves the calibration at the Guenoc gauge upstream, which is unimpacted by that loss rate. Lake elevation and volume metrics are "Good" to "Very Good" with slight underprediction across the modeled time period of 0.5% and 3.4%, respectively (Table 9-8). Elevation and volume are still overpredicted in some cases (e.g., 2011-2013), but all excess spillway events are eliminated. During drought periods (e.g., 2014-2016, 2020-2022), the simulated lake levels and volumes tend to underpredict the lowest observations, which is conservative based on the purposes of the model. These observations point to possible seasonal dynamics within the lake, and watershed as a whole, that are still unrepresented in the model but present an opportunity for further exploration and future model refinements.

Controlled, non-spillway flows from the lake closely match the CDEC observed data, indicating that the reach operations for controlled flows from the lake are operating as expected. This is indicated by the "Very Good" dry season metric in Table 9-9 and illustrated in Figure 9-17 through Figure 9-20. The slight overprediction of the other conditions is due to spillway overflows occurring over an extended amount of time compared to observations because of the slight overprediction of elevation and volume during those periods. This is especially evident during atmospheric river years such as water year 2017, as clearly seen in Figure 9-18. As shown in Figure 9-19, these events happen in March during the modeled time period; all other months have an almost perfect level of correspondence between simulated and observed values.

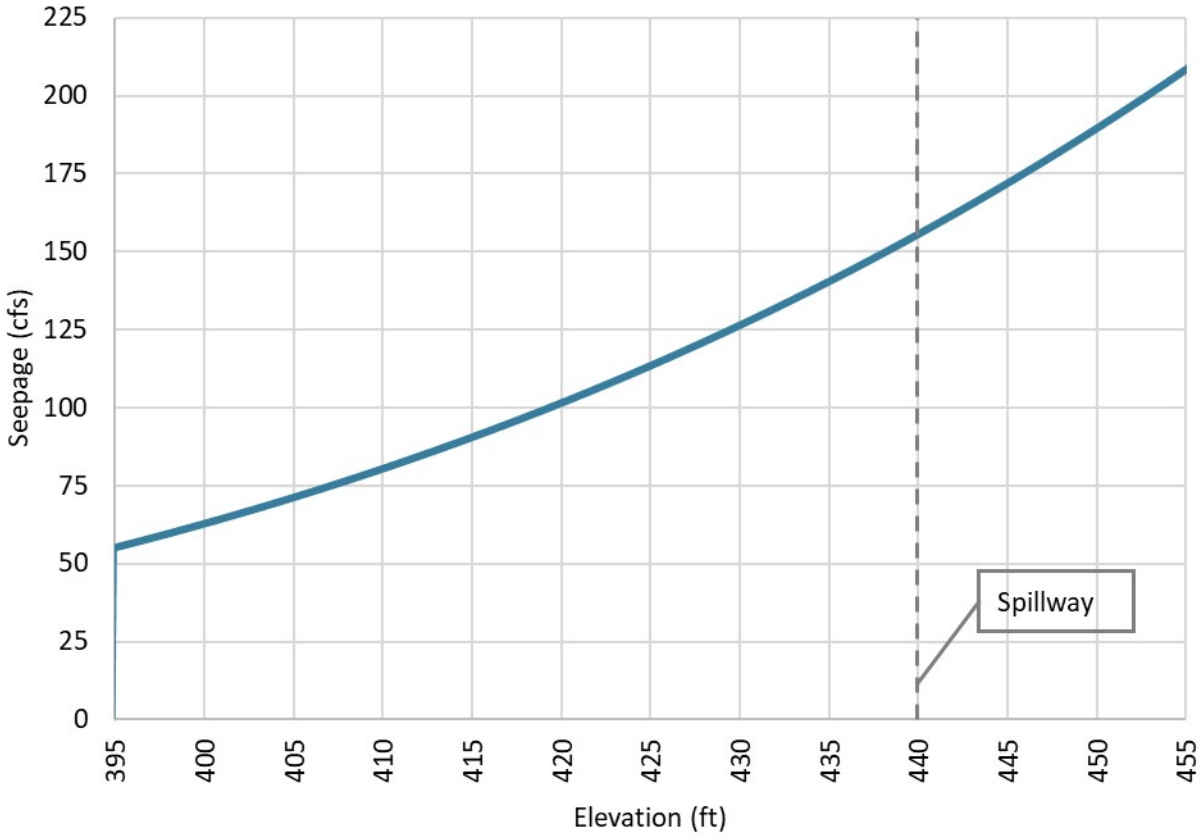

Figure 9-14. Seepage rate curve for Lake Berryessa. Note that seepage is not simulated when lake levels are below 395 ft, which corresponds to the lowest observed elevation during the modeling period.

Table 9-8. Daily calibration performance metrics for Lake Berryessa (BER) elevation and storage volume

Daily Metrics (10/01/2004 - 09/30/2023)	Elevation	Volume
Percent Bias (PBIAS)	0.5%	3.4%
RMSE-Std. Dev. Ratio (RSR)	0.30	0.34
Nash-Sutcliffe Efficiency (NSE)	0.91	0.88

Very Good Good Fair Poor
\- Overpredicts + Underpredicts

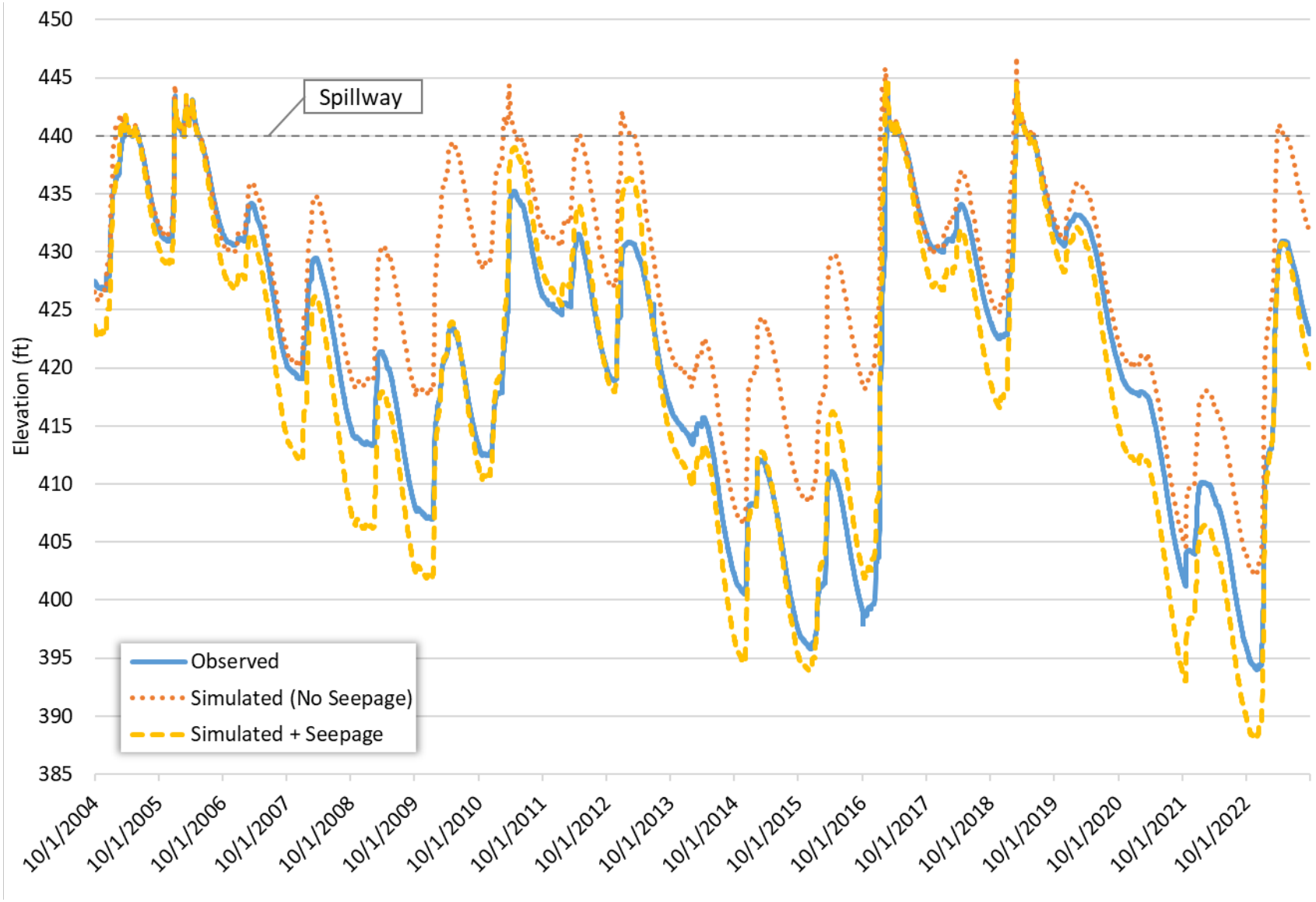

Figure 9-15. Observed and simulated elevation for Lake Berryessa, with and without seepage. Note that the spillway elevation is 440 ft.

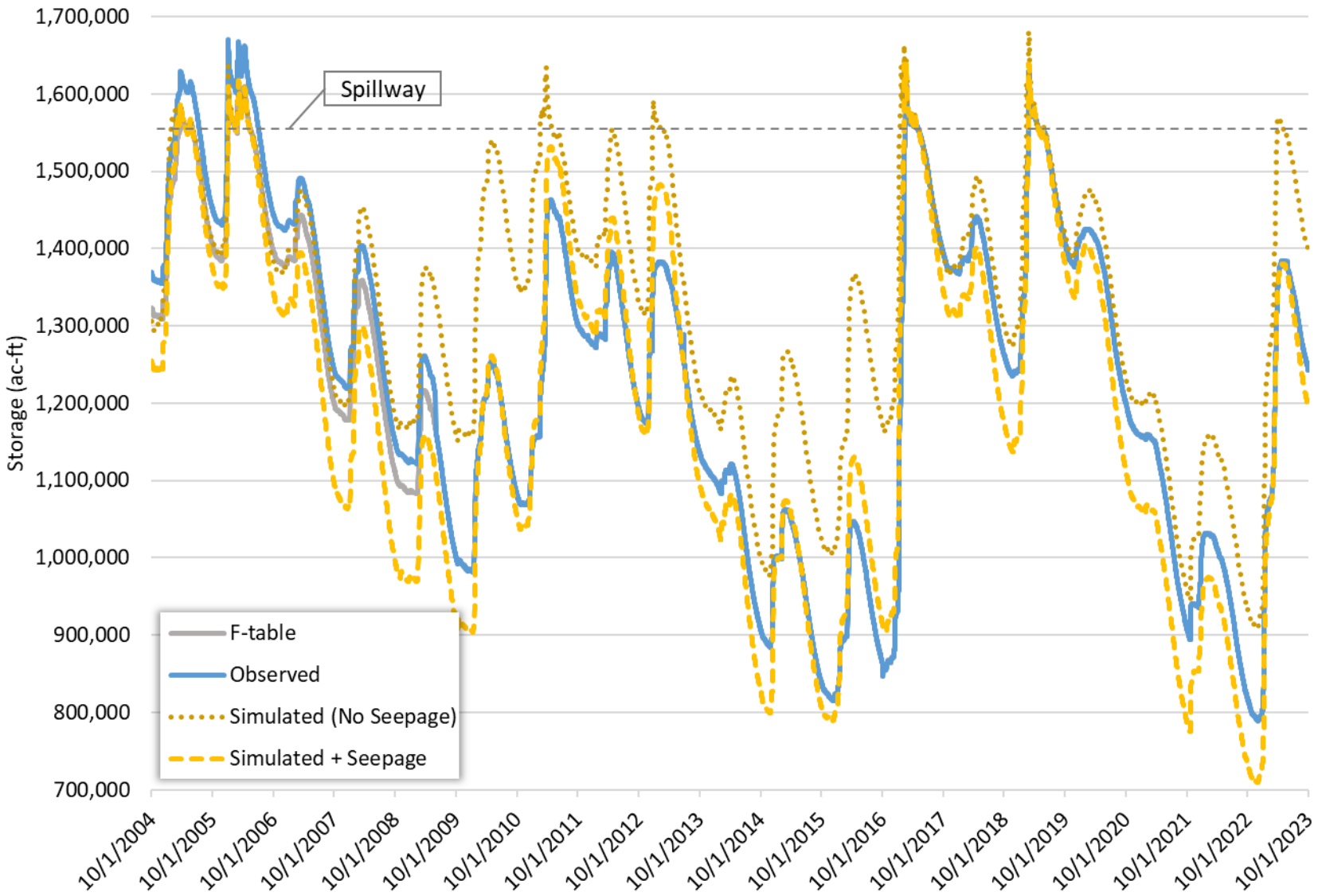

Figure 9-16. Observed and simulated storage volume for Lake Berryessa, with and without seepage. Storage volume at the spillway elevation is approximately 1,551,292 ac-ft.

Table 9-9. Summary of daily validation performance metrics for outflow from Lake Berryessa (BER)

Hydrology Monitoring Locations	Performance Metrics (10/01/2004 - 09/30/2023)														
	PBIAS						RSR			NSE			KGE[1]		
	All	Wet Season	Dry Season	>10th %ile Flows	Storm Flows	Baseflow	All	Wet Season	Dry Season	All	Wet Season	Dry Season	All	Wet Season	Dry Season
Lake Berryessa CDEC	-5.0%	-11.8%	0.3%	-9.8%	-5.3%	-4.4%	0.53	0.55	0.17	0.72	0.7	0.97	0.77	0.73	0.98

[1] Monthly, as specified in Table 8-3.

Table 9-10. Summary of validation performance metrics using monthly averages for outflow from Lake Berryessa (BER)

Calibration Metrics for Monthly Flow (10/01/2004 - 09/30/2023)	Hydrological Condition		
	All (n = 228)	Wet Season (n = 133)	Dry Season (n = 95)
Percent Bias (PBIAS)	-5.0%	-11.8%	0.3%
Nash-Sutcliffe Efficiency (NSE)	0.79	0.77	0.99
RMSE-Std. Dev. Ratio (RSR)	0.46	0.48	0.12
Kling–Gupta Efficiency (KGE)	0.77	0.73	0.98

Very Good Good Fair Poor
\- Overpredicts + Underpredicts

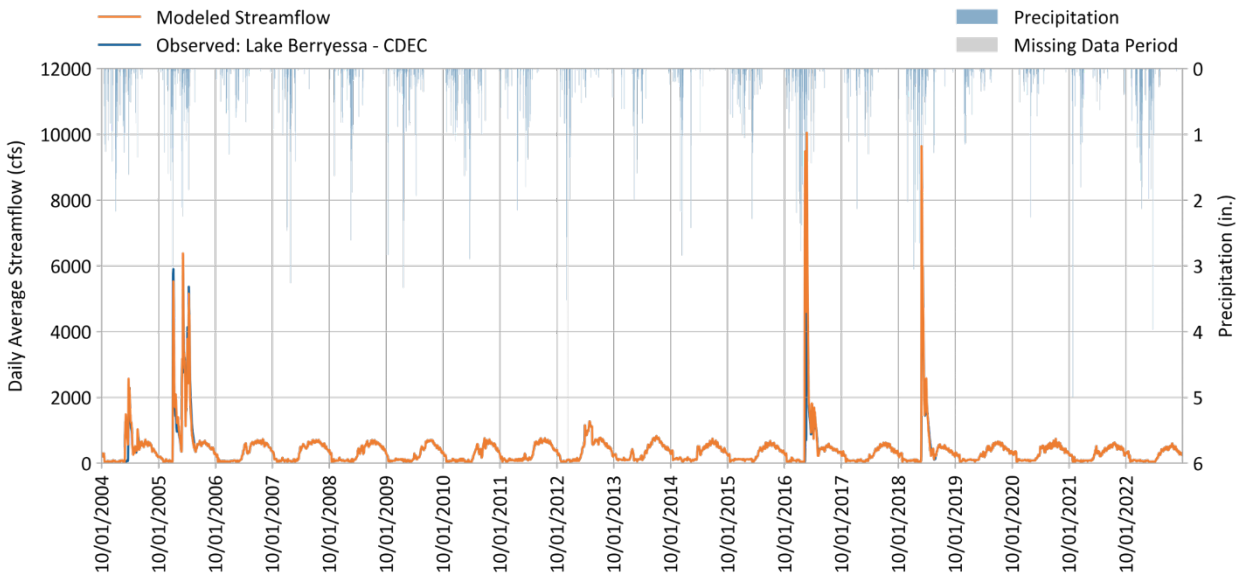

Figure 9-17. Daily simulated vs. observed outflow for Lake Berryessa (BER).

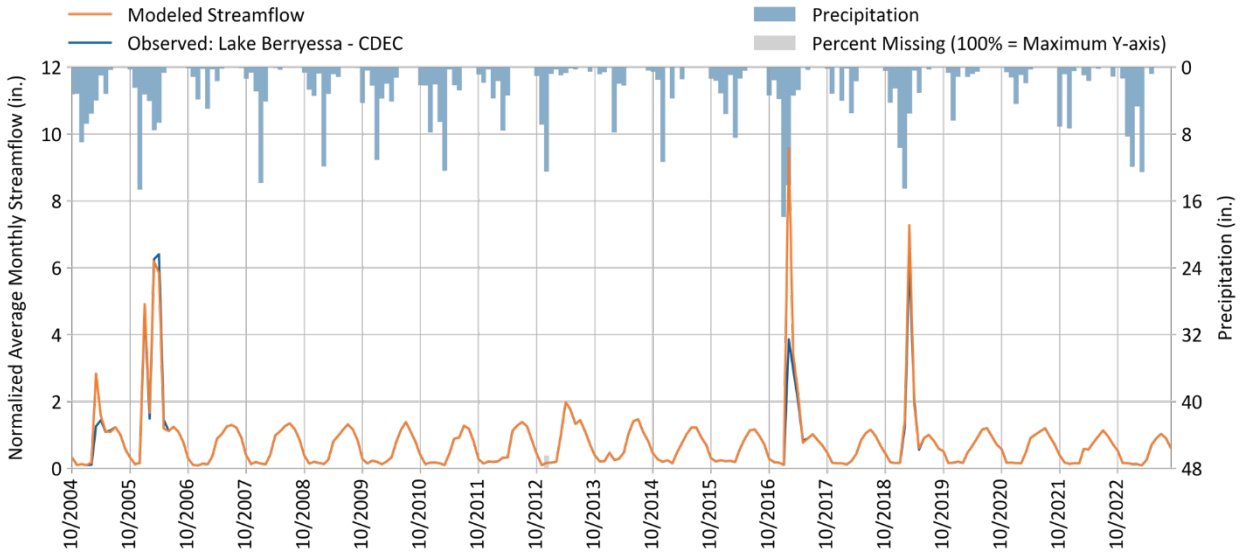

Figure 9-18. Monthly simulated vs. observed outflow for Lake Berryessa (BER).

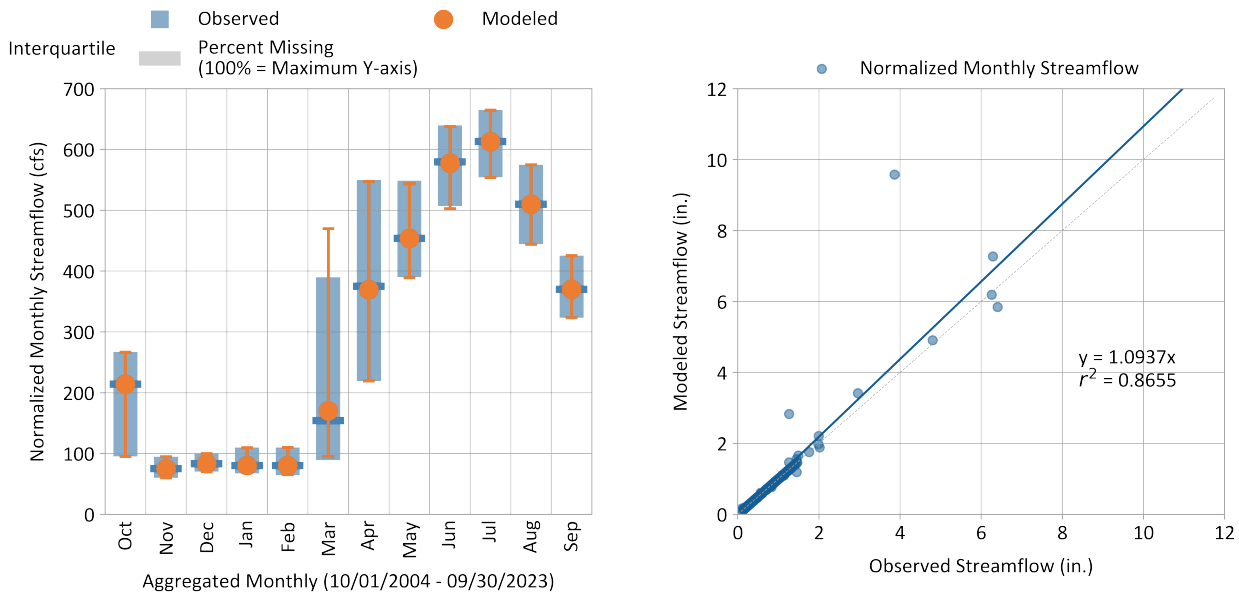

Figure 9-19. Monthly normalized simulated vs. observed outflow for Lake Berryessa (BER).

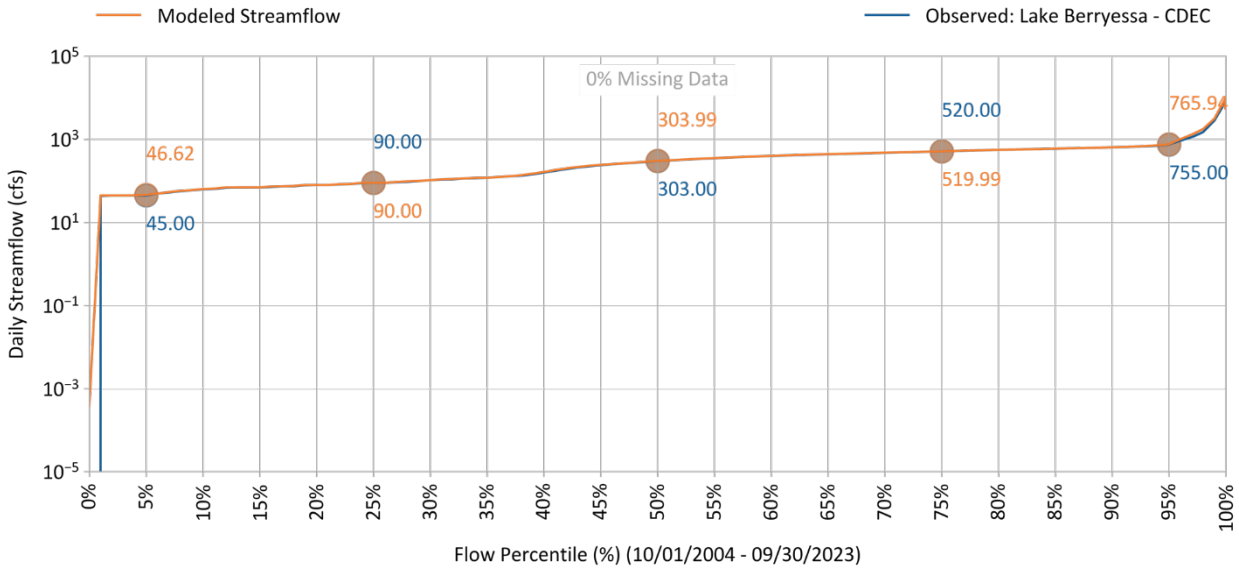

Figure 9-20. Simulated vs. observed flow duration curve for Lake Berryessa (BER).

9.4 Hydrology Downstream of Lake Berryessa

Two flow monitoring stations below Lake Berryessa, as shown in Figure 8-4 and Table 8-1, were considered for validation. Flows at the Putah Creek near Winters station are predominately controlled by the lake outflow with only a small contribution from areas below the lake. The other station is the Putah South Canal, which exports water out of the Putah Creek watershed. There are additional

stations downstream of Lake Solano where the SCWA monitors flow in Putah Creek (SCWA 2026); however, these stations were outside the scope for calibration and validation for this modeling effort[3].

Performance at the Putah Creek near Winters station is similar to the performance of the CDEC Lake Berryessa outflow station discussed in Section 9.3. The daily and monthly performance metric summaries for this station are presented in Table 9-11 and Table 9-12. Visual performance comparisons are presented in Figure 9-21 to Figure 9-25.

The Putah South Canal is controlled as diversions from Lake Solano. Only 0.5 miles of the canal is within the watershed boundary and therefore, it is not represented in the model as a reach segment. Instead, canal diversions are simulated as a withdrawal of water from Putah Creek based on the observed daily flow rates. The observed and simulated diversions were compared, as shown in Figure 9-26, to verify that the correct volume of water was diverted from the canal. The monthly performance metrics for this station are presented in Table 9-13.

Table 9-11. Summary of daily validation performance metrics for PUTAH C NR WINTERS CA (11454000)

Hydrology Monitoring Locations	Performance Metrics (10/01/2004 - 09/30/2017)														
	PBIAS						RSR			NSE			KGE[1]		
	All	Wet Season	Dry Season	>10th %ile Flows	Storm Flows	Baseflow	All	Wet Season	Dry Season	All	Wet Season	Dry Season	All	Wet Season	Dry Season
PUTAH C NR WINTERS CA	-3.6%	-12.8%	3.4%	-8.8%	-5.1%	-1.2%	0.55	0.56	0.47	0.7	0.69	0.78	0.78	0.72	0.92

[1] Monthly, as specified in Table 8-3.

Table 9-12. Summary of calibration performance metrics using monthly averages at PUTAH C NR WINTERS CA (11454000)

Calibration Metrics for Monthly Flow (10/01/2004 - 09/30/2023)	Hydrological Condition		
	All (n = 228)	Wet Season (n = 133)	Dry Season (n = 95)
Percent Bias (PBIAS)	-3.6%	-12.8%	3.4%
Nash-Sutcliffe Efficiency (NSE)	0.77	0.75	0.81
RMSE-Std. Dev. Ratio (RSR)	0.48	0.5	0.44
Kling–Gupta Efficiency (KGE)	0.78	0.72	0.92

[3] It should be noted that most reach segments of Putah Creek below Lake Solano are known to lose flow to groundwater and are within the Sacramento Valley groundwater basin: https://scwa2.com/putah-creek/.

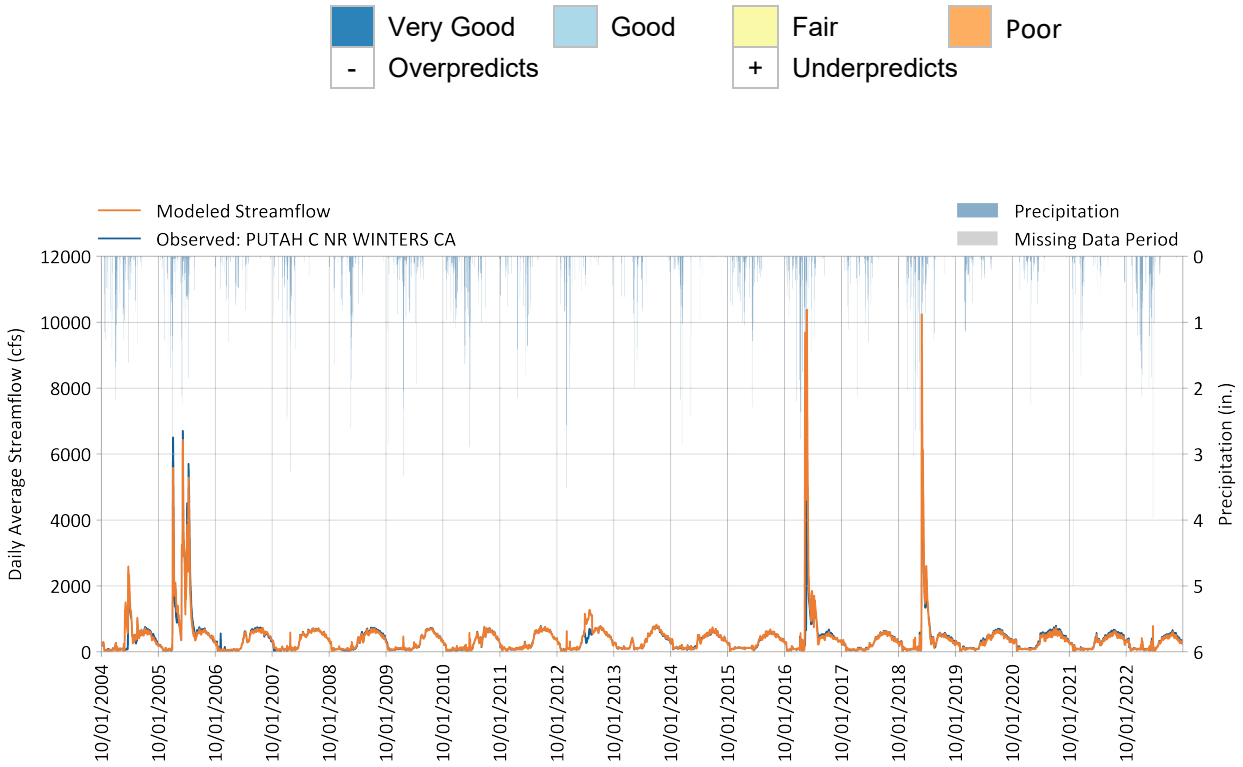

Figure 9-21. Daily simulated vs. observed streamflow for PUTAH C NR WINTERS CA (11454000).

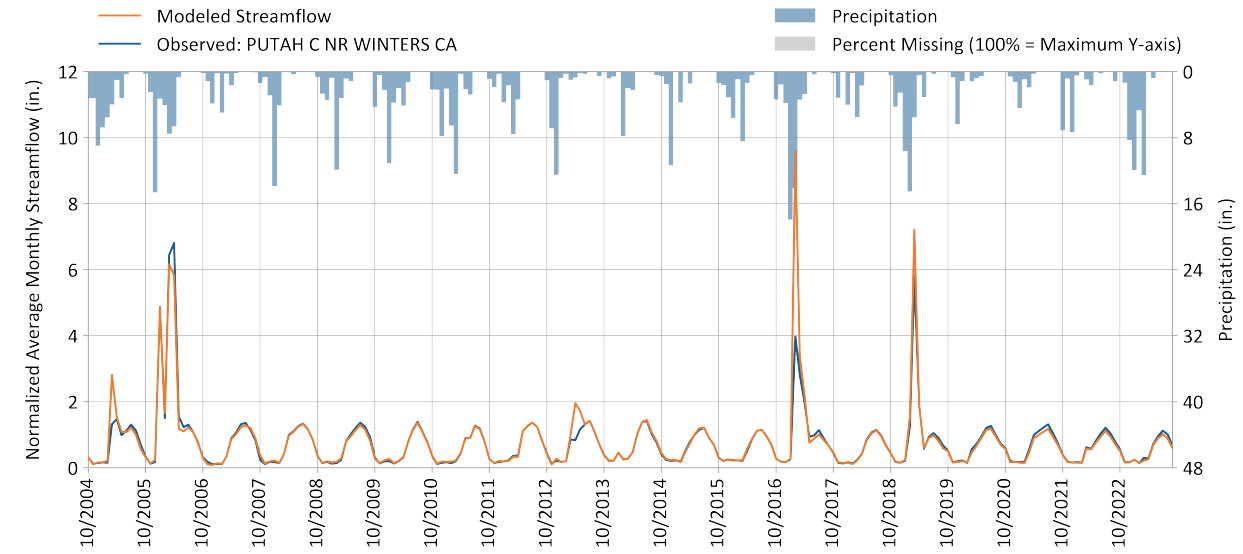

Figure 9-22. Monthly simulated vs. observed streamflow for PUTAH C NR WINTERS CA (11454000).

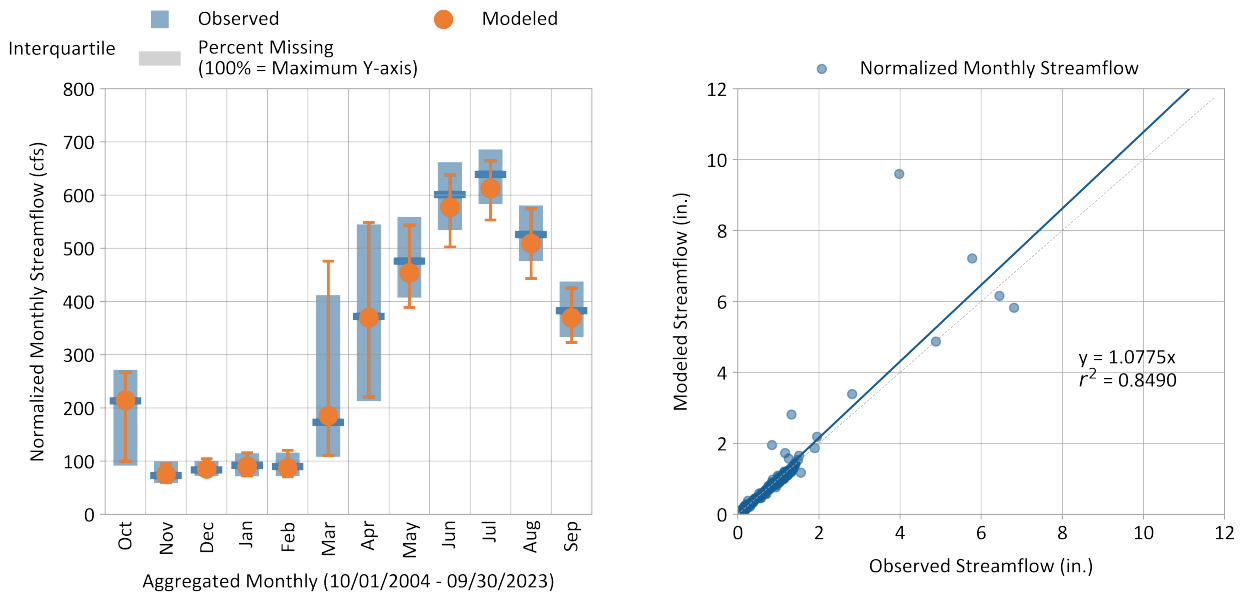

Figure 9-23. Monthly normalized simulated vs. observed streamflow for PUTAH C NR WINTERS CA (11454000).

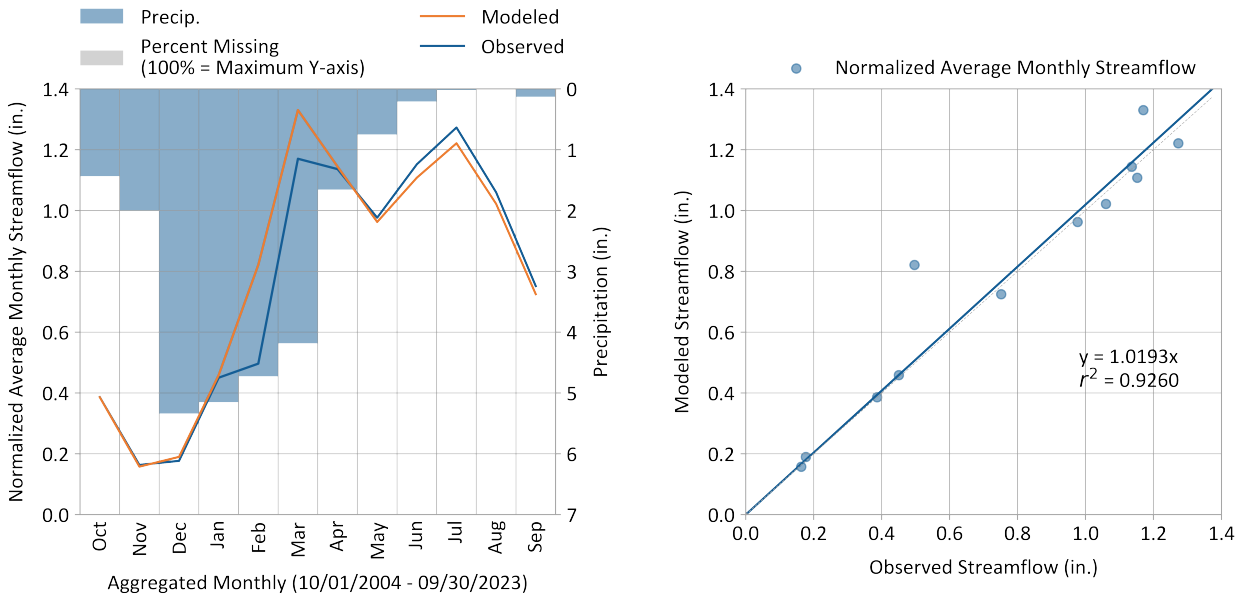

Figure 9-24. Average monthly simulated vs. observed streamflow for PUTAH C NR WINTERS CA (11454000).

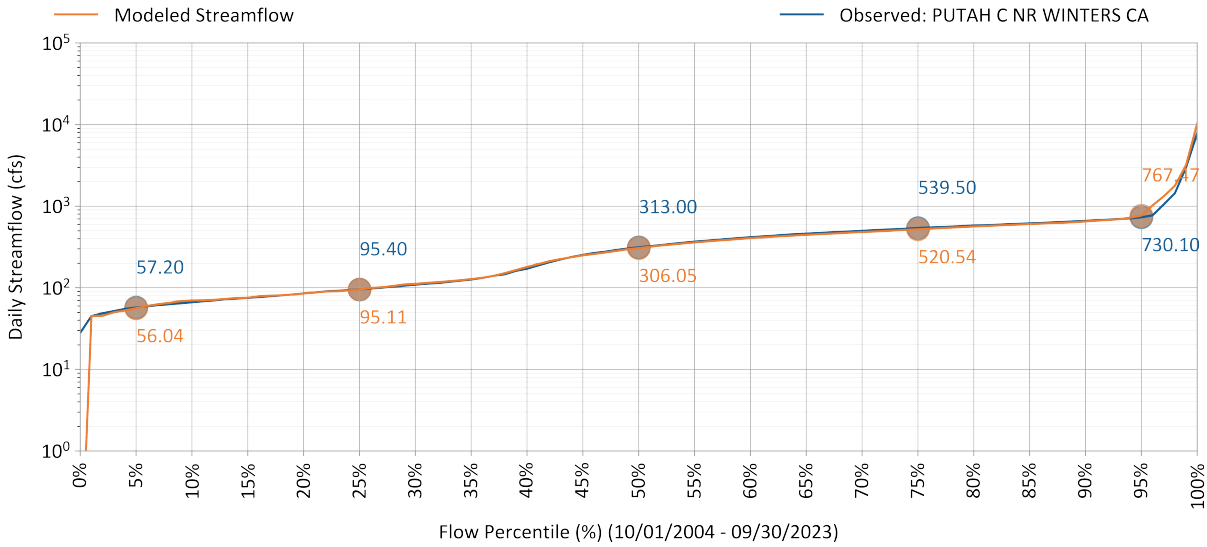

Figure 9-25. Simulated vs. observed flow duration curve for PUTAH C NR WINTERS CA (11454000).

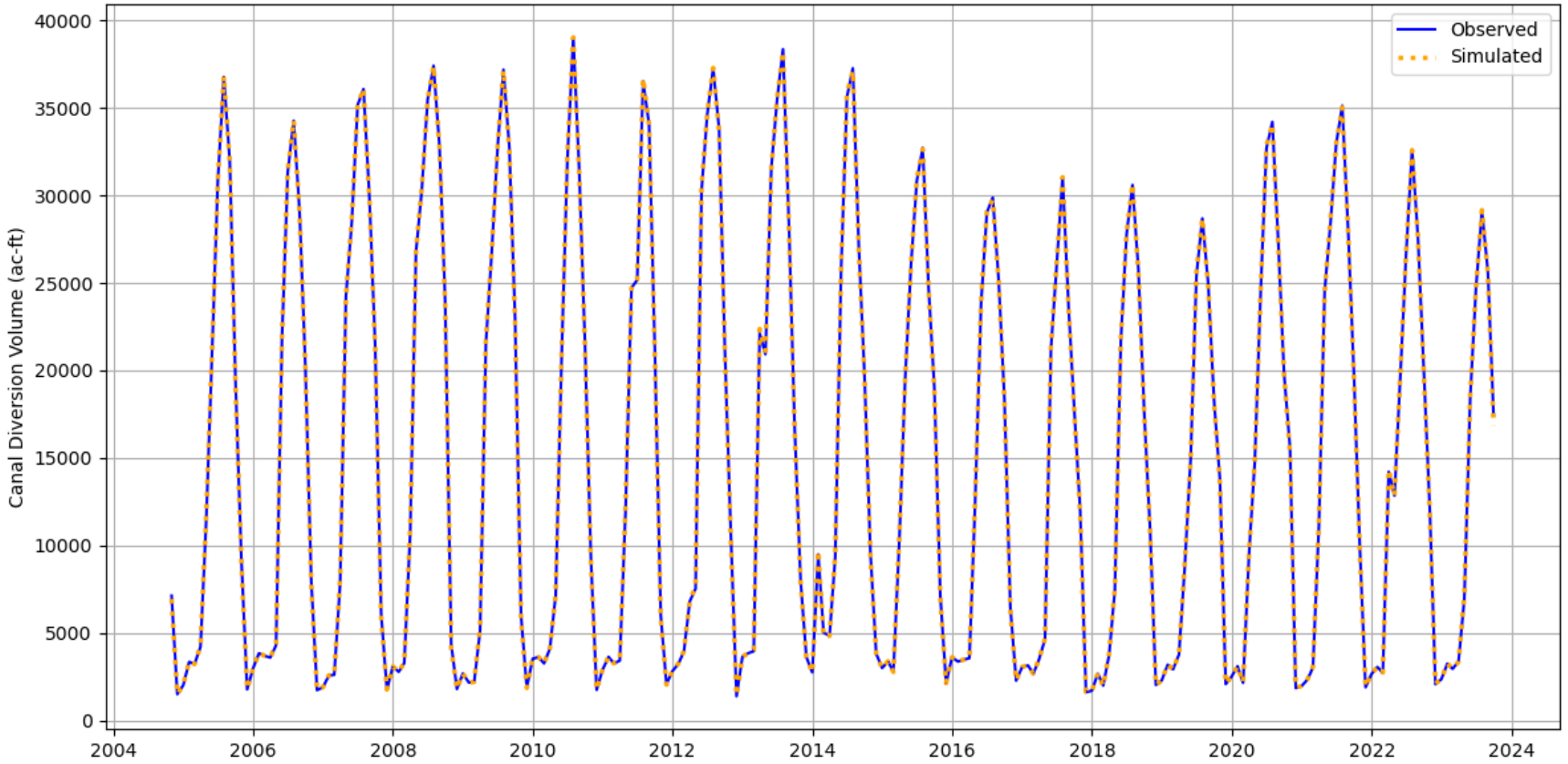

Figure 9-26. Observed and simulated monthly total volume diverted from Putah Creek into the Putah South Canal.

Table 9-13. Summary of calibration performance metrics using monthly total volume diverted from Putah Creek into the Putah South Canal

Calibration Metrics for Monthly Flow (10/01/2004 - 09/30/2023)	Hydrological Condition		
	All (n = 60)	Wet Season (n = 38)	Dry Season (n = 22)
Percent Bias (PBIAS)	0.0%	0.1%	-0.1%
Nash-Sutcliffe Efficiency (NSE)	1.0	1.0	1.0
RMSE-Std. Dev. Ratio (RSR)	0.01	0.02	0.02
Kling–Gupta Efficiency (KGE)	1.0	1.0	1.0

Very Good Good Fair Poor
\- Overpredicts + Underpredicts

9.5 Fire and Land Cover Change Impacts

The history of wildfire induced land cover change within the Putah Creek watershed can help contextualize the calibration and validation results presented in the preceding sections. The California Department of Forestry and Fire Protection (CAL FIRE) maintains a database of fire perimeters (CAL FIRE 2026) which, when paired with annual NLCD data sets available from 1985 (USGS 2024), highlights the impacts of fire in the watershed. Fire areas are summarized by year in Table 9-14 and visualized in a series of maps for clarity (Figure 9-27 to Figure 9-29). 2015, 2018, and 2020 had especially extensive fires covering 24%, 11%, and 48% of the total watershed area, respectively.

At the watershed scale, vegetation changes from the fires are visible in Figure 9-30 as decreases in forest and scrub area and increases in grassland. Evaluation of the smaller Putah Creek near Guenoc drainage area further illustrates the loss of forest from the 2015 Valley fire and the succession of grassland back to scrub and forest (Figure 9-31). This change is especially important for the calibration and validation of the Guenoc streamflow gauge. For most of the validation period (WY 2005-2017), this drainage area is approximately 45% scrub, 35% forest, and 10% grassland. After the Valley fire in 2015, however, that distribution changes to 20% scrub, 15% forest, and 60% grassland in 2017 when the calibration period begins. These changes are not reflected in the model HRUs, which are based on the 2021 NLCD snapshot (45% scrub, 15% forest, and 35% grassland).

In terms of model performance, the Guenoc drainage area fire impacts help explain the slight underprediction during the calibration period, which was chosen based on the availability of diversion data, and slight overprediction during the validation period. Because the increased pre-fire forest area is not represented in the model, the validation period is missing an important source of increased ET and therefore overpredicting; this also helps explain the overpredicted inflow to Lake Berryessa. As described in Section 8.2.1, additional parameter adjustments were made to interception and ET to help rebalance hydrology over time; however, impacts associated with fire may be better represented by changing HRU footprints over time, accordingly. While the model performs well as-calibrated, incorporating time-varying HRUs as a future model enhancement could substantially improve the current differences in over- and under-prediction for the validation and calibration periods.

Table 9-14. Total CAL FIRE historical wildland fire area by calendar year within the Putah Creek watershed

Year	2004	2005	2006	2007	2008	2009	2010	2011	2012	2013	2014	2015	2016	2017	2018	2019	2020	2021	2022	2023
Total Fire Area (ac)	33,402	695	525	1,274	187	--	--	508	--	437	10,956	100,211	5,885	11,389	45,814	584	200,253	142	1	--
Total Fire Area (%)	8.0%	0.2%	0.1%	0.3%	0.0%	--	--	0.1%	--	0.1%	2.6%	23.9%	1.4%	2.7%	10.9%	0.1%	47.8%	0.0%	0.0%	--

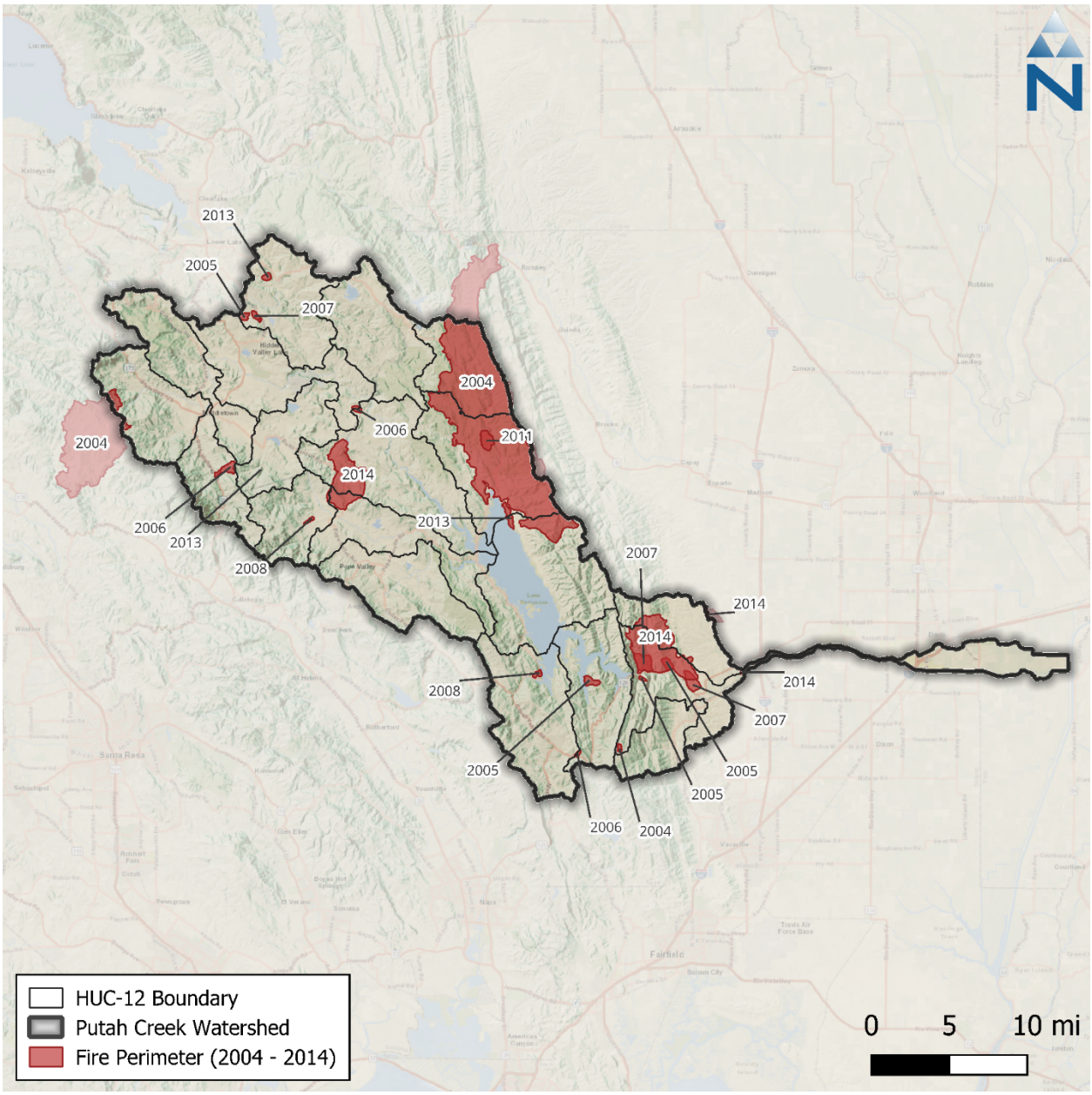

Figure 9-27. CAL FIRE historical wildland fire perimeters within the Putah Creek watershed between 2004 and 2014.

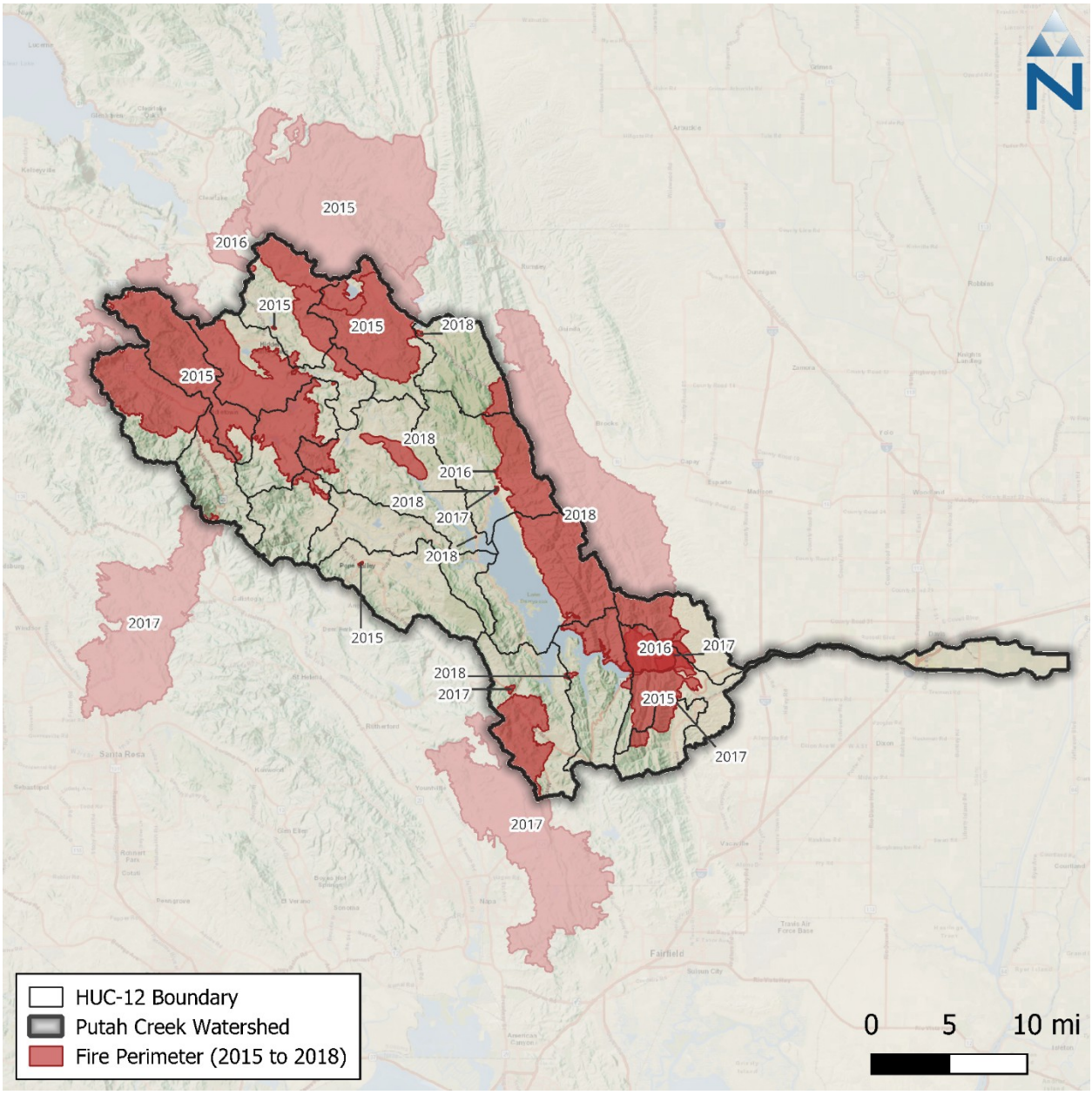

Figure 9-28. CAL FIRE historical wildland fire perimeters within the Putah Creek watershed between 2015 and 2018.

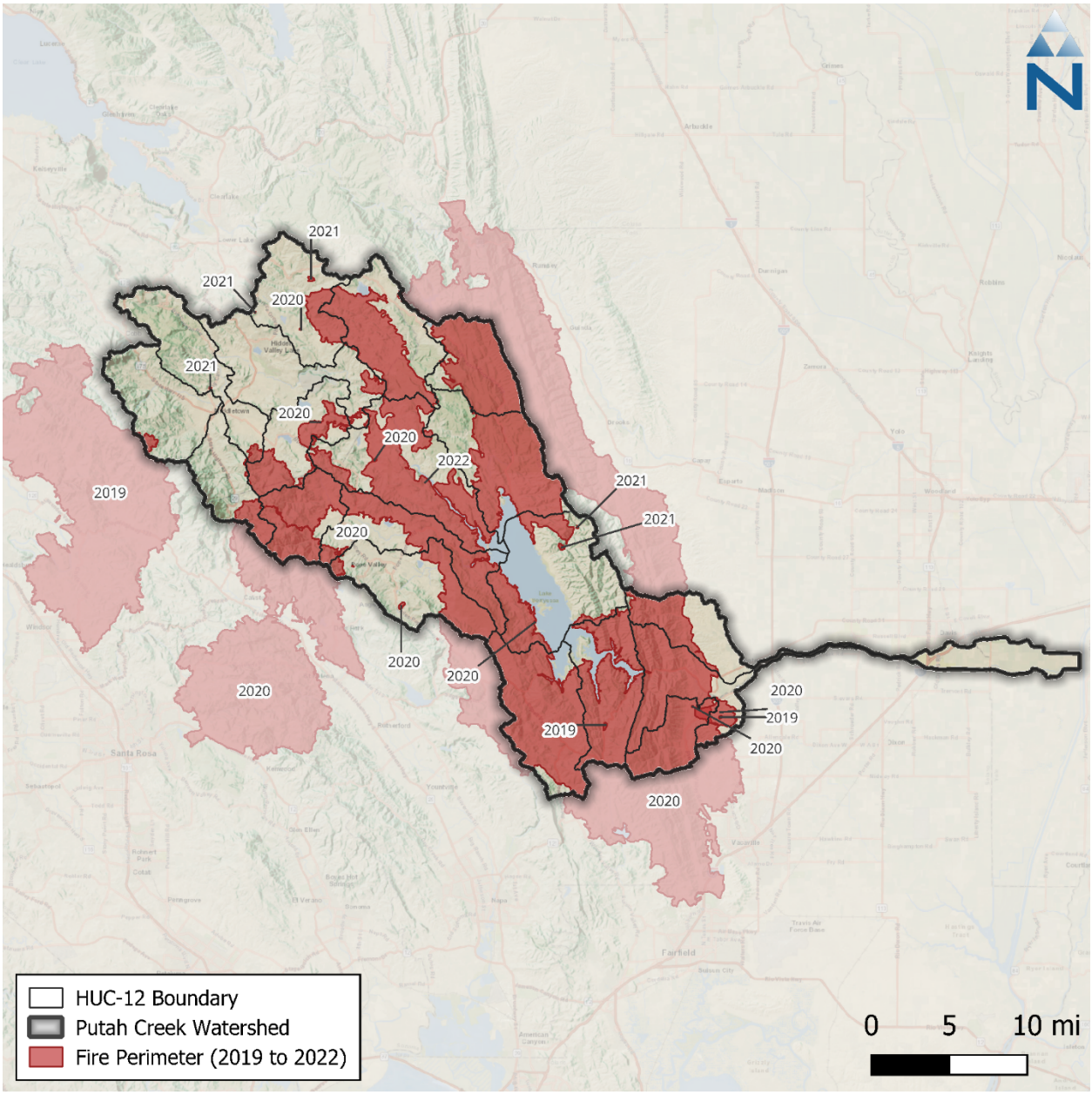

Figure 9-29. CAL FIRE historical wildland fire perimeters within the Putah Creek watershed between 2019 and 2022.

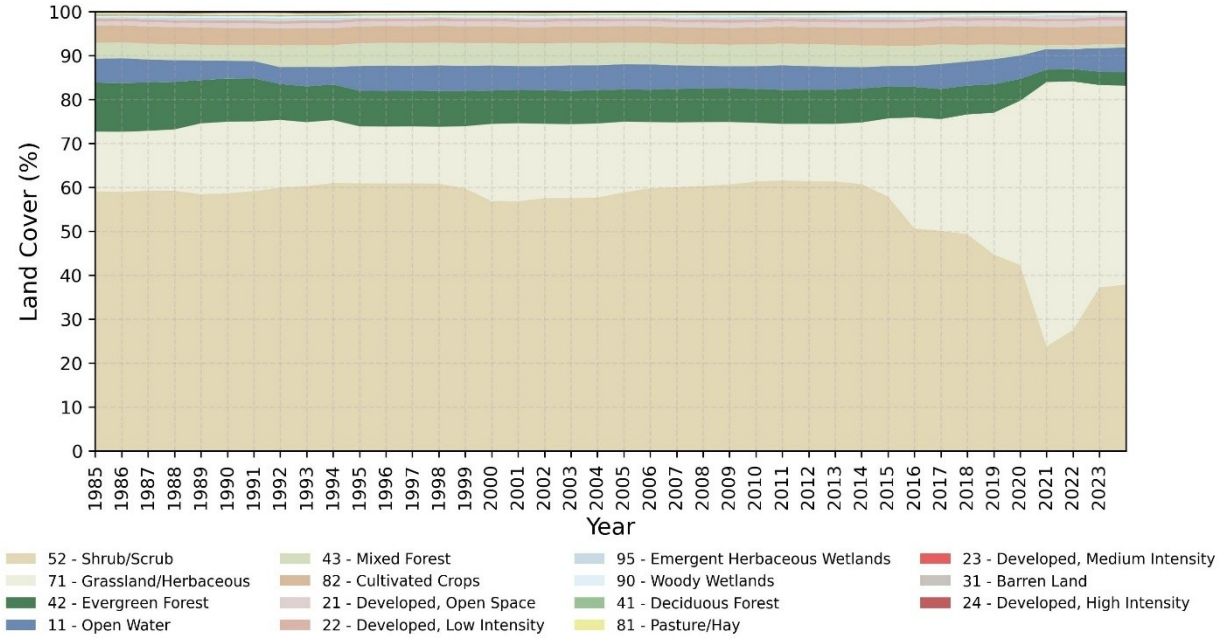

Figure 9-30. Annual NLCD landcover distribution from 1985-2023 for the entire Putah Creek watershed, excluding the Guenoc drainage area.

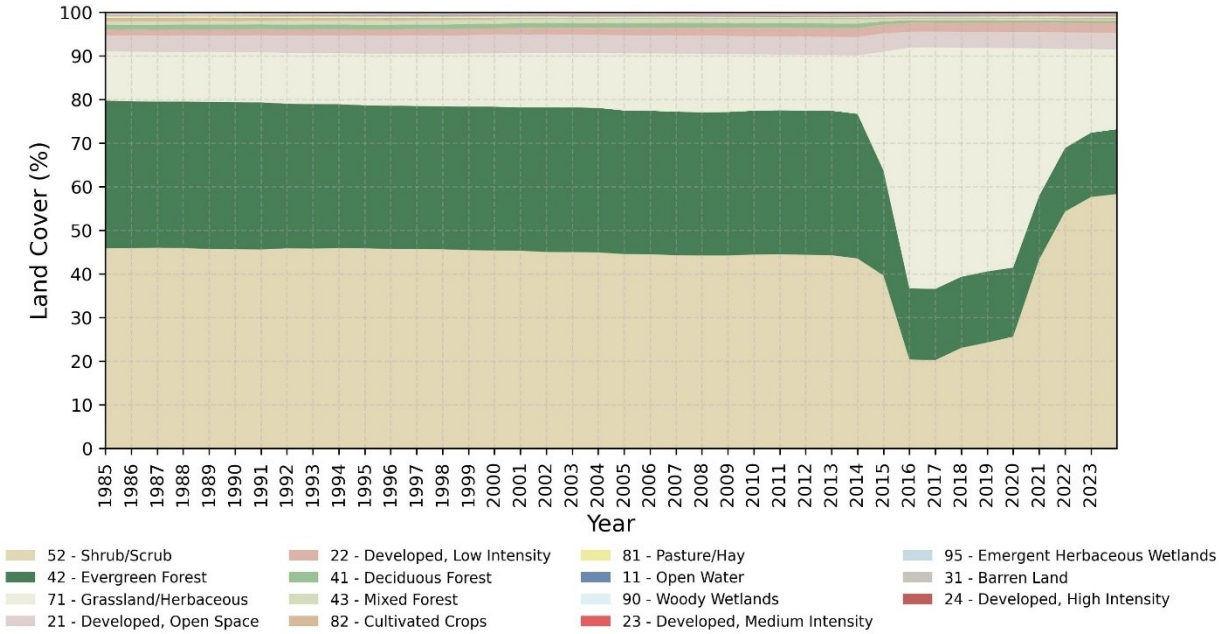

Figure 9-31. Annual NLCD landcover distribution from 1985-2023 for the Putah Creek near Guenoc drainage area.

10 SUMMARY

This report documented the configuration, calibration, and validation of an LSPC hydrology model for the Putah Creek watershed. The Water Board will use this model to facilitate water use planning to ensure adequate, minimal water supplies for critical purposes. The Putah Creek watershed model provides a comprehensive planning and decision-making tool by serving as an evaluation platform for (1) simulating existing instream flows that integrate current water management activities and consumptive uses and (2) evaluating the range of impacts of alternative management scenarios, including water allocation, changes in demand, and the impact of extreme events (e.g., droughts, atmospheric rivers, etc.).

The Putah Creek watershed model was configured based on authoritative and comprehensive data sets suitable for characterizing hydrology within the region. The model is based on HRUs, which capture physical attributes controlling the rainfall-runoff response and are driven by long-term meteorological forcing time series representing the spatial and temporal range of precipitation and evapotranspiration conditions in the watershed. The model was calibrated at the Putah Creek near Guenoc USGS streamflow station representing the headwaters and validated there as well as at Pope Creek, Lake Berryessa, and downstream of the lake at Putah Creek near Winters and the Putah South Canal for the modeled period (Water Years 2004-2023). The overall model validation performance across the evaluated performance metrics was generally "Very Good" to "Good". There is some accepted underprediction of flows at the Guenoc headwaters station during the calibration period (2018-2023); however, this was necessary to balance overprediction in the validation period. Model performance during the validation period (2004-2017) was generally "Very Good" and "Good," with a reasonably representative water balance assessment across the entire modeling period.

Some key findings on conditions within the Putah Creek watershed that should be considered during use and potential future updates to the model are:

- **Land cover change from fires**: The Putah Creek watershed has an extensive history of fires, as discussed in Section 9.5. These impacts were not explicitly represented in the model but help explain the current differences in over- and under-prediction for the validation and calibration periods at the Guenoc station. Incorporating time-varying HRUs as a future model enhancement could substantially improve the model's representation of observed conditions.
- **Seepage from Lake Berryessa**: The seepage of water from Lake Berryessa into groundwater was simulated in the model to account for uncertainty in all unknown losses of water from the vicinity of the lake as discussed in Section 9.3; reach operations are used to ensure the correct amount of water is released downstream on a daily basis. Incorporation of time-varying HRUs could also help refine the simulation of lake processes by reducing inflows and allowing seepage to be reduced correspondingly.

In conclusion, the Putah Creek watershed model is a robust platform for representing existing conditions and setting up future management scenarios. An important benefit of the model development approach used to build the watershed model and described in this report is that it is designed in a modular way, where key components can be refined and improved over time as new and better information becomes available.

11 REFERENCES

Arcement, G.J., JR., Schneider, V.R., 1989. Guide for selecting Manning's roughness coefficients for natural channels and flood plains. USGS Water-Supply Paper 2339.

Arnold, J.G., Allen, P.M., Muttiah, R., Bernhardt, G., 1995. Automated Base Flow Separation and Recession Analysis Techniques. Groundwater 33, 1010–1018. https://doi.org/10.1111/j.1745-6584.1995.tb00046.x

Bent, G.C., Waite, A.M., 2013. Equations for Estimating Bankfull Channel Geometry and Discharge for Streams in Massachusetts. U.S. Geological Survey Scientific Investigations Report 2013–5155 62. https://doi.org/https://doi.org/10.3133/sir20135155

CAL FIRE (California Dept. of Forestry and Fire Protection), 2026. California Fire Perimeters (1950+). CAL FIRE eGIS. https://gis.data.ca.gov/datasets/CALFIRE-Forestry::california-fire-perimeters-1950/explore?location=37.578990%2C-119.269051%2C6

Cosgrove, B.A., Lohmann, D., Mitchell, K.E., Houser, P.R., Wood, E.F., Schaake, J.C., Robock, A., Marshall, C., Sheffield, J., Duan, Q., Luo, L., Higgins, R.W., Pinker, R.T., Tarpley, J.D., Meng, J., 2003. Real-time and retrospective forcing in the North American Land Data Assimilation System (NLDAS) project. Journal of Geophysical Research: Atmospheres 108, 8842. https://doi.org/10.1029/2002jd003118

Daly, C., G. H. Taylor, W. P. Gibson, T. W. Parzybok, G. L. Johnson, P. A. Pasteris, 2000. High-Quality Spatial Climate Data Sets for the United States and Beyond. Transactions of the ASAE 43, 1957–1962. https://doi.org/10.13031/2013.3101

Daly, C., Neilson, R.P., Phillips, D.C., 1994. A Statistical-Topographic Model for Mapping Climatological Precipitation over Mountainous Terrain. J Appl Meteorol Climatol 33, 140–158.

Daly, C., Taylor, G., Gibson, W., 1997. The Prism Approach to Mapping Precipitation and Temperature, in: 10th AMS Conf. on Applied Climatology. Reno, NV, pp. 10–12.

Doherty, J. 2015. Calibration and Uncertainty Analysis for Complex Environmental Models - PEST: complete theory and what it means for modelling the real world. ISBN: 978-0-9943786-0-6

Duda, P.B., P.R. Hummel, A.S. Donigian, and J.C. Imhoff, 2012. BASINS/HSPF: Model Use, Calibration, and Validation. Trans ASABE 55, 1523–1547. https://doi.org/10.13031/2013.42261

DWR (California Department of Water Resources), 2020. California's groundwater—Update 2020: Sacramento, Calif., California Department of Water Resources Bulletin 118, 485 p., accessed September 25, 2023, at https://water.ca.gov/Programs/Groundwater-Management/Bulletin-118.

EPA (U.S. Environmental Protection Agency), 2000. BASINS Technical Note 6 Estimating Hydrology and Hydraulic Parameters for HSPF, Office of Water 4305. EPA-823-R00-012.

Gibson, W.P., Daly, C., Kittel, T., Nychka, D., Johns, C., Rosenbloom, N., McNab, A., Taylor, G.H., 2002. Development of a 103-Year High-Resolution Climate Data Set for the Conterminous United States, in: Proceedings of the 13th AMS Conference on Applied Climatology. Portland, OR, pp. 181–183.

Gupta, H. V., Kling, H., Yilmaz, K.K., Martinez, G.F., 2009. Decomposition of the mean squared error and NSE performance criteria: Implications for improving hydrological modelling. J Hydrol (Amst) 377, 80–91. https://doi.org/10.1016/j.jhydrol.2009.08.003

Henn, B., Newman, A.J., Livneh, B., Daly, C., Lundquist, J.D., 2018. An assessment of differences in gridded precipitation datasets in complex terrain. J Hydrol (Amst) 556, 1205–1219. https://doi.org/10.1016/j.jhydrol.2017.03.008

Jensen, M. E., Dotan, A., Sanford, R., 2005. Penman-Monteith Estimates of Reservoir Evaporation. Impacts of Global Climate Change, 1–24. https://doi.org/10.1061/40792(173)548

Kim, S., Paik, K., Johnson, F.M., Sharma, A., 2018. Building a Flood-Warning Framework for Ungauged Locations Using Low Resolution, Open-Access Remotely Sensed Surface Soil Moisture, Precipitation, Soil, and Topographic Information. IEEE J Sel Top Appl Earth Obs Remote Sens 11, 375–387. https://doi.org/10.1109/JSTARS.2018.2790409

Knoben, W.J.M., Freer, J.E., Woods, R.A., 2019. Technical note: Inherent benchmark or not? Comparing Nash–Sutcliffe and Kling–Gupta efficiency scores. Hydrol Earth Syst Sci 23, 4323–4331. https://doi.org/10.5194/hess-23-4323-2019

Kouchi, D.H., Esmaili, K., Faridhosseini, A., Sanaeinejad, S.H., Khalili, D., Abbaspour, K.C., 2017. Sensitivity of calibrated parameters and water resource estimates on different objective functions and optimization algorithms. Water (Basel) 9. https://doi.org/10.3390/w9060384

LACFCD (Los Angeles County Flood Control District), 2020. WMMS Phase I Report: Baseline Hydrology and Water Quality Model. Prepared for the Los Angeles County Flood Control District by Paradigm Environmental. Alhambra, CA.

Looper, J.P., Vieux, B.E., 2012. An assessment of distributed flash flood forecasting accuracy using radar and rain gauge input for a physics-based distributed hydrologic model. J Hydrol (Amst) 412–413, 114–132. https://doi.org/10.1016/j.jhydrol.2011.05.046

McCandless, T.L., 2003a. Maryland stream survey: Bankfull discharge and channel characteristics in the Allegheny Plateau and the Valley and Ridge hydrologic region. Annapolis, MD.

McCandless, T.L., 2003b. Maryland Stream Survey: Bankfull Discharge and Channel Characteristics in the Coastal Plain Hydrologic Region. Annapolis, MD.

McCandless, T.L., Everett, R.A., 2002. Maryland stream survey: Bankfull discharge and channel characteristics in the Piedmont hydrologic region. Annapolis, MD.

McGourty, G., Lewis, D., Metz, J., Harper, J., Elkins, R., Christian-Smith, J., Papper, P., Schwankl, L., Prichard, T., 2020. Agricultural water use accounting provides path for surface water use solutions. Calif Agric (Berkeley) 74, 46–57. https://doi.org/10.3733/CA.2020A0003

Mitchell, K.E., Lohmann, D., Houser, P.R., Wood, E.F., Schaake, J.C., Robock, A., Cosgrove, B.A., Sheffield, J., Duan, Q., Luo, L., Higgins, R.W., Pinker, R.T., Tarpley, J.D., Lettenmaier, D.P., Marshall, C.H., Entin, J.K., Pan, M., Shi, W., Koren, V., Meng, J., Ramsay, B.H., Bailey, A.A., 2004. The multi-institution North American Land Data Assimilation System (NLDAS): Utilizing multiple GCIP products and partners in a continental distributed hydrological modeling system. Journal of Geophysical Research: Atmospheres 109. https://doi.org/10.1029/2003jd003823

Moriasi, D.N., Arnold, J.G., Van Liew, M.W., Bingner, R.L., Harmel, R.D., Veith, T.L., 2007. Model Evaluation Guidelines for Systematic Quantification of Accuracy in Watershed Simulations. Trans ASABE 50, 885–900. https://doi.org/10.13031/2013.23153

Moriasi, D.N., Gitau, M.W., Pai, N., Daggupati, P., 2015. Hydrologic and water quality models: Performance measures and evaluation criteria. Trans ASABE 58, 1763–1785. https://doi.org/10.13031/trans.58.10715

Nash, J.E., Sutcliffe, J. V., 1970. River flow forecasting through conceptual models part I - A discussion of principles. J Hydrol (Amst) 10, 282–290. https://doi.org/10.1016/0022-1694(70)90255-6

Nathan, R.J., McMahon, T.A., 1990. Evaluation of automated techniques for base flow and recession analyses. Water Resour Res 26, 1465–1473. https://doi.org/10.1029/WR026i007p01465

NHDPlus (National Hydrography Dataset Plus) Data, 2022. EPA (United States Environmental Protection Agency). https://www.epa.gov/waterdata/get-nhdplus-national-hydrography-dataset-plus-data

Quirmbach, M., Schultz, G.A., 2002. Comparison of rain gauge and radar data as input to an urban rainfall-runoff model. Water Science and Technology 45, 27–33. https://doi.org/10.2166/wst.2002.0023

SCWA (Solano County Water Agency), 2009. Area and Capacity Table for Lake Berryessa at Monticello, California (June 1, 2009). https://rms.waterboards.ca.gov/DownloadAttachment.aspx?ATTACHMENT_ID=17303

SCWA (Solano County Water Agency), 2026. Putah Creek. https://scwa2.com/putah-creek/

Sloto, R.A., Crouse, M.Y., 1996. HYSEP: A Computer Program for Streamflow Hydrograph Separation and Analysis: U.S. Geological Survey Water-Resources Investigations Report 1996–4040. https://doi.org/10.3133/wri964040

Smakhtin, V.U., 2001. Low flow hydrology: a review. J Hydrol (Amst) 240, 147–186. https://doi.org/10.1016/S0022-1694(00)00340-1

SWRCB (State Water Resource Control Board). 2025. Supply and Demand Assessment (SDA) – Navarro River. Watershed Supply and Demand Allocations. https://www.waterboards.ca.gov/waterrights/water_issues/programs/supply-and-demand/navarro-river.html

SWRCB (State Water Resource Control Board), 2024. Watershed Supply and Demand Allocations: Putah Creek Work Plan. https://www.waterboards.ca.gov/waterrights/water_issues/programs/supply-and-demand/docs/putah-creek-workplan.pdf

Sutherland, R.C., 2000. Methods for Estimating the Effective Impervious Area of Urban Watersheds, Technical Note 58, in: Scueler, T.R., Holland, H.K. (Eds.), The Practice of Watershed Protection. Center for Watershed Protection, Ellicot City, MD, pp. 193–195.

Thomasson, H.G., Olmsted, F.H., Lfiroux, E.F., 1960. Geology, water resources and usable ground-water storage capacity of part of Solano County, California (2nd print. (with corrections).): U.S. Geological Survey Water Supply Paper 1464. https://doi.org/10.3133/wsp1464

USDA (United States Department of Agriculture), 2024. Cropland Data Layer. https://croplandcros.scinet.usda.gov/

USGS (United States Geological Survey), 2024. Annual National Land Cover Database (NLCD) Collection 1 Products (ver. 1.1, June 2025). https://doi.org/10.5066/P94UXNTS

Xia, Y., Mitchell, K., Ek, M., Cosgrove, B., Sheffield, J., Luo, L., Alonge, C., Wei, H., Meng, J., Livneh, B., Duan, Q., Lohmann, D., 2012a. Continental-scale water and energy flux analysis and validation for North American Land Data Assimilation System project phase 2 (NLDAS-2): 2. Validation of model-simulated streamflow. Journal of Geophysical Research Atmospheres 117. https://doi.org/10.1029/2011JD016051

Xia, Y., Mitchell, K., Ek, M., Sheffield, J., Cosgrove, B., Wood, E., Luo, L., Alonge, C., Wei, H., Meng, J., Livneh, B., Lettenmaier, D., Koren, V., Duan, Q., Mo, K., Fan, Y., Mocko, D., 2012b. Continental-scale water and energy flux analysis and validation for the North American Land Data Assimilation System project phase 2 (NLDAS-2): 1. Intercomparison and application of model products. Journal of Geophysical Research Atmospheres 117, 3109. https://doi.org/10.1029/2011JD016048